NAVIGATION STUDY FOR

JACKSONVILLE HARBOR, FLORIDA

DRAFT INTEGRATED GENERAL REEVALUATION REPORT II

AND

SUPPLEMENTAL ENVIRONMENTAL IMPACT STATEMENT

APPENDIX A

ATTACHMENT K

PHASE I

ENGINEERING – Hydrodynamic and Salinity Modeling for Ecological Impact Evaluation

EFDC Salinity Modeling for Jacksonville Harbor GRR-2 Deepening Project
(Phase 1)

Final Report

Prepared for

U.S. Army Corps of Engineers, Jacksonville District
Jacksonville, Florida

by

Taylor Engineering, Inc.
10151 Deerwood Park Blvd.
Bldg. 300, Ste. 300
Jacksonville, Florida 32256
(904) 731-7040

C2009-040

February 2013

EXECUTIVE SUMMARY

The Jacksonville Harbor General Re-evaluation Study Project Management Plan (PMP) provides a plan to identify solutions to improve navigation in federally-maintained channels in the St. Johns River and to evaluate the impacts of these solutions. One of the solutions identified in the plan is modification of the federal navigation channel. The USACE-SAJ, as part of its General Re-evaluation Study to improve Jacksonville Harbor navigation, is assessing the effects of potential channel modifications on the general circulation, salinity, ecology, and water quality in the St Johns River. The USACE-SAJ chose to use the Environmental Fluid Dynamics Code (EFDC) model to characterize river circulation and salinity for pre- and post-project conditions. This report documents the setup, sensitivity analyses, validation, and preliminary application of the EFDC model to evaluate the direct impacts to salinity of navigation channel modifications.

The EFDC hydrodynamic model was calibrated and verified with monitoring data of water level and salinity collected during 1995 to 2005 for three conditions (wet period, dry period, and wind condition). The overall good agreement between simulated and observed water levels and salinity demonstrates the capability of the model to reasonably simulate these processes in the Lower St. Johns River. Based on the calibration and verification results and preliminary model application, the model is suitable for predicting hydrodynamic and salinity changes in the Lower St. Johns River from the potential channel deepening projects.

To test the model to evaluate the possible impacts from the potential channel dredging projects, this study simulated two preliminary project alternatives during a four-month dry period. To present the current condition of the channel more accurately, the study employed a model with 2009 survey bathymetric data to establish baseline conditions. This baseline model was then adjusted to reflect project modifications (dredging) in two additional models – one for Alternative Plan A and one for Alternative Plan B. Alternative Plan A involves dredging the navigation channel to 50 ft below mean lower low water (MLLW), widening some areas along the channel, and building new turning basins. Alternative Plan B, is similar to Alternative Plan A but limits deepening the navigation channel to 50 ft below MLLW for only the first 14 miles from the mouth of the river. Comparisons of simulation results from the models show that while potential dredging would not likely bring the ocean level salinity (35 ppt) any farther upstream, dredging could increase salinity along the river from its mouth to Buckman Bridge. Model results suggest small salinity changes at Shands Bridge and upstream.

TABLE OF CONTENTS

6.0 SUMMARY AND CONCLUSIONS **90**

REFERENCES..**91**

APPENDIX A   Governing Hydrodynamic

LIST OF FIGURES

LIST OF TABLES

1.0 INTRODUCTION

The Jacksonville Harbor, as described by the U.S. Army Corps of Engineers Jacksonville District (USACE-SAJ), includes the first 20 river miles from the St. Johns River mouth in the Atlantic Ocean. The harbor consists of three segments (Figure 1.1) namely (a) Segment 1 — from the entrance channel to River Mile 14 — has an authorized existing depth of 40 ft, (b) Segment 2 — from River Mile 14 to River Mile 20 — has an authorized depth of 40 feet, and (c) Segment 3 (West Blount Island Channel) has an existing authorized depth of 38 feet.

Figure 1.1 Jacksonville Harbor Segments (Source: USACE-SAJ)

The Jacksonville Harbor General Re-evaluation Study Project Management Plan (PMP) provides a plan to identify solutions to improve navigation in federally-maintained channels in the St. Johns River and to evaluate the impacts of these solutions. One of the solutions identified in the plan is modification of the federal navigation channel. The USACE-SAJ, as part of its General Re-evaluation Study to improve Jacksonville Harbor navigation, is assessing the effects of potential channel modifications on the general circulation, salinity, ecology, and water quality in the St Johns River. For the hydrodynamic modeling, the USACE-SAJ chose to use the Environmental Fluid Dynamics Code (EFDC) to characterize river circulation and salinity for pre- and post-project conditions.

On June 5, 2009, the USACE-SAJ provided Taylor Engineering, Inc. a Notice-to-Proceed for Work Order W912EP-06D-0012 (Delivery Order 0010) to perform the St. Johns River EFDC circulation and salinity modeling for the Jacksonville Harbor GRR-2 Deepening Project. Specifically, the purpose of the modeling is to provide an assessment of the direct effects of channel modifications on salinity, and to assess the cumulative effects of other projects including the Mayport Deepening Project for the U.S. Navy

and freshwater withdrawals in the St. Johns River. For the above Work Order, USACE-SAJ directed Taylor Engineering to refine the existing EFDC model from the St. Johns River Water Management District (SJRWMD) to accommodate details of the potential channel modifications. Simulating effects of the proposed channel deepening template was not possible in the SJRWMD version of the model due to limited model mesh resolution on the river bottom. Also, USACE-SAJ directed Taylor Engineering to evaluate the influence of the number of horizontal mesh elements across the navigation channel and the number of vertical elements in the water column on simulated water levels and salinity. The SJRWMD calibrated and verified its model for the period 1996 – 2005 for the St. Johns River Water Supply Impact Study (WSIS) (Sucsy et al., 2010).

This report describes the model refinement, sensitivity analyses, re-calibration, re-verification, and preliminary application in the project area. Following this introduction, Chapter 2 describes the study area. Chapter 3 describes the EFDC model refinement and sensitivity analysis. Chapter 4 describes model calibration and verification. Chapter 5 describes the modeling of some of the initial channel modifications. Chapter 6 provides a summary and conclusions.

2.0 STUDY AREA

The study area encompasses the lower (northern) 124 mi of the St. Johns River from its mouth near Mayport to upstream of Astor. The study area includes portions of the Atlantic Ocean, the Lower St. Johns River, Chicopit Bay, White Shells Bay, Mill Cove, major river tributaries, sections of the Atlantic Intracoastal Waterway (AIWW), and Lake George. Figure 2.1 shows a map of the study area. As described in the following paragraphs, the project area extends only to the first 20 miles of the St. Johns River (i.e., Segments 1, 2, and 3 of Jacksonville Harbor).
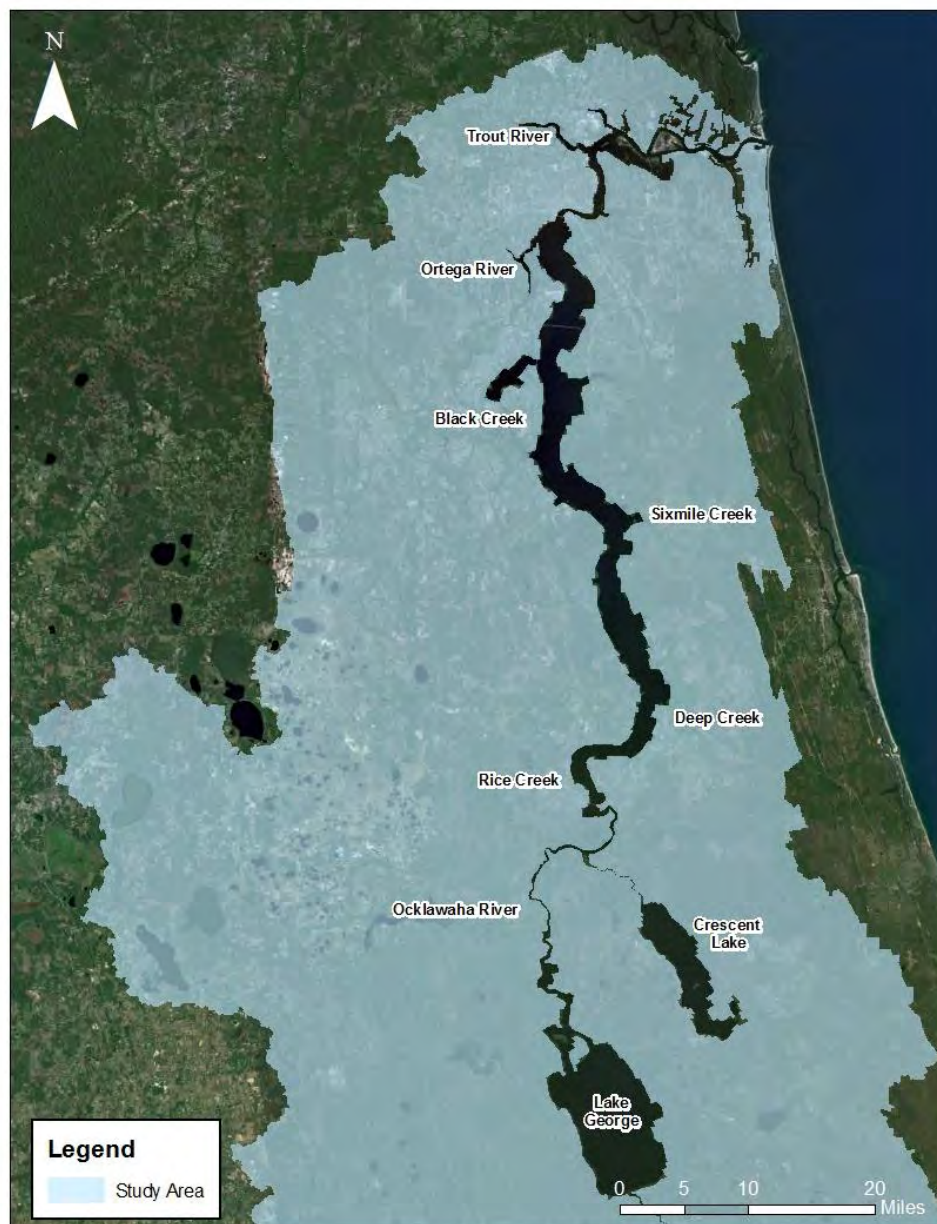
Figure 2.1 Study Area

Tides, winds, and freshwater flows from upstream and tributaries mainly influence the river flow in the study area. Semi-diurnal tide propagates from the Atlantic Ocean and reaches up to Crescent Lake. Measured data shows salinity is highest in the project area, lowest from Green Cove south to Palatka, and increases south of Palatka as the ground water inflows contain salts and calcium.

2.1 Project Area

The proposed Federal navigation channel deepening project area stretches from just east of mouth of the St Johns River to mile-marker 20. Along this stretch of the river, the navigation channel width ranges 400 – 1,200 ft. Figure 2.2 shows the main Federal channel mile markers, authorized channel depths, and dredged material sites. The USACE-SAJ plans to evaluate the impacts of dredging portions of this stretch for depths that range 40 – 50 ft. Although channel deepening considerations extend only up to around the Talleyrand Terminal (Mile 20), the USACE-SAJ would like to assess the extent of the channel deepening impacts at river areas located further upstream. Thus, the study area includes most of the Lower St. Johns River.
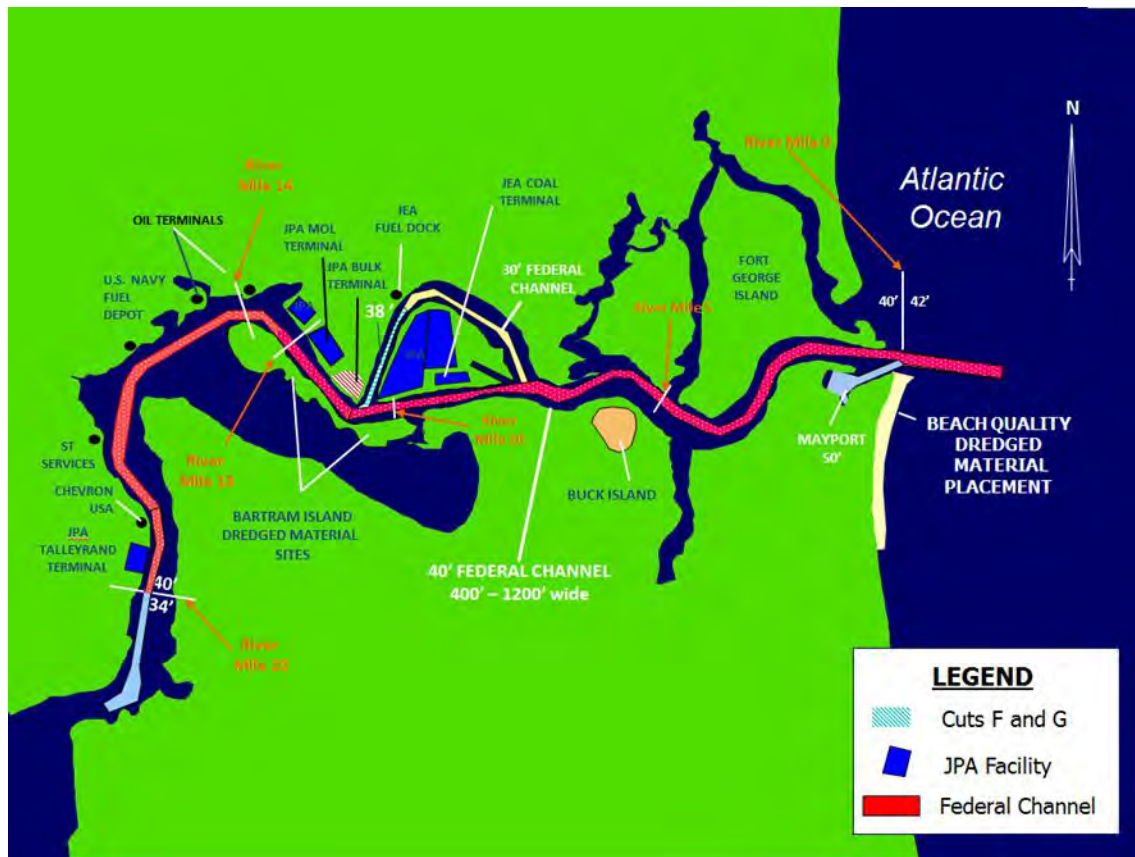
Figure 2.2 St. Johns River Federal Navigation Channel Mile Markers and Authorized Depths
(Source: USACE-SAJ)

2.2   St. Johns River Basin

The St. Johns River, spanning 310 miles (mi), is the longest river in Florida. The St. Johns River drainage basin encompasses over 8,840 square miles (sq. mi) spread across 16 counties (Sucsy and Morris, 2002). A slow-moving water body with very mild slope, the St. Johns River drops an average 0.1 foot per mile (ft/mi) (Toth, 1993). The mild slope of the river allows tidal effects to extend at least 106 mi from the river mouth in Duval County to Lake George in Volusia County. Lake George, with an area of 67 sq mi, is the second largest lake in Florida. The filling and draining of Lake George, due to subtidal variability of Atlantic Ocean water levels, causes intermittent periods of reverse flow extending far upstream in the Lower St. Johns River. Periods of reverse flow, when the daily net discharge moves upstream, extend the upstream movement of salt as well as upstream dispersal of pollutants entering the river.

The St. Johns River Water Management District (SJRWMD) manages and divides the basin into three sub-basins — Upper, Middle, and Lower St. Johns River. The Upper St. Johns River sub-basin extends from the headwaters of the St. Johns River in Okeechobee and Indian River Counties to the confluence of Econlockhatchee River in Seminole County. The Middle St. Johns River sub-basin extends from Lake Harney (Seminole and Volusia Counties) to the confluence of the Ocklawaha River near Welaka. The Lower St. Johns River sub-basin extends from the confluence of the Ocklawaha River to the river mouth at the Atlantic Ocean in Duval County (http://www.protectingourwater.org/watersheds/map). In addition, to these three sub-basins, the Lake George and Ocklawaha River Basins also drain into the St. Johns River (Figure 2.3). Located in the Lower St. Johns River, the Jacksonville Harbor main shipping channel, a 23-mi stretch of the river, extends from the river mouth to the Jacksonville Port Authority (JAXPORT) Talleyrand Marine Terminal just north of downtown Jacksonville. The incoming ocean tide acts as a nearly pure progressive shallow-water wave over the lower 31 mi, from the river mouth to Jacksonville (Sucsy and Morris, 2002).

2.3   Lower St. Johns River Area

The Lower St. Johns River receives 42% of its total annual freshwater flow from sources upstream of Astor. Astor is approximately 4.5 river miles south of the southern end of Lake George. The surrounding local watersheds of the Lower St. Johns River encompass 2,300 sq. mi, about 27% of the total watershed area (Sucsy and Morris, 2002). The main tributaries of the Lower St. Johns River include Black Creek, Deep Creek, Sixmile Creek, Etonia Creek, Julington Creek, McCullough Creek, Arlington River, Broward River, Dunns Creek, Ortega River, Trout River, and Atlantic Intracoastal Waterway.
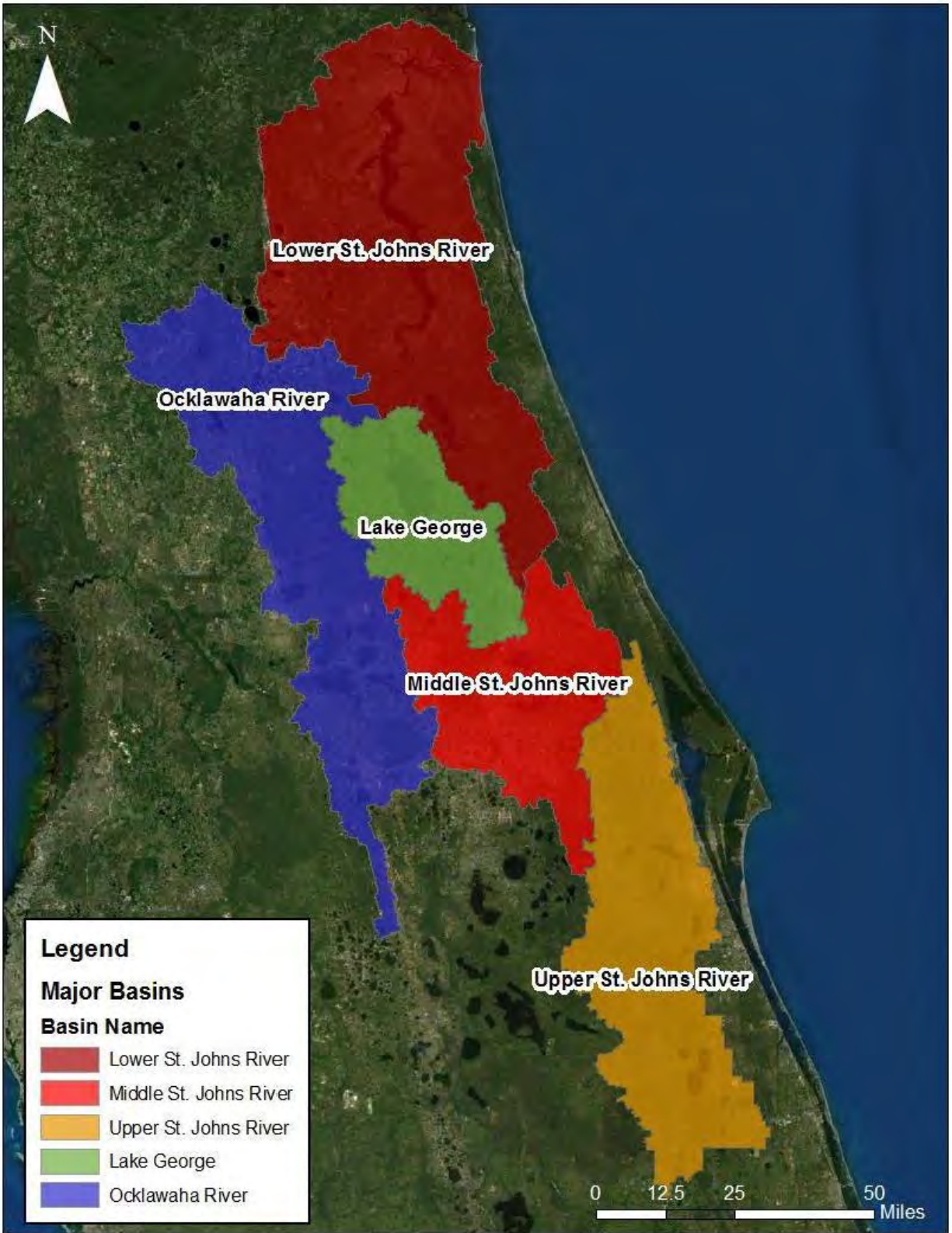
Figure 2.3 Major Tributary Basins and Sub-Basins of the St. Johns River Basin

In the Lower St. Johns River, three major factors govern the upstream extent of salinity: net freshwater discharge entering the upper estuary through Astor, subtidal variability of ocean water levels, and wind. The SJRWMD's EFDC calibration and verification (covering 1996 – 2001 and 1996 – 2005), showed the salinity front reached an area between Buckman Bridge (river mile 35) and Shands Bridge (river mile 47). Moderate levels of salinity intrusion rarely reached Shands Bridge. Although a water quality monitoring station located about 4.3 mi upstream of Shands Bridge recorded salinity at 5 practical salinity units (psu, approximately equal to 5 ppt) during May 1994, neither a theoretical maximum nor probability of the extent of upstream salinity intrusion has been determined (Sucsy and Morris, 2002).

Between the river mouth and downtown Jacksonville, highly variable salinity ranges from completely fresh conditions to near ocean levels. At the Acosta Bridge near downtown Jacksonville, salinity ranges from completely fresh conditions due to high river discharges to 28 psu during dry conditions. At Dames Point, farther downstream near Blount Island, salinity ranges from 0.4 to 34.9 psu (Sucsy and Morris, 2002).

3.0   MODEL DESCRIPTION AND LOWER ST. JOHN RIVER EFDC SALINITY MODEL SETUP

This chapter describes the hydrodynamic and advection-dispersion model applied in this study. The chapter also describes the sensitivity analysis conducted for model resolution.

3.1   Model Description

This study employed the Environmental Fluid Dynamics Code (EFDC), the three-dimensional (3-D) numerical model developed by John Hamrick (1996). A public domain modeling package, EFDC simulates multidimensional flow, transport, and biochemical processes in surface water systems including lakes, rivers, estuaries, reservoirs, wetlands, and coastal regions. This model, currently maintained by Tetra Tech with support from the U.S. Environmental Protection Agency (USEPA), has a history of extensive use in the United States (e.g., Wool et al., 2003; Sucsy and Morris, 2002; Jin et al., 2000; and Hamrick et. al, 1995). More recently, the SJRWMD (2011) presents the completed application of the model to quantify the effects of water withdrawals on hydrodynamics throughout the St. Johns River. The EFDC model has undergone extensive tests, documentation, and applications in more than 200 modeling studies worldwide by research institutions, governmental agencies, and consulting organizations (Hamrick, 2011).

The hydrodynamic model, based on the 3-D shallow water equations of motion, includes dynamically coupled salinity and temperature transport. The physics of the EFDC model, and many aspects of the computational scheme, are similar to the widely used Blumberg-Mellor model, which later became Princeton Ocean Model (Blumberg and Mellor, 1987). The EFDC model employs a curvilinear-orthogonal horizontal grid, and a stretched or sigma vertical coordinate. In addition to hydrodynamic, salinity, and temperature transport simulation capabilities, EFDC can also simulate cohesive and non-cohesive sediment transport, near field and far field discharge dilution from multiple sources, eutrophication processes, transport and fate of toxic contaminants in the water and sediment phases, and transport and fate of various life stages of finfish and shellfish (USEPA, 2007). Appendix A describes the governing equations of the EFDC model.

3.2 Model Setup

3.2.1 Model Domain

The model applied for this study originated from the Lower St. Johns River Hydrodynamic Model developed by the St. Johns River Water Management District (SJRWMD) for its Water Supply Impact Study (WSIS), hereinafter called the 2001 SJRWMD EFDC model. However, during the course of the Jacksonville Harbor GRR-2 Deepening Project study, the SJRWMD updated the 2001 model and released a newer model, hereinafter called the 2010 SJRWMD EFDC. The SJRWMD calibrated and verified the 2001 model with data from a five-year period (1996 – 2000) and the 2010 model with data from a 10-year period (1996 – 2005). The SJRWMD applied the 2010 model on its St. Johns River Water Supply Impact Study (WSIS) (SJRWMD, 2011).

The 2010 SJRWMD EFDC model domain covers the entire Lower St. Johns River (LSJR) and major tributaries from Astor upstream of Lake George to the Atlantic Ocean (Figure 3.1). The model domain comprises 4,295 curvilinear horizontal water cells with the model variables (water surface elevation, velocity, temperature, salinity, etc.) calculated within each cell over the model simulation period. Each horizontal cell comprises six equally divided layers in the vertical direction. Thus, six equally stretched layers compose the model's vertical dimension.

3.2.2 Boundary Conditions

Boundary conditions used for model forcing include ocean water level, ocean salinity, lateral discharge and salinity, wind, rainfall, and evaporation. Ocean water level and salinity define the seaward (downstream) open ocean boundary. Notably, the SJRWMD provided the 2001 and 2010 SJRWMD EFDC models with the temperature variable switched off which means the models do not include the effect of temperature changes in the model simulations. Model boundary conditions span a period that allows the model to run for the 1995 through 2005 period. The USACE-SAJ scope of work states the SJRWMD processed and quality-assured the boundary conditions data.
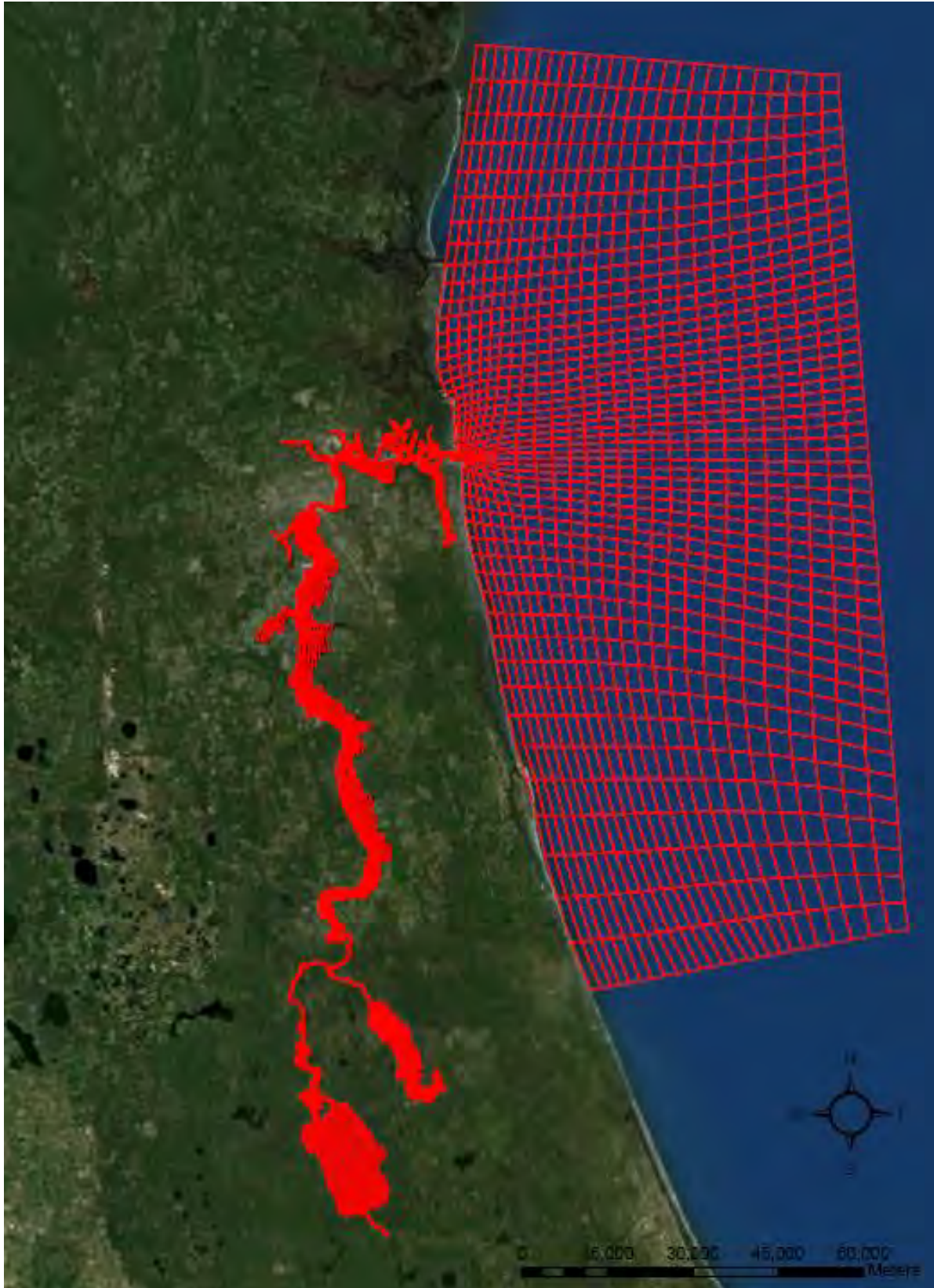
Figure 3.1 2010 SJRWMD EFDC Model Mesh

3.2.2.1 Ocean Water Level and Salinity

Fifty-four cells form the open ocean boundary along the eastern side of the LSJR grid. Ocean water level provides the forcing function along the open ocean boundary. SJRWMD provided a time-series of hourly water surface elevation — vertical displacements above or below the mean tide level. Sucsy et al. (2010) stated creation of the ocean water level time-series by a superposition of predicted astronomical tide and observed meteorological tide. During the simulation years, ocean water levels — dominated by semidiurnal tides — ranged from -5.18 to +4.33 ft NAVD. Ocean salinity was set at a constant value of 35.5 ppt along the open ocean boundary.

3.2.2.2 Lateral Discharge and Salinity

Lateral discharges included in the model are (a) tributary discharge, (b) spring (localized groundwater) discharge, (c) diffuse groundwater discharge, and (d) wastewater treatment plant discharge. Lateral discharges, either observed or estimated, provide model boundary conditions. Tributary discharge, obtained from either USGS gaging stations or from SJRWMD hydrologic modeling, enters the LSJR model at 100 separate locations. Tributary discharge for the 1995 – 2005 period averaged 2,494 million gallons per day (mgd) (Sucsy et al., 2010). Springs enter the model at 11 locations. Monthly discharges, which capture seasonal variability, establish boundary conditions for most of the springs. Spring discharge observations are sparse for most springs in the study area. For springs with insufficient discharge data, Sucsy et al. (2010) stated that discharge time-series were estimated either by correlation to stage with a nearby well or by correlation to a neighboring spring discharge. Water flows from the Upper Floridan Aquifer account for diffuse groundwater into the river through the river bottom. It enters a broad area of the LSJR throughout Lake George and Crescent Lake. Belaineh (2010) developed the groundwater model for the diffuse groundwater boundary conditions, with discharge provided as constant discharge. The EFDC model also includes discharge from 34 wastewater treatment facilities, with discharge specified as a constant for each facility.

SJRWMD 2010 model developers assigned all water entering the EFDC model domain an associated salinity. Data used to develop salinity time-series for boundary conditions came from four sources: observed data, site-specific discharge-salinity relationships, generic discharge-salinity relationships, or established constants. Observed data were used at three locations — Astor, Rice Creek, and Deep Creek — where observations spanned the entire model simulation period (1995 – 2005) with adequate temporal resolution. Sucsy et al. (2010) stated that (a) site-specific discharge-salinity

11

relationships were developed for tributaries with limited observed data; (b) generic discharge-salinity relationships were used in areas with no data; (c) discharge-salinity relationships were developed for the Crescent Lake watershed; and (d) a low, constant value of 0.04 ppt was assigned to all the LSJR surface tributaries downstream of Rice and Deep creeks.

3.2.2.3 Meteorology: Rainfall, Evaporation, and Wind

For the selected model simulation periods, wind, rain, and evaporation all vary spatially and temporally over the model grid. The EFDC model accounts for the spatial variability of this input data by inverse distance interpolation of each variable based on the three nearest stations to a given model grid cell. The National Weather Service maintains five rainfall stations that provide daily-averaged rainfall (metadata shown in Table 3.1) near the river.

Estimates of potential evapotranspiration (PET) are based on the 1985 Hargreaves Method (Hargreaves and Allen, 2003) at the same location as the rainfall stations above. PET, a direct estimate of actual evaporation over open water, was directly applied to the hydrodynamic model. The Hargreaves Method, the highest-ranked temperature-based method for calculating PET, requires only observed minimum and maximum air temperature and estimated solar radiation (Jensen et al., 1990).

Table 3.1 Stations with Observed Rainfall and Evaporation Data near the Lower St. Johns River

NOAA Station ID	Station Name	Period of Record	Latitude	Longitude
4538	Jacksonville Int'l Airport	1948 – Present	# ").'	(! $!.&
4366	Jacksonville Beach	1948 – Present	# !'.#	(! "#.&
2915	Federal Point	1931 – Present	") $%.#	(! #".#
1978	Crescent City	1931 – Present	") "%.	(! # .(
2229	Deland	1931 – Present	") !.!	(! !(.&

Hourly wind data (Table 3.2) are available from National Oceanic and Atmospheric Administration (NOAA) sites located at airports and the Florida Automated Weather Network (FAWN). All the stations provide hourly wind speed and direction, and record wind at a standard height of 10 meters or 32.8 ft (Sucsy et al., 2010).

Table 3.2 Stations with Observed Wind Data near the Lower St. Johns River

Station ID	Station Name	Period of Record	Latitude	Longitude
NOAA 13384	Jacksonville Int'l Airport	1948 – Present	# ").'	(! $!.&
FAWN 270	Hastings	1999 – Present	") $!.&	(! "&.'
NOAA 12816	Gainesville Regional Airport	1984 – Present	") $!.%	(" !&.%
NOAA 12834	Daytona Beach Int'l Airport	1948 – Present	") !!.	(! ".)
FAWN 302	Umatilla	1998 – Present	"(%%."	(! #'.)

3.3   Model Setup Sensitivity Analysis

Model sensitivity analyses, as applied to model setup (as opposed to model sensitivity with respect to model input data), test a model's response to changes in model setup. The sensitivity analyses for the current study involved evaluating changes in model results (water level and salinity) in response to changes in the number of vertical layers and number of cells in the navigation channel model mesh.

As directed by the USACE-SAJ, Taylor Engineering performed model sensitivity analyses for both the 2001 and 2010 SJRWMD EFDC models because soon after completion of the 2001 model sensitivity analyses, the SJRWMD provided to the USACE-SAJ the 2010 model. Thus, the USACE decided to apply the 2010 model instead of the 2001 model for the Jacksonville Harbor GRR-2 Deepening Project study. The following paragraphs describe the procedure for the 2010 SJRWMD EFDC sensitivity analysis. The procedure is identical to the analysis for 2001 SJRWMD EFDC.

The analysis of model sensitivity to the number of vertical layers began by increasing the number of SJRWMD model's vertical layers from the original & layers to (layers, and then to 10 layers. Increasing the number of vertical layers required decreasing the computational time step to   maintain computational stability. With the time step reduced, model computation time increased 400% (8 vertical layers) and 500% (10 vertical layers) compared to the time required to run the original model (6 vertical layers). Figure 3.2 to Figure 3.4 show a comparison (with observed data) of salinity values at three stations (Dames Point, Acosta Bridge, and Shands Bridge) from models with three different vertical layers. The figure shows salinity values for the surface layer (the upper 17% of the water column) and bottom layer (the lower 17% of the water column). The comparison indicates that an increase in the number of layers has no significant effect on model results. Thus, for this study, higher vertical resolution does not necessarily improve the accuracy of the results but significantly increases the computation time. Therefore, this study conducted the rest of the sensitivity analysis with six vertical layers in the model.
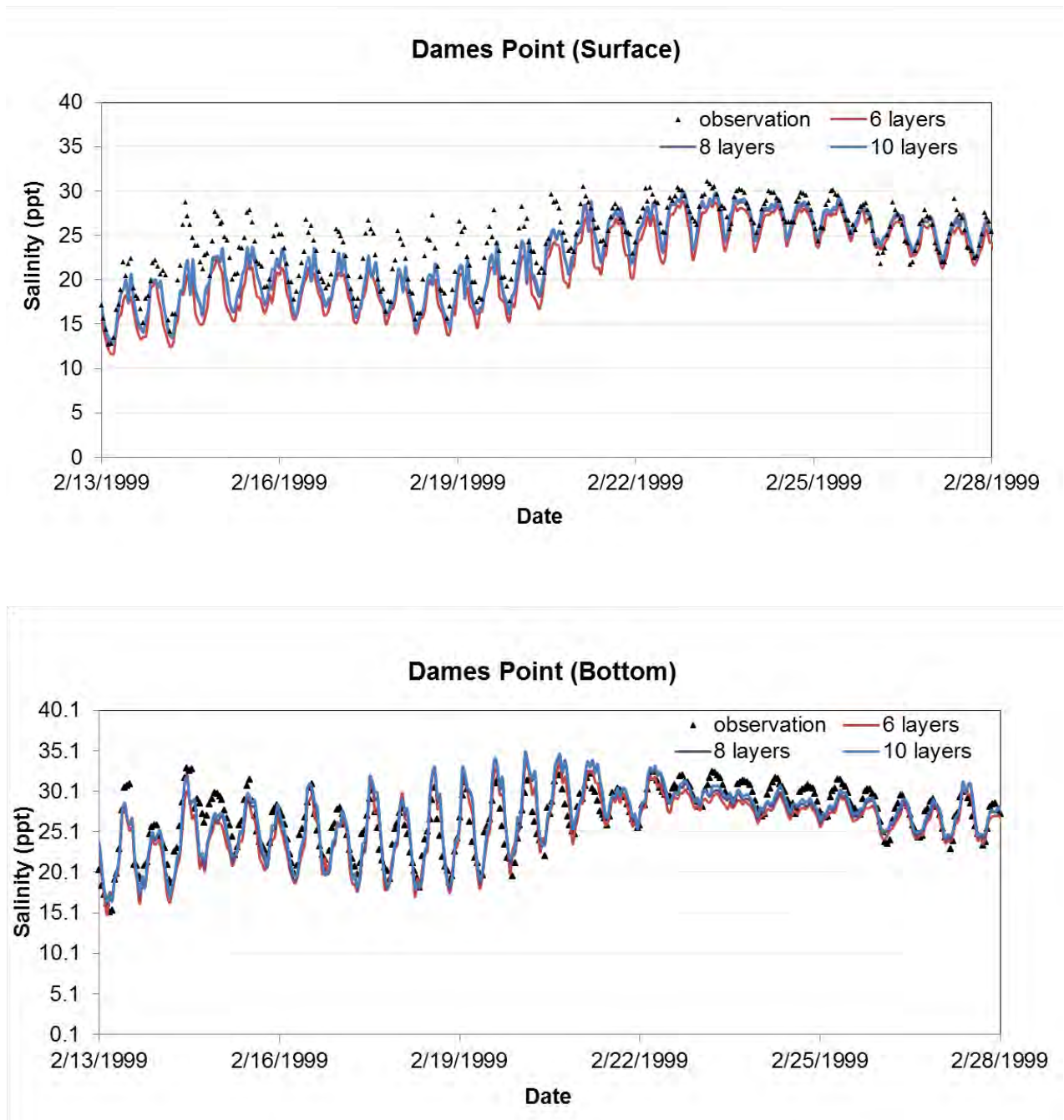
Figure 3.2 Surface and Bottom Salinity from Models with 6, 8, and 10 Vertical Layers at Dames Point
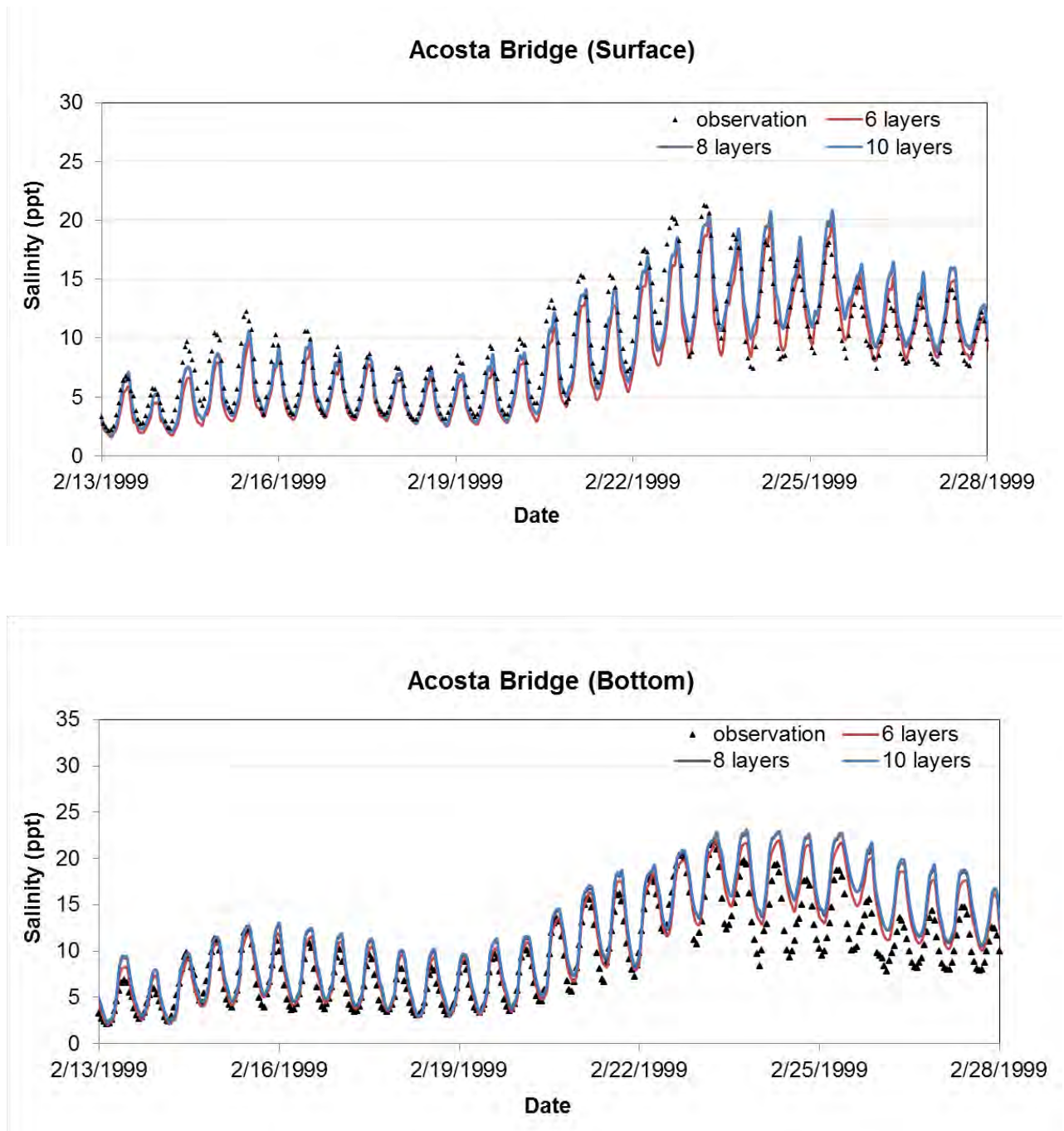
Figure 3.3 Surface and Bottom Salinity from Models with 6, 8, and 10 Vertical Layers at Acosta Bridge
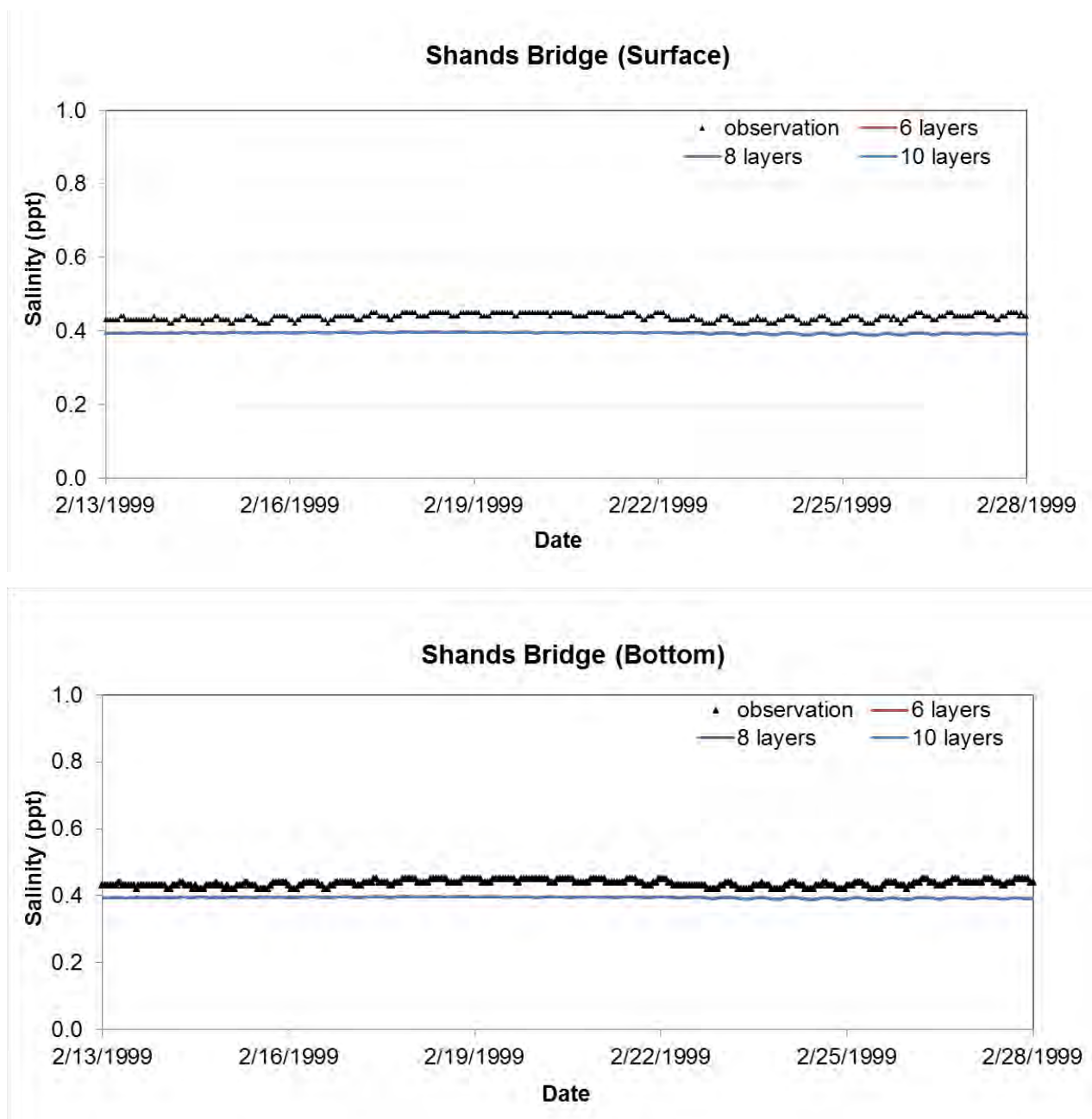
Figure 3.4 Surface and Bottom Salinity from Models with 6, 8, and 10 Vertical Layers at Shands Bridge

To refine the proposed dredge templates in the navigation channel, this study evaluated the sensitivity of the model to improved horizontal mesh resolution in the channel from the river mouth to River Mile 20. As shown in Figure 3.5, the SJRWMD EFDC model provides limited resolution inside and near the channel. Ideally, the model would simulate continuous, longitudinal unidirectional flow through the deep channel as much as possible. Achieving these ends first required two adjustments to the model mesh — realigning the model's single element in the navigation channel and splitting the single element

to multiple elements. Representing the trapezoidal channel accurately required at least three cross channel elements (Figure 3.6). To ensure that the sensitivity analyses provide only the effect due to mesh refinement, the study maintained the same element bed elevations outside the navigation channel, and the refined elements in the navigation channel adopted the bed elevation of the SJRWMD 2010 EFDC model single element in the navigation channel.

While at least three elements are required to accurately represent the navigation channel modifications, more than three elements require additional computation time with potentially negligible improved accuracy. Notably, the cells inside the channel are much smaller than their adjacent cells outside the channel. The differing element sizes increase the numerical instability of the model, which then requires longer computing time to arrive at a suitable numerical solution. To test the improvements gained by adding more elements, a sensitivity analysis was performed. Investigating model sensitivity to different numbers of elements across the channel required testing two model meshes — one mesh with two elements and one mesh with three elements defining the channel. (An investigation of the 2001 model with four channel elements showed no appreciable increase in model accuracy, but showed a significant increase in model instability and computation time.) Water level and salinity at the surface and bottom were compared with observed data along with the original SJRWMD 2010 EFDC model results at three stations (Acosta Bridge, Buckman Bridge, and Shands Bridge). Comparisons of water levels over a 60-day period (1/21/1999 – 3/22/1999) at all three stations (Figure 3.8 to Figure 3.9) show very small differences between the two-element and three-element models (figures show only 30 days to distinguish tidal cycles). Table 3.3 provides the root mean square error (RMSE) and correlation coefficient at each station of model-calculated and measured hourly water levels. A smaller RMSE value and a larger correlation value indicate closer agreement with the data. The RMSE and correlation statistics show little differences in model performance.

Salinity at both surface and bottom from different models were compared at all stations over a 60-day period (1/21/1999 – 3/22/1999) (Figure 3.10 – Figure 3.12 show only 15 days to distinguish tidal cycles), and the RMSE and correlation coefficient at each station of model-calculated and measurements were calculated (Table 3.4). Results from the three-element model show less agreement with observed data than results from the other two models. The main reason for this difference is the refined models were not recalibrated at this point. Some key calibration parameters such as horizontal diffusion coefficient are cell-size sensitive. The original horizontal diffusion coefficient has a greater effect on the three-element model than the two-element model. Thus, to improve the refined model performance, a refined model recalibration becomes necessary. Detailed in Chapter 4, recalibration with the refined mesh improved the performance of the three-element model. In fact, the recalibrated three-element model

provided slightly improved model performance in the project area. After recalibration, the updated Jacksonville Harbor EFDC model (hereinafter referred to as the USACE model) comprises three elements in the navigation channel from Mile 0 to Mile 20, six vertical layers, and 4,824 horizontal cells with lengths varying between 233 ft to 29,320 ft.
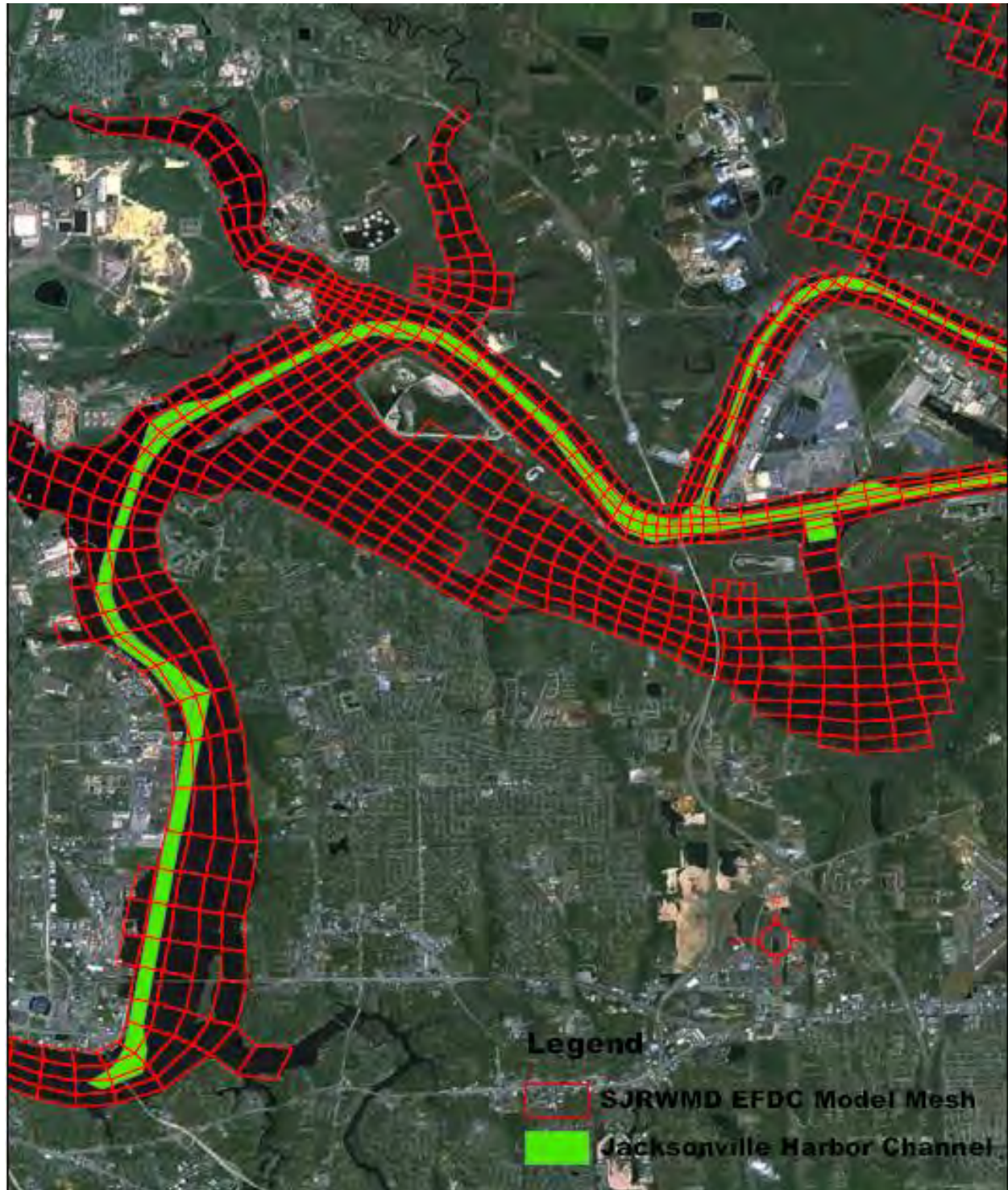
Figure 3.5 SJRWMD EFDC Model Mesh in the Navigation Channel from River Mile 10 to 20
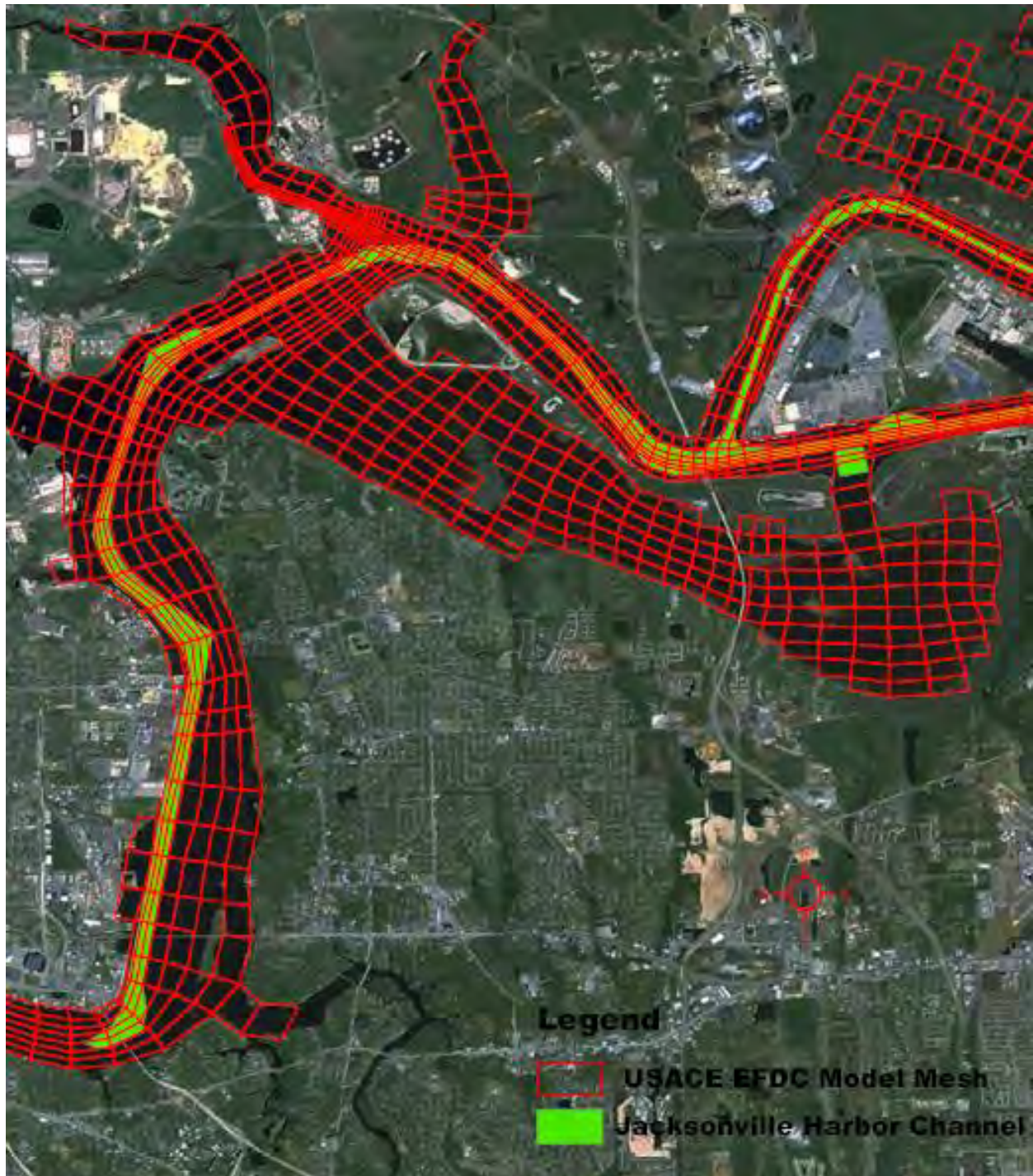
Figure 3.6 Updated Model Mesh with Three Elements in the Navigation Channel
from River Mile 10 to 20
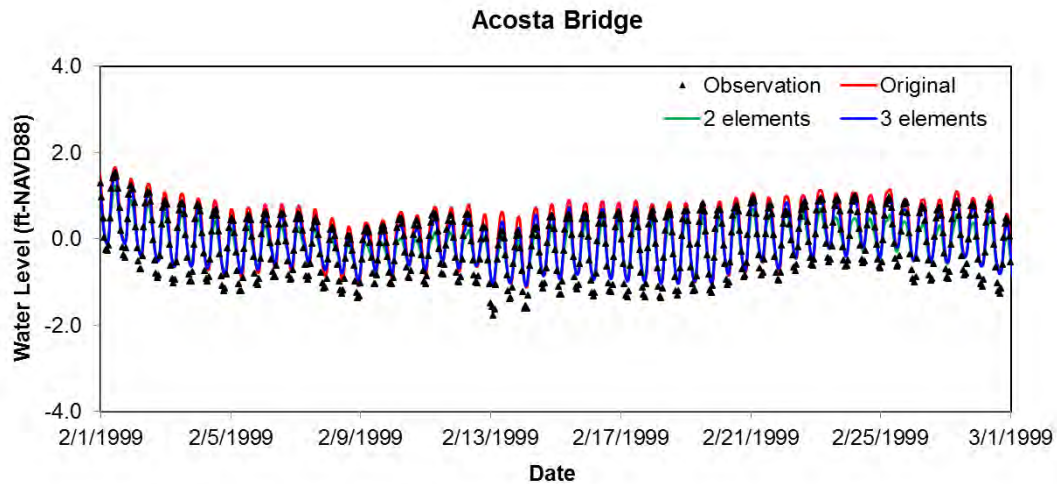
Figure 3.7 Comparison of Water Surface Elevation from Models with Different Channel Horizontal Elements at Acosta Bridge
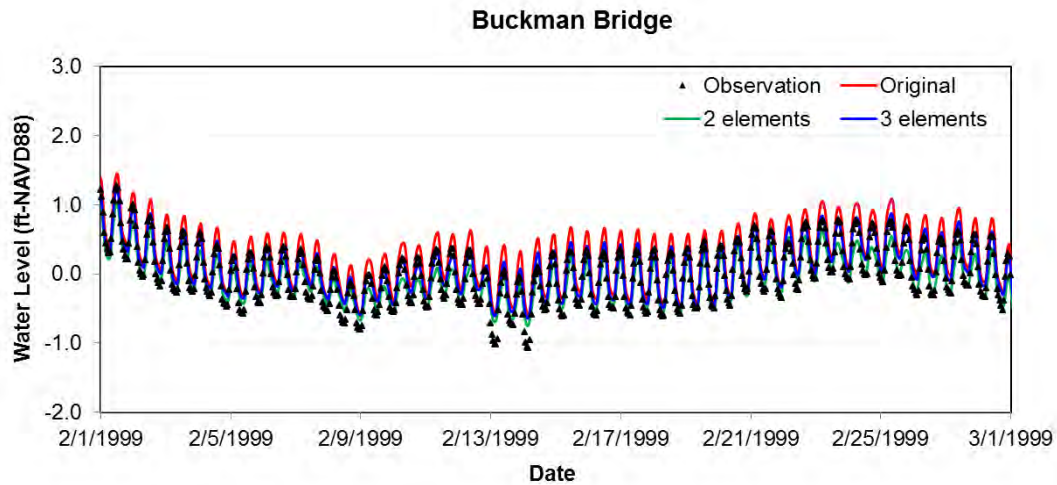
Figure 3.8 Comparison of Water Surface Elevation from Models with Different Channel Horizontal Elements at Buckman Bridge
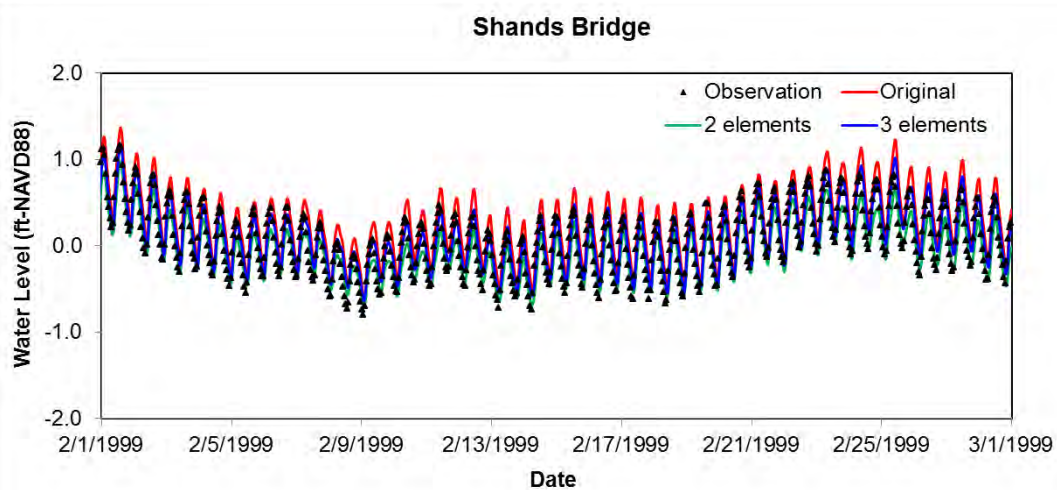
Figure 3.9 Comparison of Water Surface Elevation from Models with Different Channel Horizontal Elements at Shands Bridge

20

Table 3.3 Statistics for Water Level for Mesh Refinement Sensitivity Analysis (1/21/1999 – 3/22/1999)

Water Level	Original Model			Two-Element Model			Three-Element Model		
	Acosta Bridge	Buck-man Bridge	Shands Bridge	Acosta Bridge	Buck-man Bridge	Shands Bridge	Acosta Bridge	Buck-man Bridge	Shands Bridge
Correlation Coefficient	0.981	0.970	0.965	0.980	0.973	0.970	0.975	0.967	0.962
Root Mean Square Error	0.084	0.078	0.068	0.071	0.056	0.047	0.076	0.048	0.039
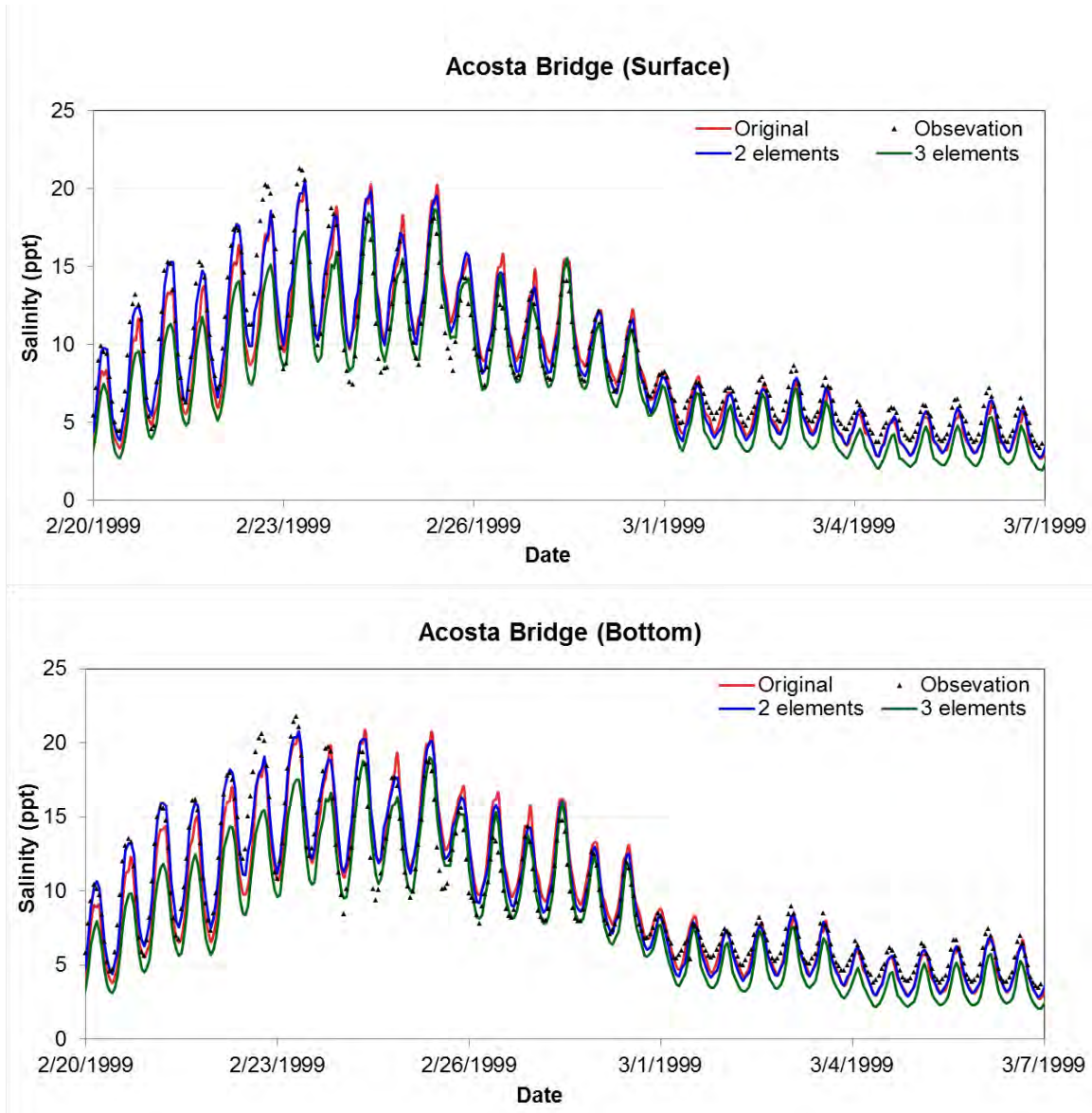
Figure 3.10 Comparison of Salinity at Acosta Bridge from Models with Different Channel Horizontal Elements during Spring Tide
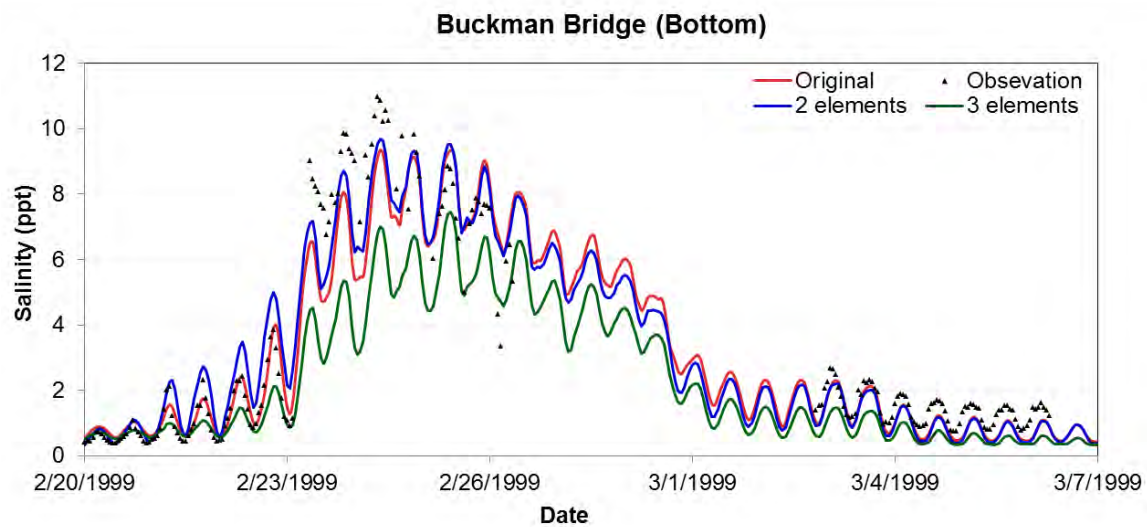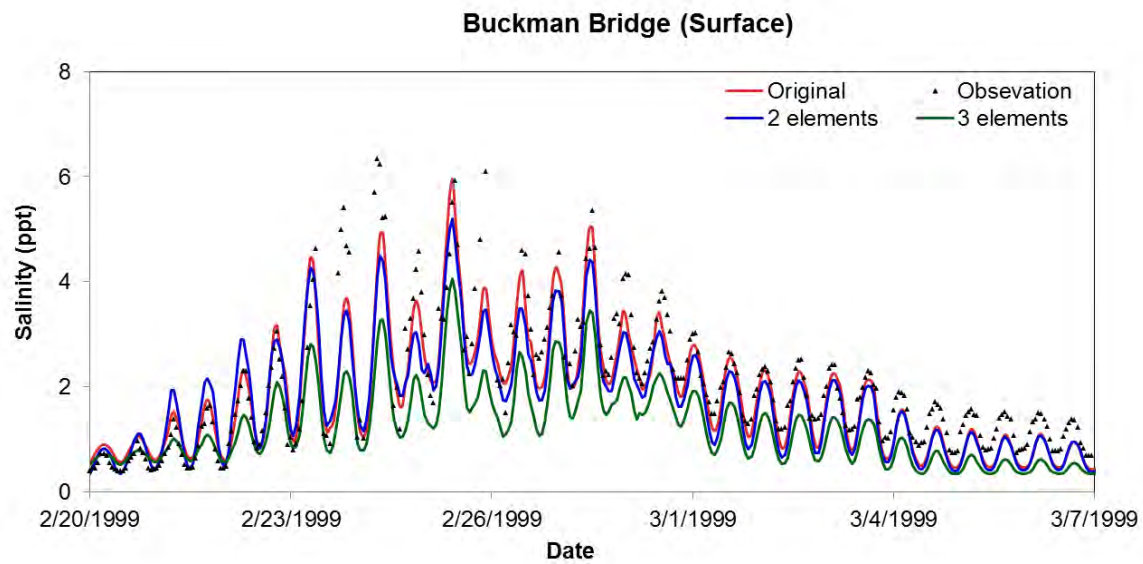
Figure 3.11 Comparison of Salinity at Buckman Bridge from Models with Different Channel Horizontal Elements during Spring Tide
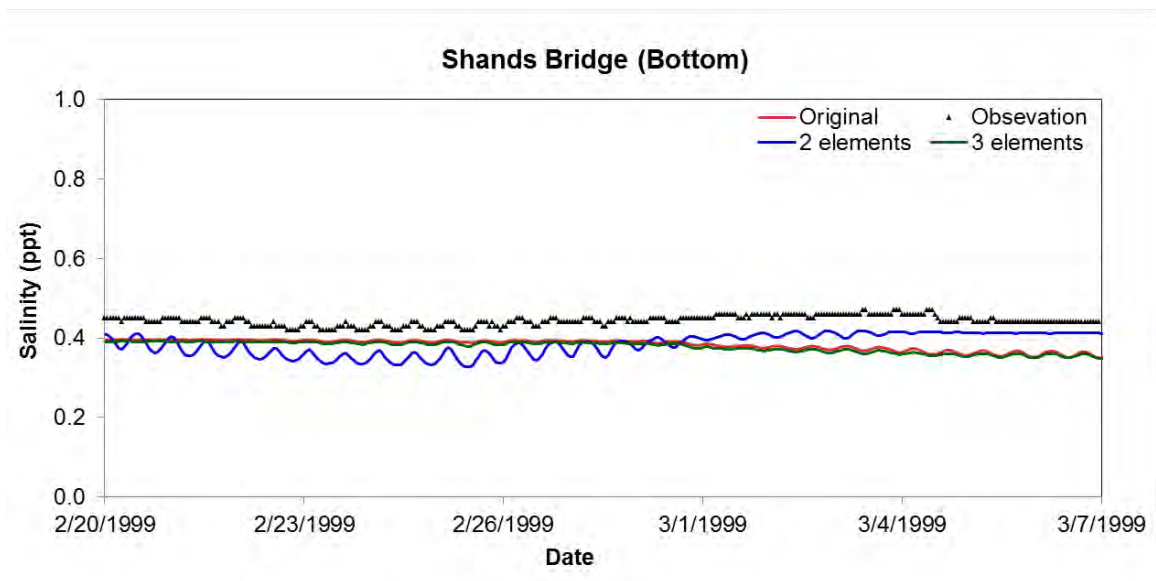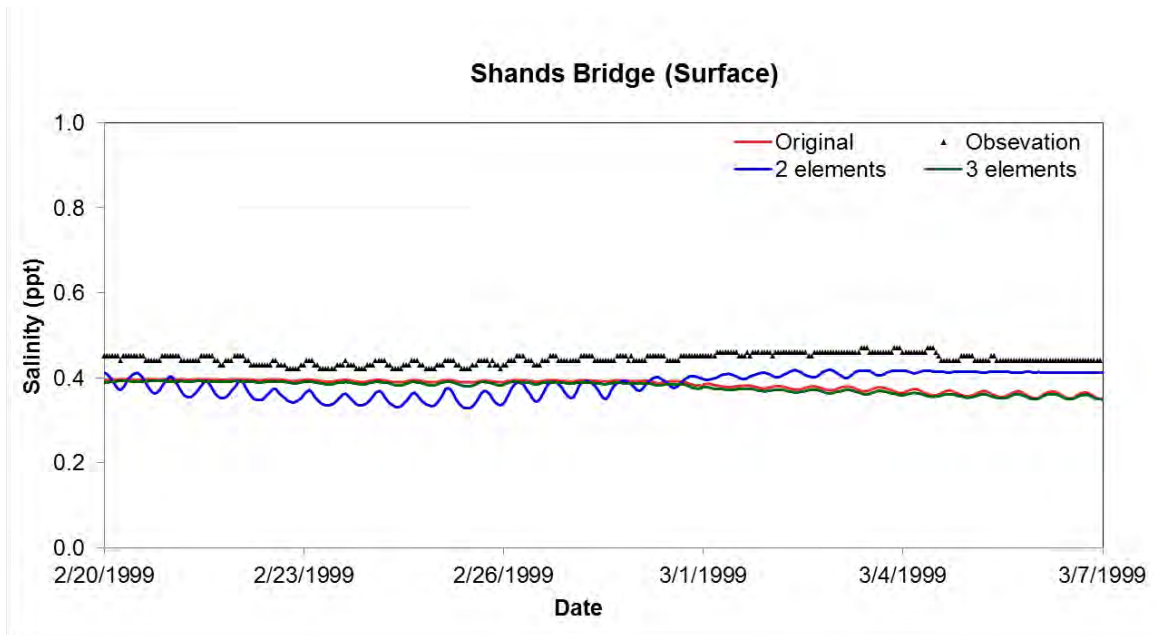
Figure 3.12 Comparison of Salinity at Shands Bridge from Models with Different Horizontal Elements during Spring Tide

Table 3.4 Statistics for Salinity for Mesh Refinement Sensitivity Analysis (1/21/1999 – 3/22/1999)

	Original Model			Two-Element Model			Three-Element Model		
Salinity (Surface)	**Acosta Bridge**	**Buck-man Bridge**	**Shands Bridge**	**Acosta Bridge**	**Buck-man Bridge**	**Shands Bridge**	**Acosta Bridge**	**Buck-man Bridge**	**Shands Bridge**
Correlation Coefficient	0.913	0.850	0.342	0.907	0.883	0.372	0.912	0.750	0.368
Root Mean Square Error	1.550	0.576	0.097	1.829	0.466	0.070	1.784	0.667	0.082
Salinity (Bottom)									
Correlation Coefficient	0.921	0.826	0.315	0.919	0.926	0.406	0.914	0.835	0.336
Root Mean Square Error	1.619	1.134	0.101	1.970	0.820	0.069	1.799	1.099	0.087

4.0   VALIDATION OF HYDRODYNAMIC AND SALINITY MODEL

Validation of the model provides confidence the model accurately simulates its intended parameters and conditions. Model validation comprises two components – calibration and verification. Calibration fine tunes a model to improve estimation of simulated conditions for a specific study domain and period of record. In general, the calibration process is an iterative procedure to select model parameters that improve the accuracy of model outputs, such that model results provide the best comparison with field measured data. Model verification involves model application and comparison of the model results with an independent set of data (not used for model calibration) to make sure that the calibrated model's good performance extends beyond the calibration period. Once calibrated and verified, a numerical model can serve as a reliable tool to simulate changes in modeled processes (e.g., water level and salinity) in the model domain This chapter describes the calibration and verification of the Jacksonville Harbor EFDC model (hereinafter referred to as the USACE model) and the results of the model calibration and verification simulations.

4.1   Model Calibration Methodology

Calibration of the St. Johns River USACE model included qualitative and quantitative comparisons of model results with field measured data. Qualitative comparisons consisted of visual inspections of model results with the data via comparisons of time series plots and spatial graphics of water level and salinity. Visual inspections determined whether the model could reproduce field-measured data in time and space. In contrast, quantitative comparisons used statistical analyses to measure the goodness-of-fit of model results to the data. For the quantitative evaluations of model calibration and verification, this study applied the RMSE and correlation statistical calculations. The RMSE is measure of the size of the discrepancies between model-calculated and field-measured values and provides an indication of model accuracy. The correlation coefficient measures the tendency of the model-calculated and observed values to vary together linearly.

The comparisons of model results first started with comparisons of water levels followed by comparisons with salinity concentration data. Each of these two parameters has its own importance in judging the success of the model calibration. Calibration with water levels improves confidence that the modeling process properly simulates parameters relevant to the driving transport mechanisms such as flow volume and velocity, bed friction, tidal phasing, and hydraulic boundary conditions. A good

calibration with salinity concentration improves confidence that the model properly simulates advection-dispersion processes.

4.2   Hydrodynamic Model Parameters

Frequently adjusted parameters in EFDC modeling setup and calibration include bottom friction, such as the bottom roughness height, and the horizontal momentum diffusion coefficient.

Adjustments to bottom roughness height usually occur before adjustments of horizontal momentum diffusion coefficient during hydrodynamic model calibration. Bottom roughness differs from a friction coefficient because it corresponds to the logarithmic boundary layer roughness height in meters. The solution of momentum equations requires a bottom stress τ_b

$$\tau_b = \rho u_*^2 = c_b \rho U^2 \tag{4.1}$$

where u_* is the friction or shear velocity , c_b is the bottom stress coefficient (friction coefficient), and U is the flow velocity at the bottom layer. Applying a logarithmic distribution of velocity profile between the solid bottom and the middle of the bottom cell layer provides the bottom stress coefficient:

$$c_b = \kappa^2 [\ln(\frac{H}{2z_0^*})]^{-2} \tag{4.2}$$

where z_0^* is the dimensional bottom roughness height , κ is von Karman constant, and H is the height of the bottom layer.

The SJRWMD optimized the bottom roughness height in the LSJR to minimize the difference between observed and simulated harmonic tide given the importance of tidal dynamics to circulation and mixing in this area. Grid cells were grouped into different segments within which bottom roughness was optimized and varied from 3.281 x 10^{-4} to 8.202 x 10^{-2} ft.

The horizontal momentum diffusion coefficient is pre-specified or calculated with the Smagorinsky formula:

$$A_H = C\Delta x\Delta y[(\frac{\partial u}{\partial x})^2 + (\frac{\partial v}{\partial y})^2 + \frac{1}{2}(\frac{\partial u}{\partial y} + \frac{\partial v}{\partial x})^2]^{1/2} \tag{4.3}$$

where C is the horizontal mixing constant, and Δx and Δy are the model grid size in x and y horizontal directions. The Smagorinsky formula links the numerical model's horizontal mixing to current shear and model grid size.

4.3   USACE Model Calibration

The USACE model calibration consisted of model simulations (with one-year model ramp up period) to reflect three hydraulic conditions: wet period (December 1, 1997 – April 1, 1998), dry period (December 1, 1998 – April 1, 1999), and wind condition period (August 1 – December 1, 1996). Calibration consisted of comparisons of model-calculated and measured water levels at five stations – Bar Pilot Dock, Long Branch, Main Street Bridge, Buckman Bridge, and Shands Bridge (Figure 4.1) and comparisons of model-calculated and measured salinity at four stations – Dames Point, Acosta Bridge, Buckman Bridge, and Shands Bridge (Figure 4.2).

The abovementioned stations provide continuous records of measured water level or salinity. The SJRWMD provided all the measured water level and salinity hourly data in 1995 – 2005 in cooperation with the Florida Department of Environmental Protection (FDEP) and the U.S. Geological Survey (USGS). For water level data, the FDEP measures water level at six-minute intervals at these five stations. This water level network began in early 1995 as a cooperative effort between FDEP, National Oceanic and Atmospheric Administration (NOAA), and SJRWMD to provide continuous water level data for the total maximum daily loads (TMDL) modeling study (Sucsy and Morris, 2002). Salinity data came from the U.S. Geological Survey (USGS), which monitors salinity at hourly intervals at the four stations in the Lower St. Johns River. This salinity network began in the early 1995 as a joint effort between USGS and SJRWMD to provide continuous salinity data for the TMDL modeling study.

The initial model calibration considered three model calibration conditions (e.g., wet, dry, wind conditions) separately and applied different sets of model parameters to get the best result for each condition. The final calibration process consisted of selecting one set of model parameters appropriate for all three conditions. Figure 4.3 shows the final calibrated bottom roughness height. The following sections describe the final calibration and verification results.
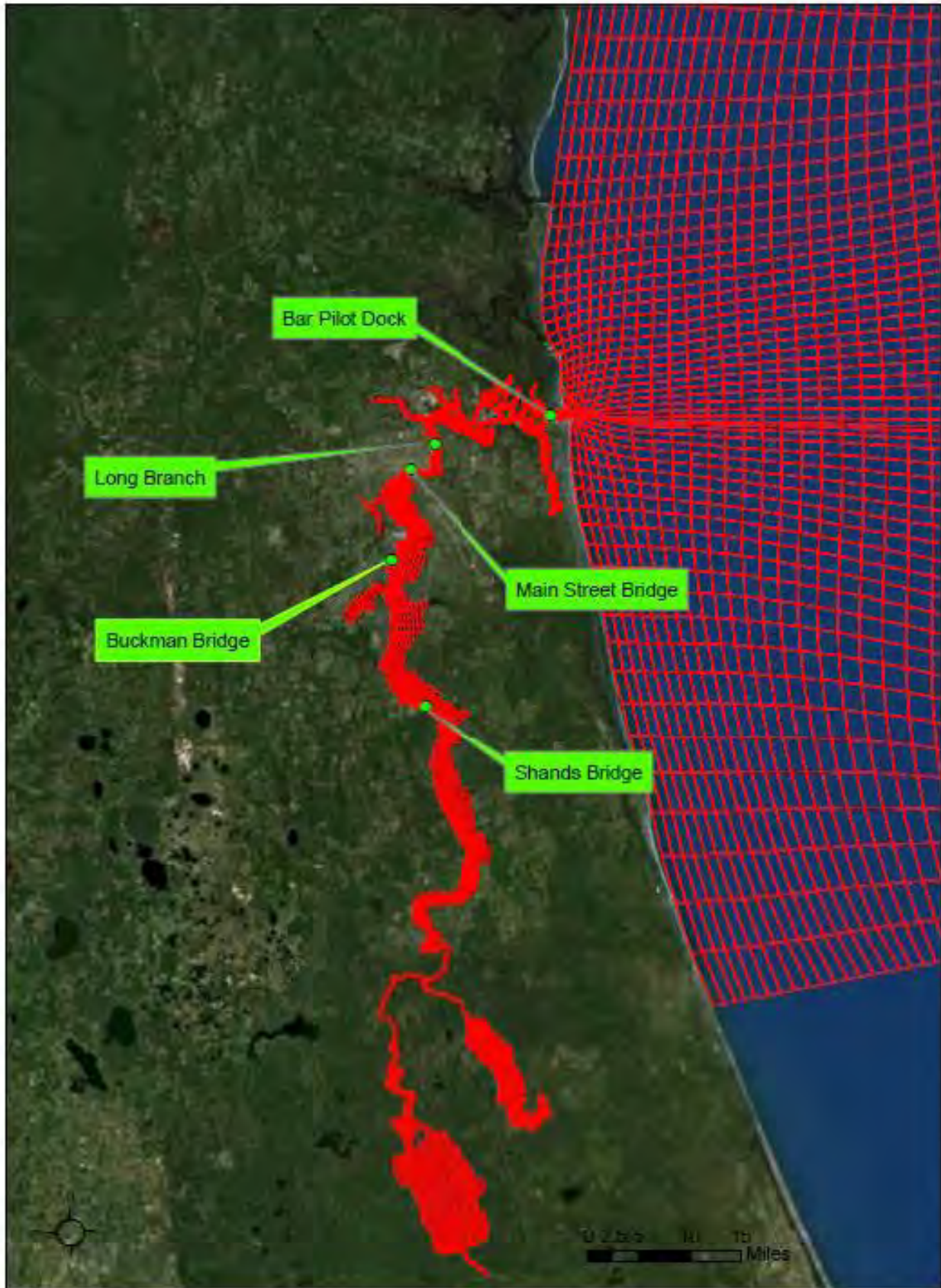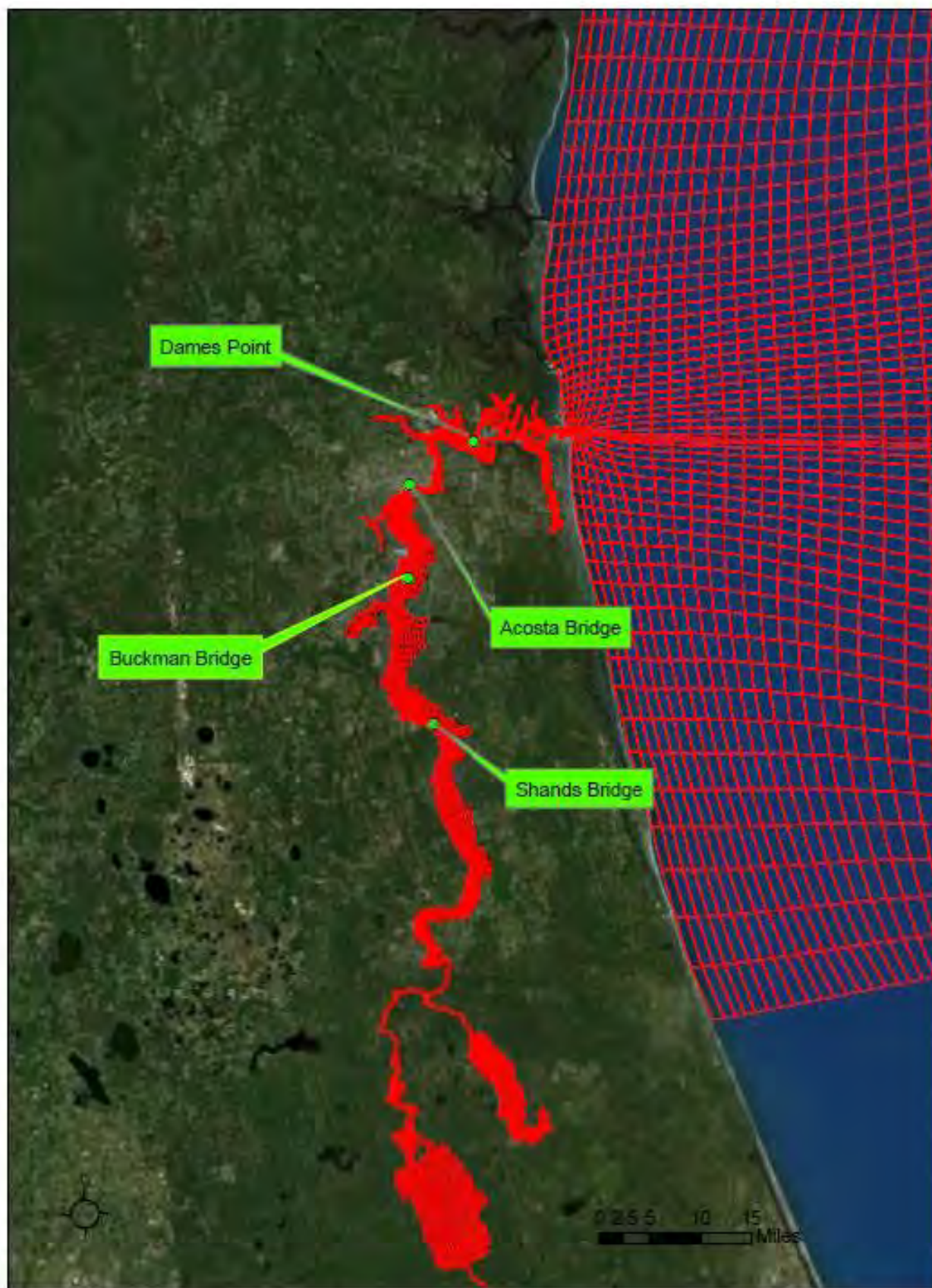
Figure 4.1 Locations of Water Level Stations
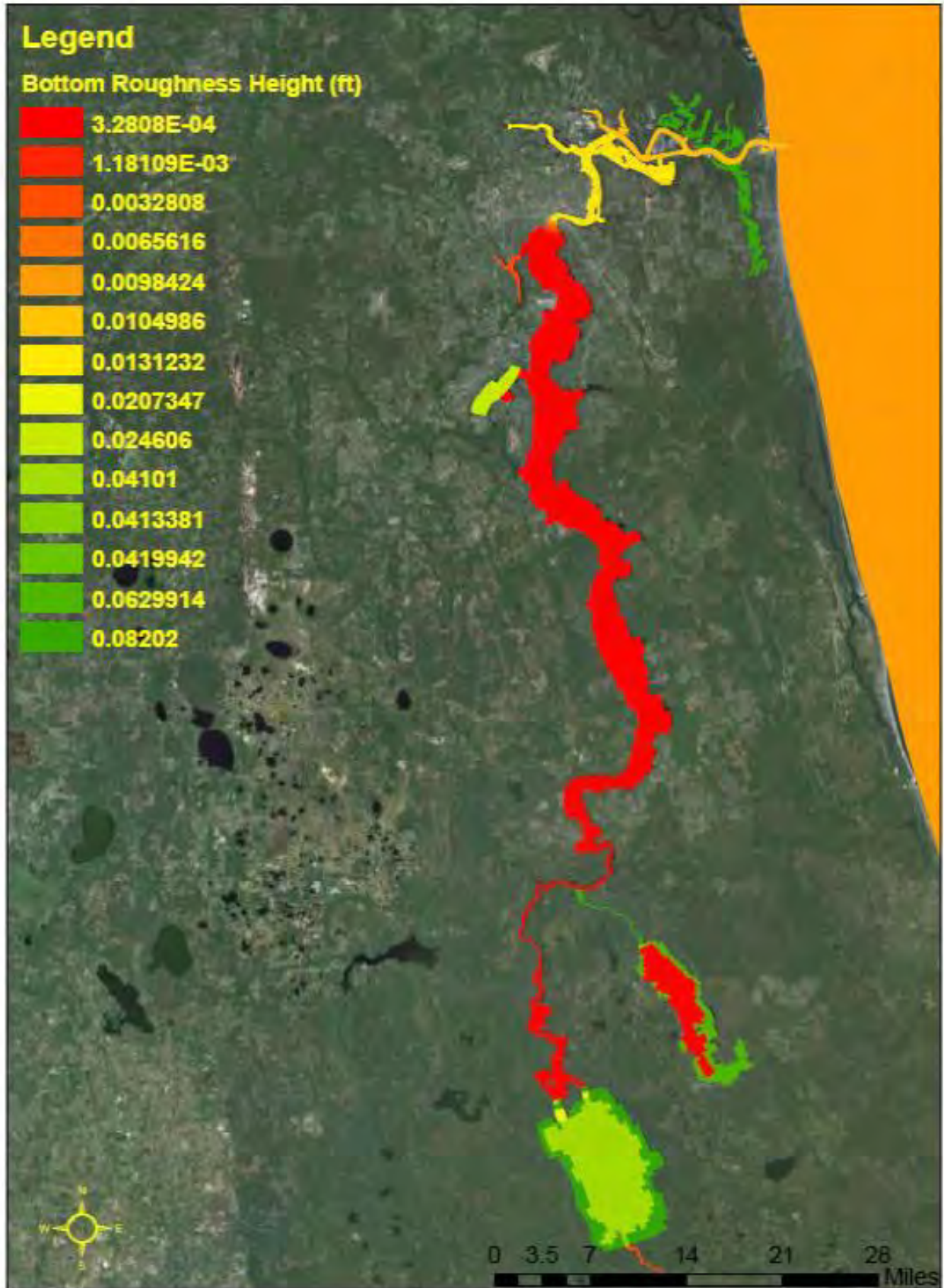
Figure 4.2 Locations of Salinity Stations

Figure 4.3 EFDC Model Bottom Roughness Height

4.3.1   *Water Surface Level Calibration*

Comparisons of simulated and measured hourly water levels at the five water level stations along the Lower St. Johns River provided the means to evaluate model performance of the USACE model during the water level calibration period. Figure 4.4 – Figure 4.18 show the comparison plots and Table 4.1 – Table 4.3 provide the RMSE and correlation coefficients of simulated and measured hourly water levels for each of the water surface stations for the wet, dry, and wind condition calibration periods. Visual observation of the figures and examination of the statistical results show that the model accurately represents the tidal propagation from near the river mouth (Bar Pilot Dock), through the navigation channel (Long Branch Station and Main Street Bridge), to the middle of the Lower St. Johns River at Shands Bridge.

To discern tidal periods in the plot, a one-month period from each calibration condition was selected to show the observed and simulated time-series of water level. The graphs show that semidiurnal tides dominate water levels although lower frequency variability occurs, especially during the dry season, when the influence from freshwater inflow weakens. Root mean square errors (RMSE) are less than 0.310 ft and the correlation coefficient R is greater than 0.970 at all stations. The correlation coefficient generally decreases from downstream to upstream. Overall, the comparisons show good agreement between the measured and simulated water surface level for all three conditions.
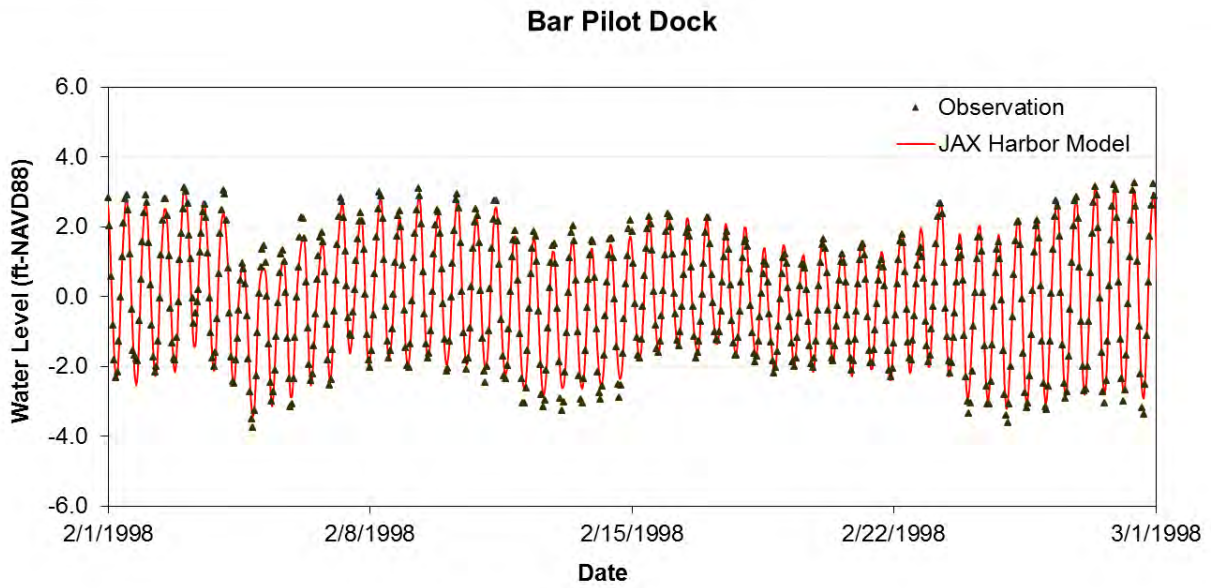
Figure 4.4 Comparison of Computed and Observed Water Levels during a Portion of the Wet Period Calibration (Bar Pilot Dock)
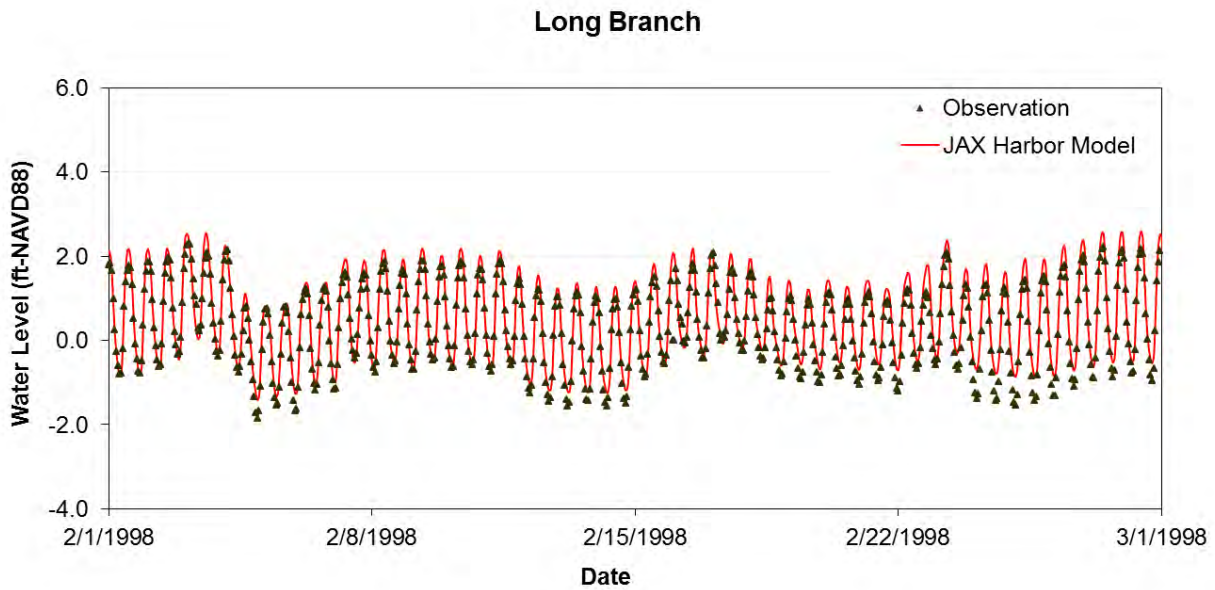
Figure 4.5 Comparison of Computed and Observed Water Level during a Portion of the Wet Period Calibration (Long Branch)

Figure 4.6 Comparison of Computed and Observed Water Level during a Portion of the Wet Period Calibration (Main Street Bridge)

Figure 4.7 Comparison of Computed and Observed Water Level during a Portion of the Wet Period Calibration (Buckman Bridge)

Figure 4.8 Comparison of Computed and Observed Water Level during a Portion of the Wet Period Calibration (Shands Bridge Station)

Table 4.1 Statistics for Water Level for Wet Period Model Calibration (12/1/1997 – 4/1/1998)

| Station / Parameters	Bar Pilot Dock	Long Branch Station	Main Street Bridge	Buckman Bridge	Shands Bridge
Correlation Coefficient, R	0.990	0.982	0.980	0.975	0.970
Root Mean Square Error, RMSE (ft)	0.282	0.282	0.310	0.281	0.299
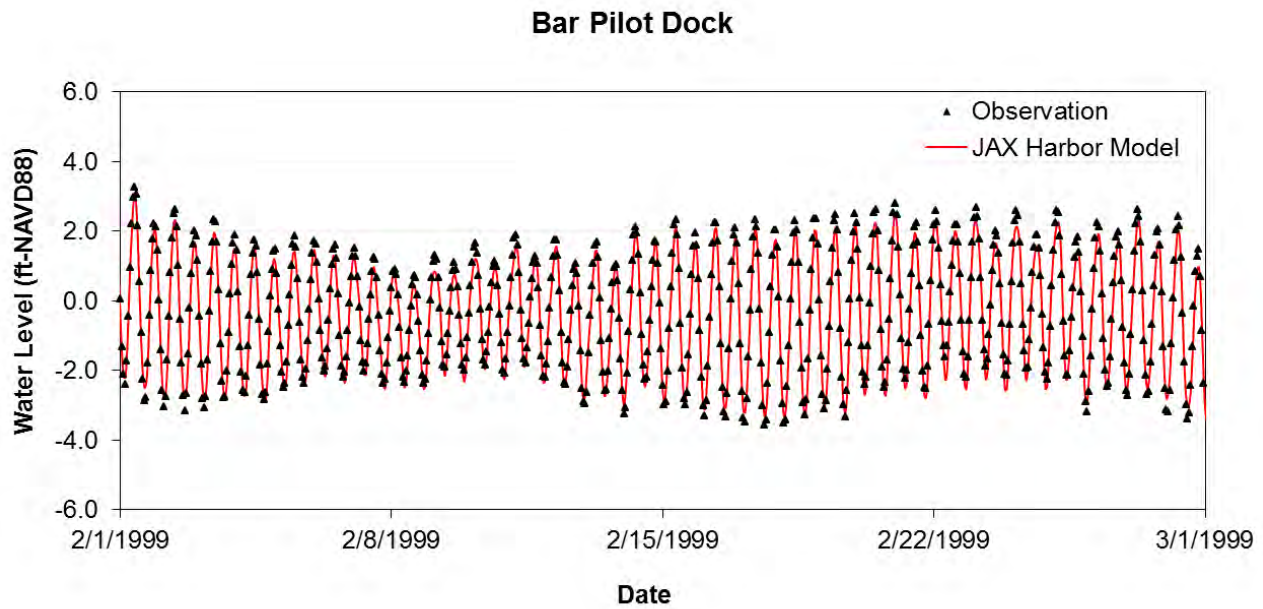
Figure 4.9 Comparison of Computed and Observed Water Levels during a Portion of the Dry Period Calibration (Bar Pilot Dock)
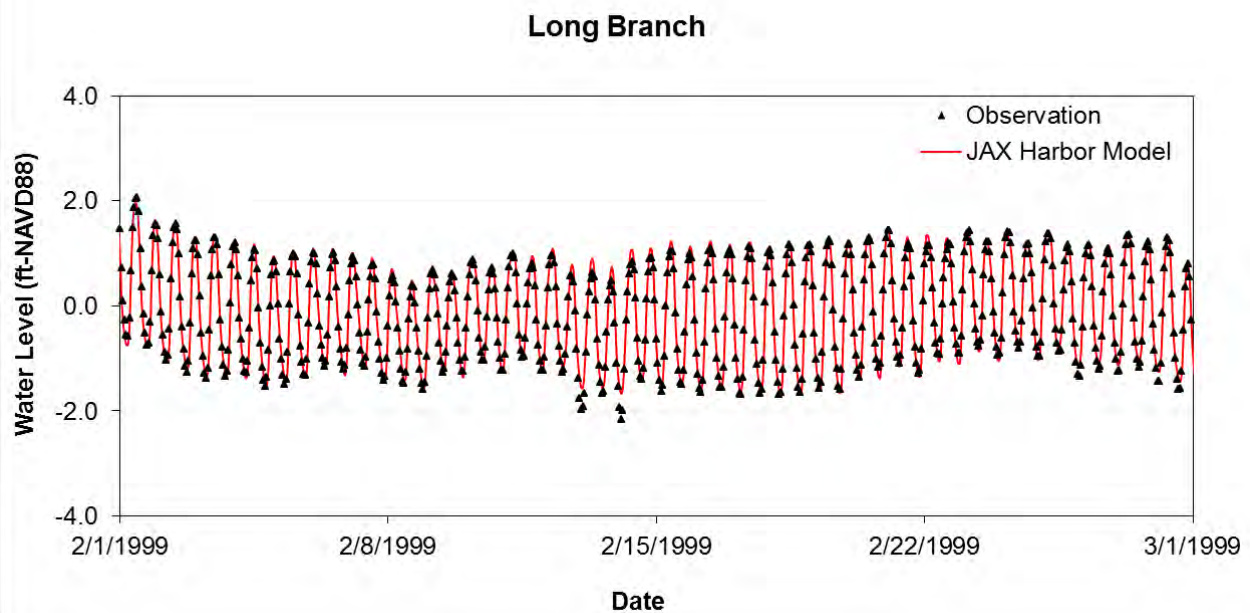
Figure 4.10 Comparison of Computed and Observed Water Levels during a Portion of the Dry Period Calibration (Long Branch)
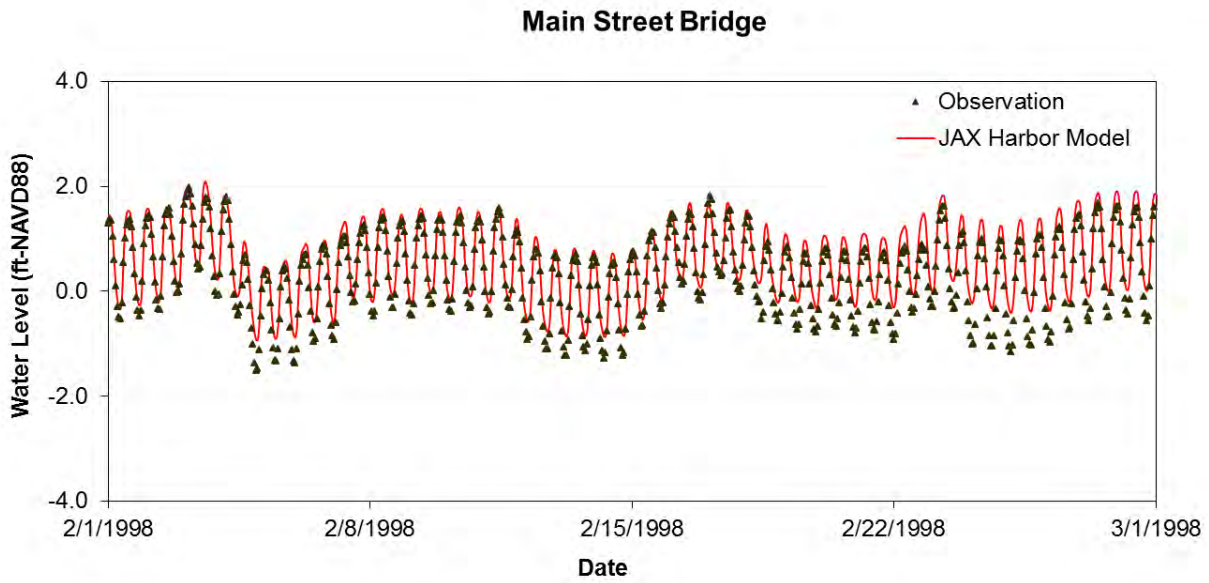
Figure 4.11 Comparison of Computed and Observed Water Levels during a Portion of the Dry Period Calibration (Main Street Bridge)
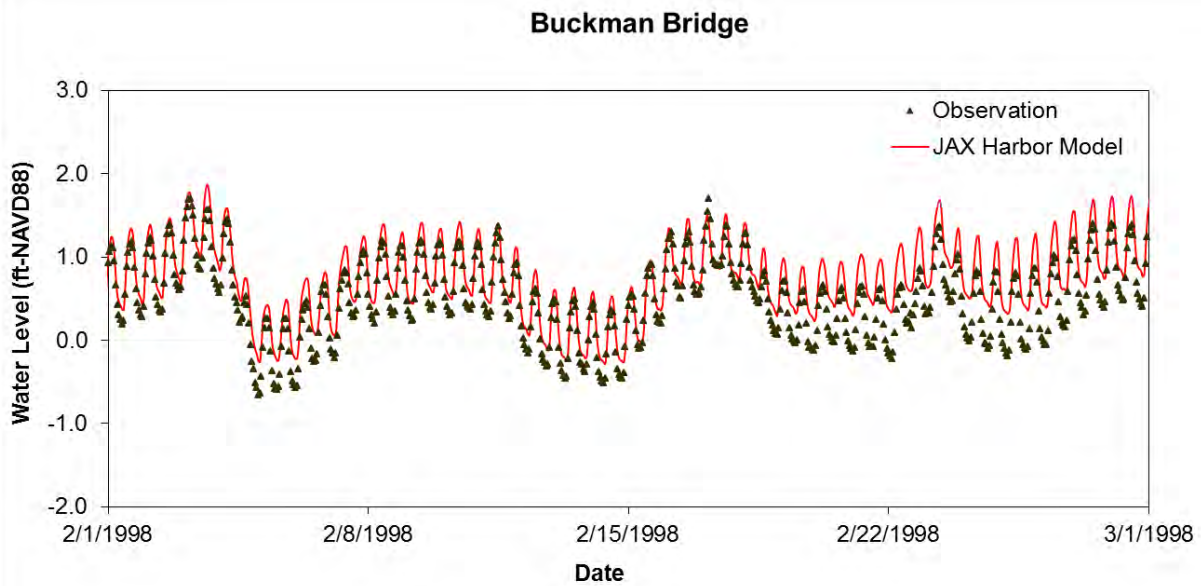

Figure 4.12 Comparison of Computed and Observed Water Levels during a Portion of the Dry Period Calibration (Buckman Bridge)
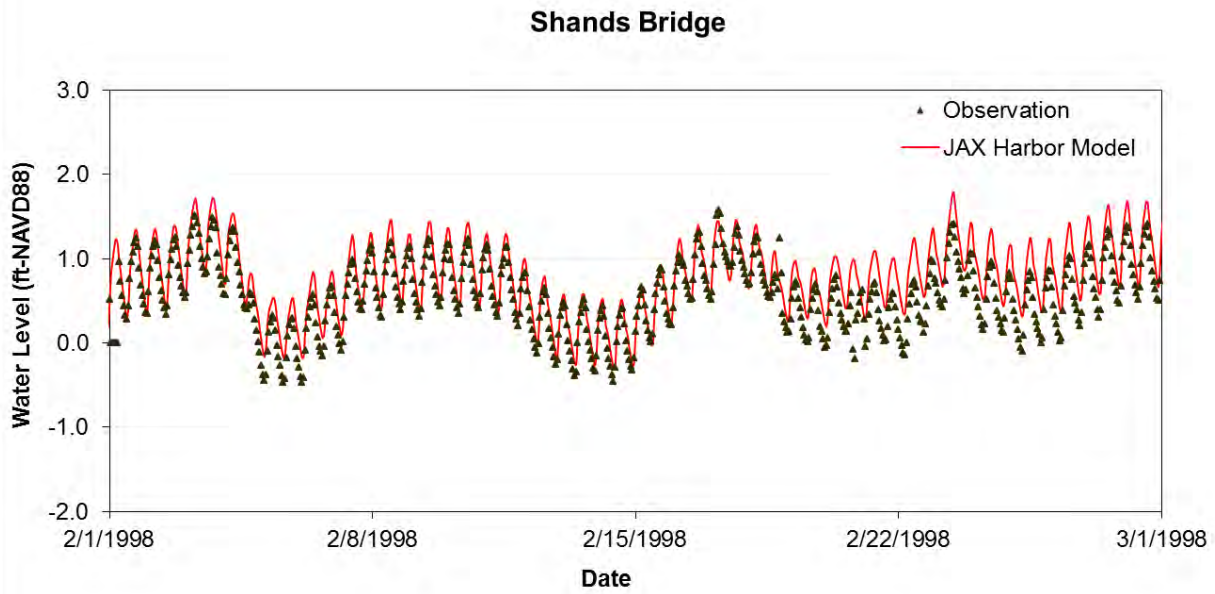
Figure 4.13 Comparison of Computed and Observed Water Levels during a Portion of the Dry Period Calibration (Shands Bridge)

Table 4.2 Statistics for Water Level for Dry Period Model Calibration (12/1/1998 – 4/1/1999)

| Station / Parameters	Bar Pilot Dock	Long Branch Station	Main Street Bridge	Buckman Bridge	Shands Bridge
Correlation Coefficient, R	0.992	0.989	0.987	0.976	0.974
Root Mean Square Error, RMSE (ft)	0.290	0.149	0.141	0.136	0.109

37
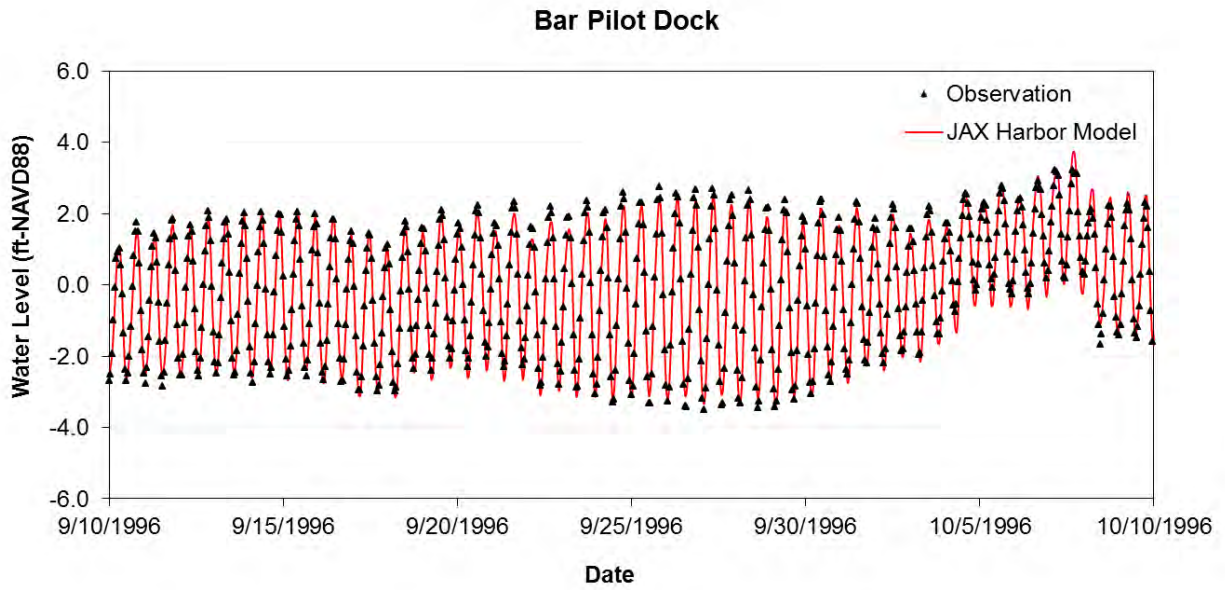
Figure 4.14 Comparison of Computed and Observed Water Levels during a Portion of the Wind Calibration Period (Bar Pilot Dock)
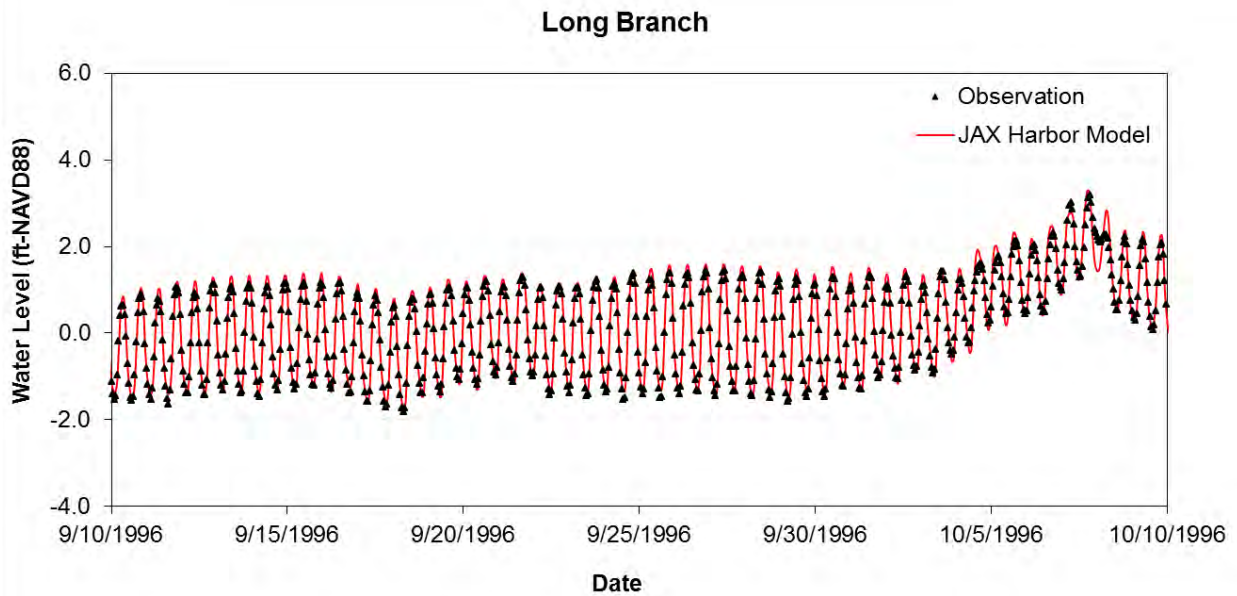
Figure 4.15 Comparison of Computed and Observed Water Levels during a Portion of the Wind Calibration Period (Long Branch)
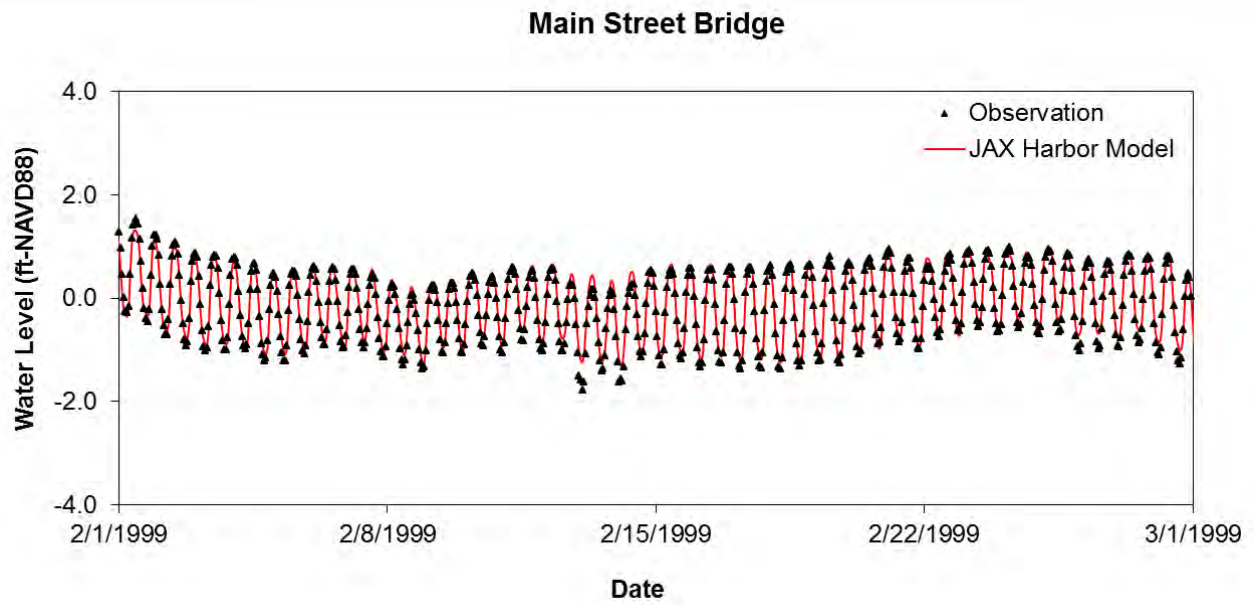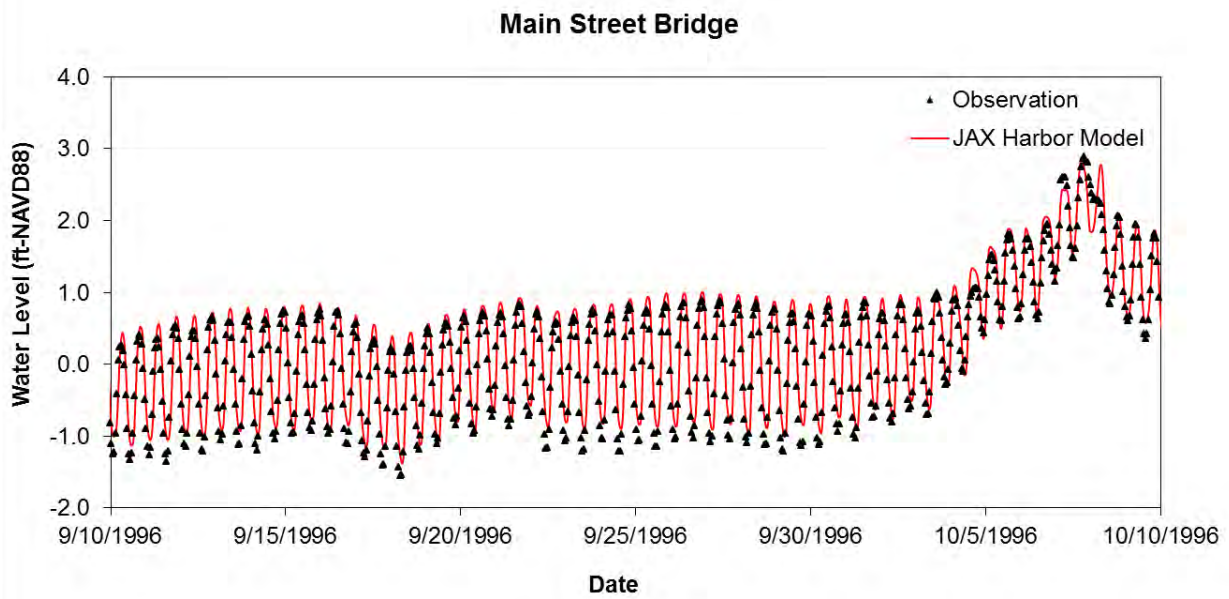
Main Street Bridge

Figure 4.16 Comparison of Computed and Observed Water Levels during a Portion of the Wind Calibration Period (Main Street Bridge)
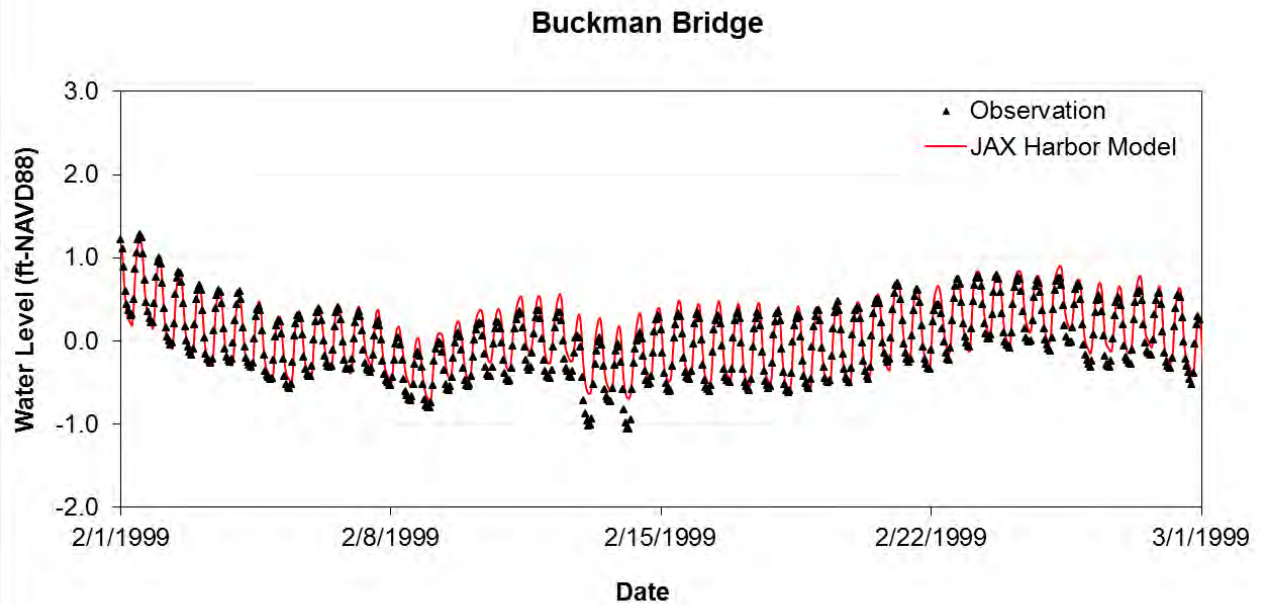
Buckman Bridge

Figure 4.17 Comparison of Computed and Observed Water Levels during a Portion of the Wind Calibration Period (Buckman Bridge)
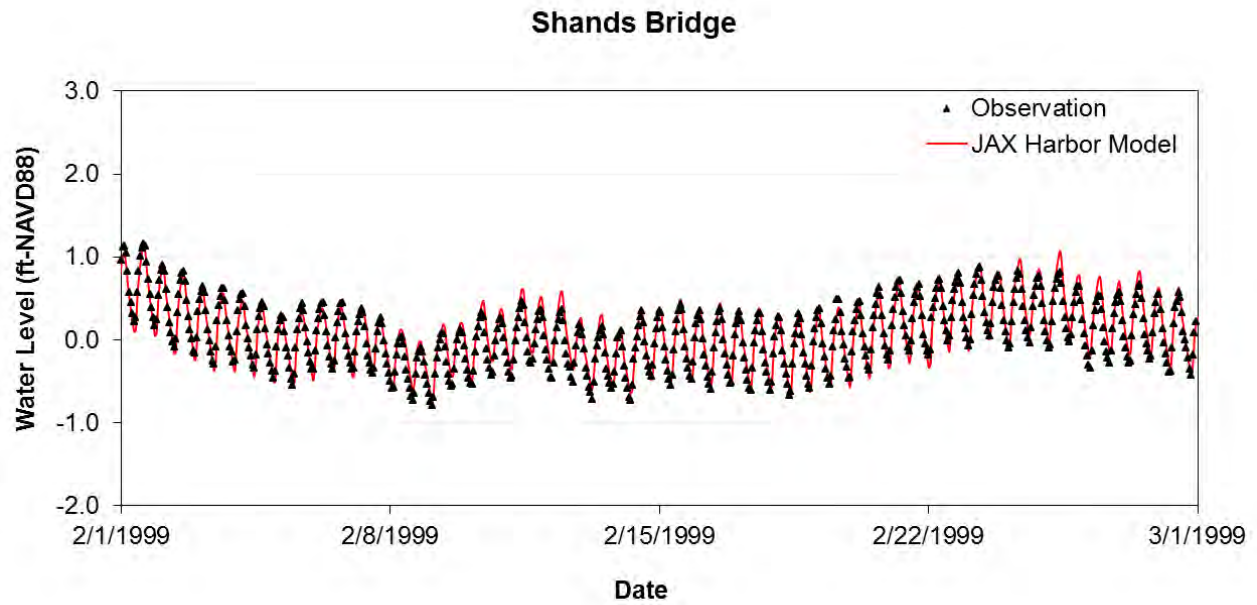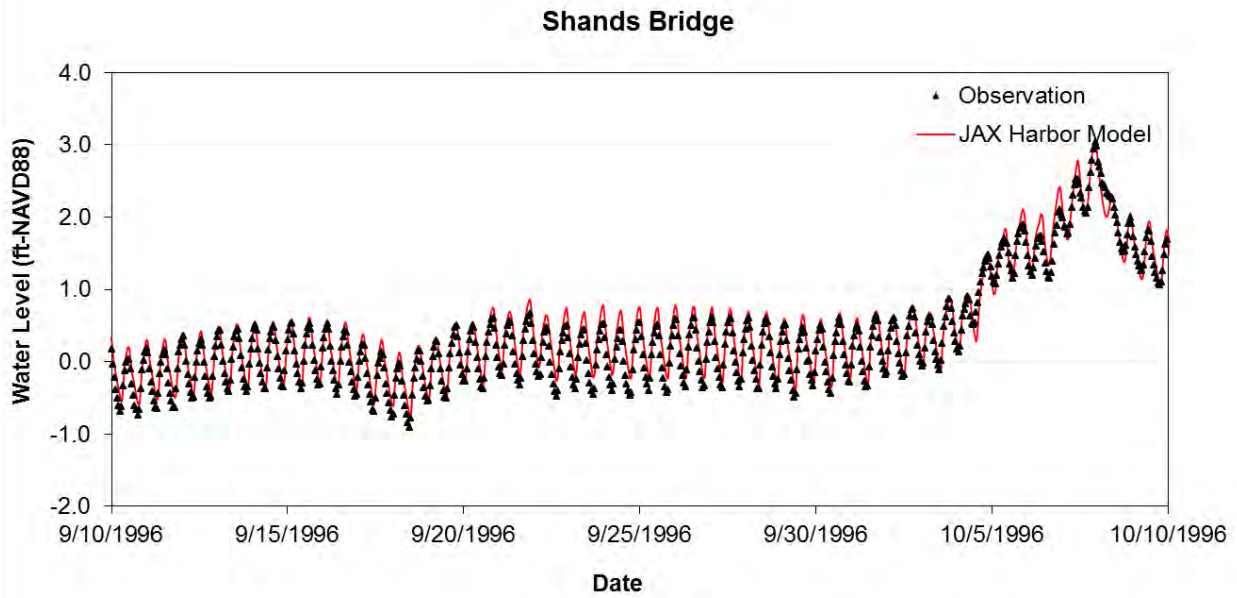
Figure 4.18 Comparison of Computed and Observed Water Levels during a Portion of the Wind Calibration Period (Shands Bridge)

Table 4.3 Statistics for Water Level for Wind Condition Period Model Calibration (8/1/1996 –12/1/1996)

Station / Parameters	Bar Pilot Dock	Long Branch Station	Main Street Bridge	Buckman Bridge	Shands Bridge
Correlation Coefficient, R	0.991	0.985	0.984	0.986	0.989
Root Mean Square Error, RMSE (ft)	0.257	0.195	0.184	0.171	0.156

4.3.2   Salinity Calibration

As a conservative constituent, salinity provides a means to assess the integration of all forces that drive the transport, circulation, and mixing processes. Additionally, salinity is a critical factor affecting the marine environment in estuaries. Thus, accurate simulation of salinity is critical to this study as the USACE model will serve to evaluate the response of salinity transport to channel deepening. Comparisons of observed and simulated hourly salinity at four stations (Dames Point, Acosta Bridge, Buckman Bridge and Shands Bridge) along the Lower St. Johns River provide the means to evaluate model performance during the salinity calibration period.

Figure 4.19 – Figure 4.30 show the comparison plot of the one-month simulation (chosen to discern tidal variability in plots) for the wet, dry, and wind condition calibration periods. Notably, only five days of observation data are available for Dames Point during the wet period calibration. Table 4.4 – Table 4.6 provide statistical comparisons of simulated and measured hourly salinity. The tables provide the RMSE and correlation coefficient at each station.

The plots of hourly salinity illustrate the high correlation of salinity variability with tide for stations downstream of Buckman Bridge. During certain dry periods, both Shands Bridge and Buckman Bridge salinity also follows a tidal signature. The signature follows the tides semi-diurnal frequency as well as the neap to spring cycles. For example, Figure 4.25 shows the daily salinity range at Buckman fell to about 0.5 ppt during the week of February 17, 1999 but exceeded 4 ppt during the week of February 25, 1999. In contrast, essentially no tidal signature is apparent in the salinity range at Shands Bridge during the wet periods. At Shands Bridge, the lack of correlation is due to the very low tidal influence and slight horizontal gradients of salinity from larger freshwater flows. Notably, simulating low salinities at locations far away from the source (ocean) is very difficult. Inaccurate estimates of freshwater flows can also account for the isolated poor comparison of modeled salinity to data. The bottom salinity comparison shown in Figure 4.25 likely exhibit this case on February 25, 1999 when model input lateral inflow may have been less than actual inflow. Overall, visual observation of figures and examination of the statistical results show generally good agreement between the measured and simulated salinity.
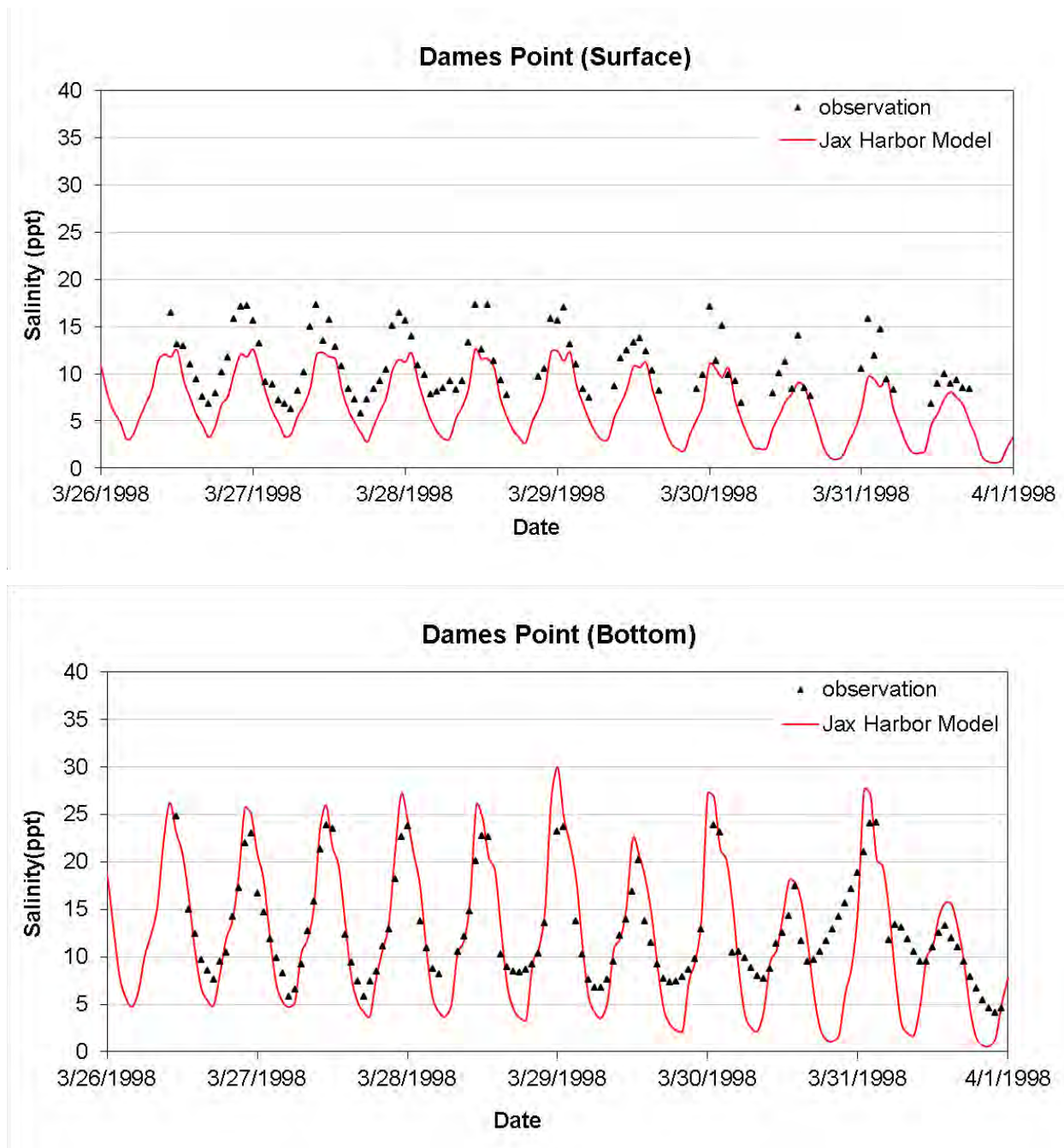
Figure 4.19 Comparison of Computed and Observed Salinity during a Portion of the Wet Period Calibration (Dames Point)

Figure 4.20 Comparison of Computed and Observed Salinity during a Portion of the Wet Period Calibration (Acosta Bridge)
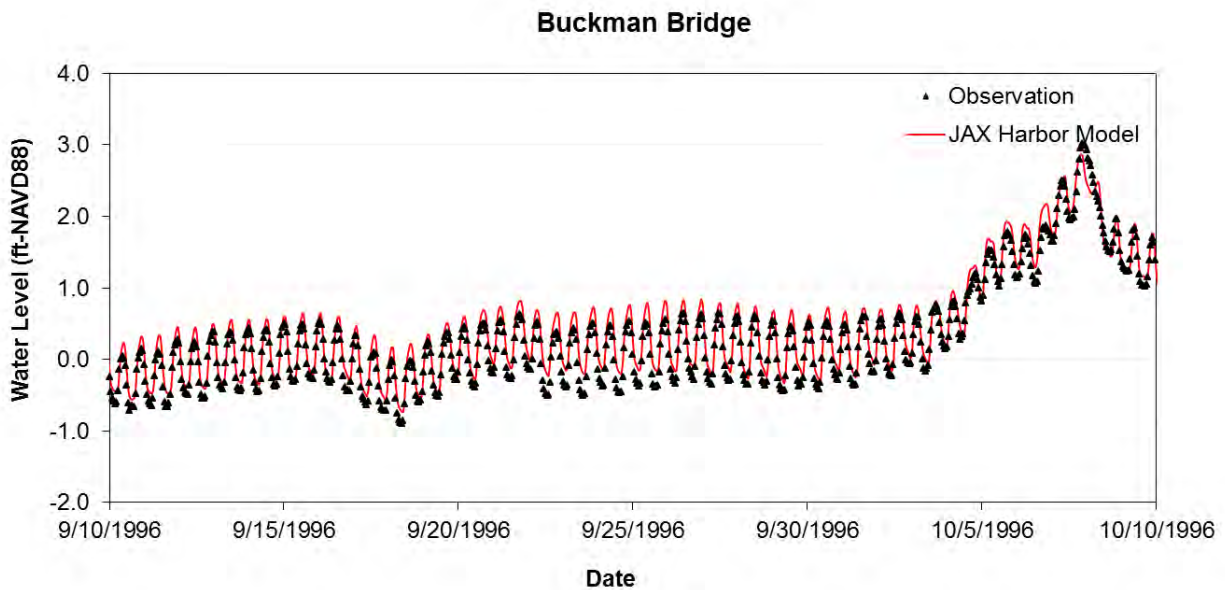
Figure 4.21 Comparison of Computed and Observed Salinity during a Portion of the Wet Period Calibration (Buckman Bridge)

Figure 4.22 Comparison of Computed and Observed Salinity during a Portion of the Wet Period Calibration (Shands Bridge)

Table 4.4 Model Calibration Statistics for Salinity during Wet Period (12/1/1997 – 4/1/1998)

| Station / Parameters	Dames Point	Acosta Bridge	Buckman Bridge	Shands Bridge
Surface				
Correlation Coefficient, R	0.873	0.957	0.927	0.916
Root Mean Square Error, RMSE (ppt)	3.468	0.410	0.024	0.022
Bottom				
Correlation Coefficient, R	0.878	0.953	0.926	0.916
Root Mean Square Error, RMSE (ppt)	3.971	0.533	0.024	0.022

Figure 4.23 Comparison of Computed and Observed Salinity during a Portion of the Dry Period Calibration (Dames Point)
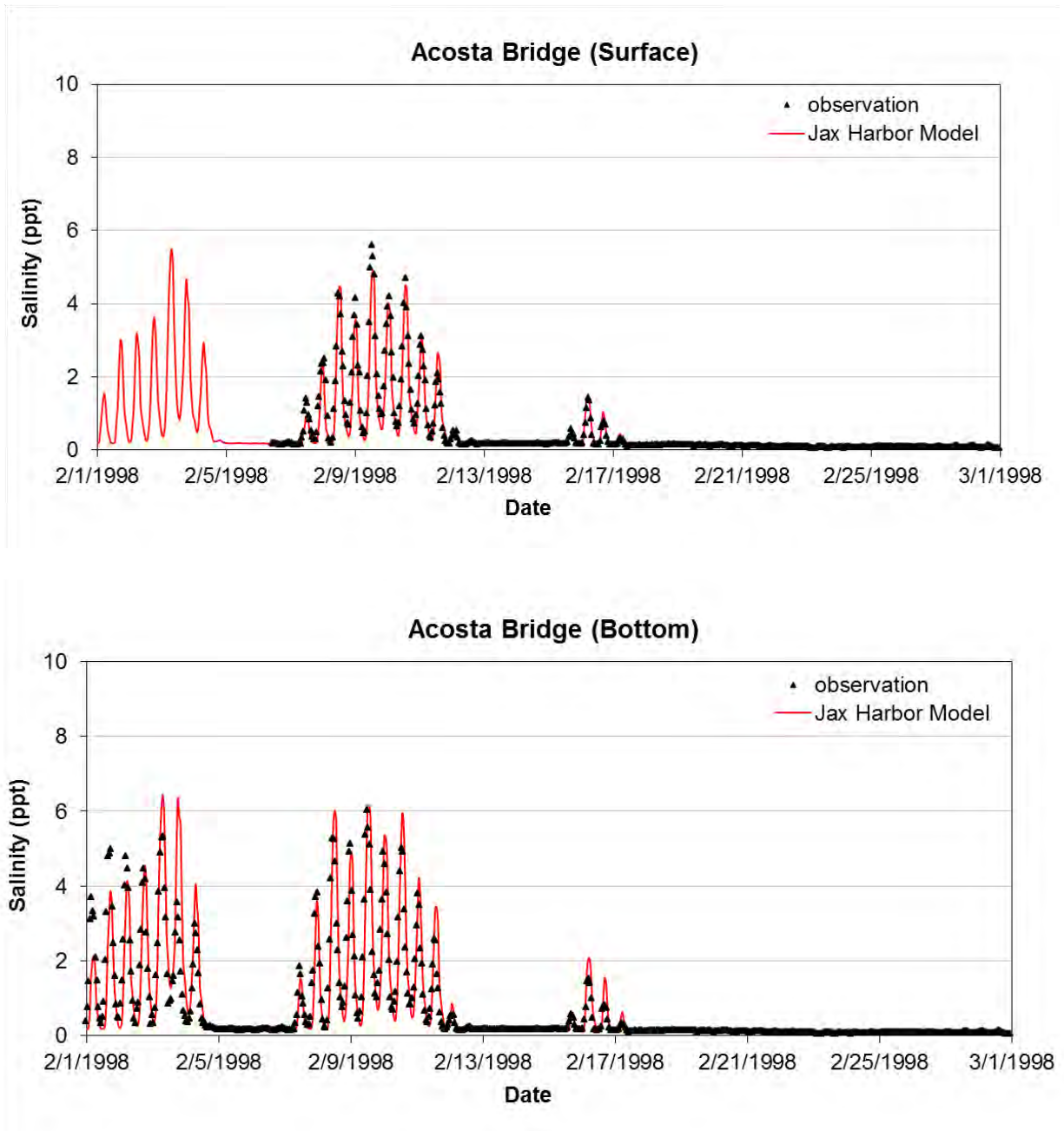
Figure 4.24 Comparison of Computed and Observed Salinity during a Portion of the Dry Period Calibration (Acosta Bridge)
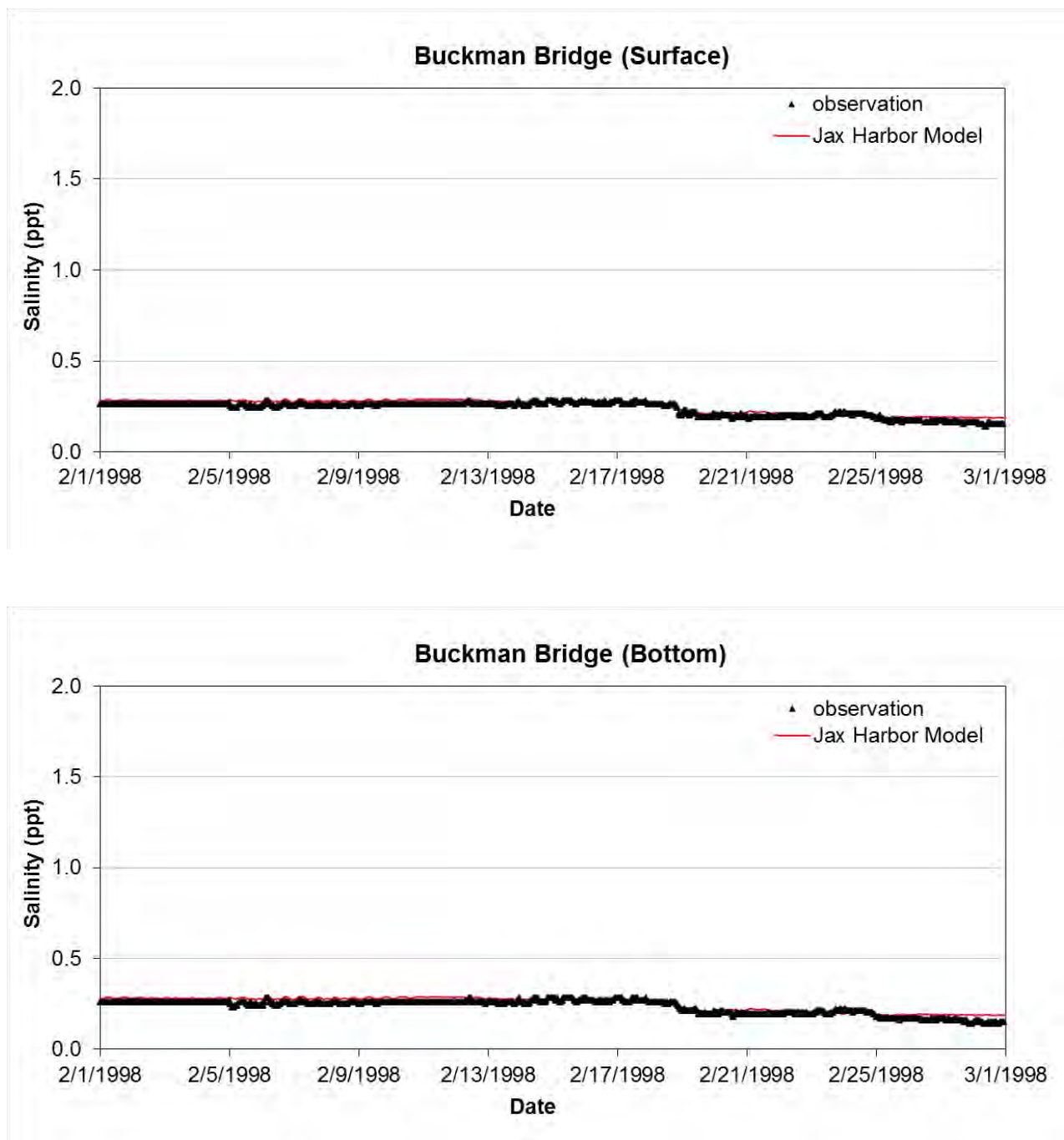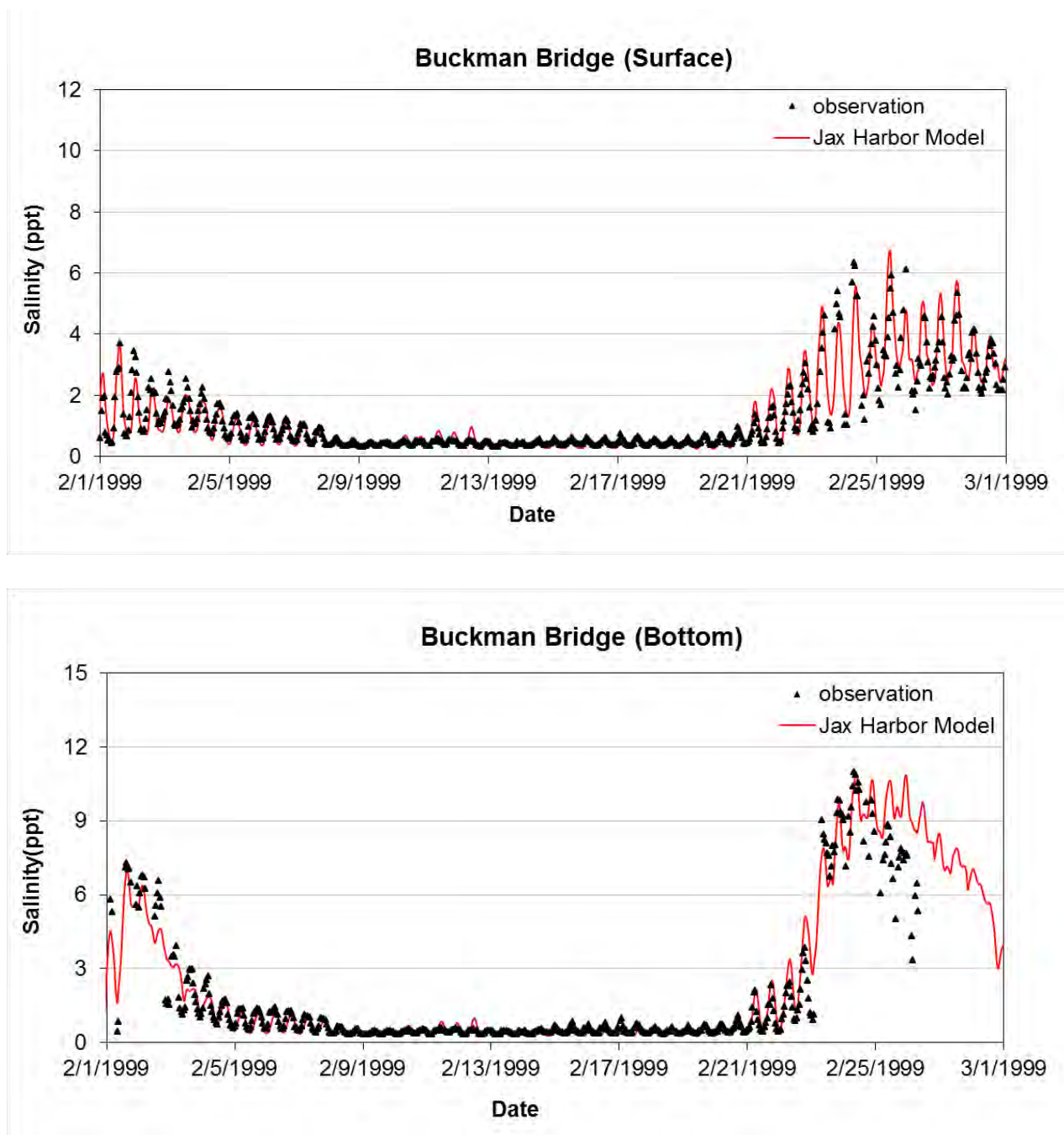
Figure 4.25 Comparison of Computed and Observed Salinity during Dry Period Calibration (Buckman Bridge)
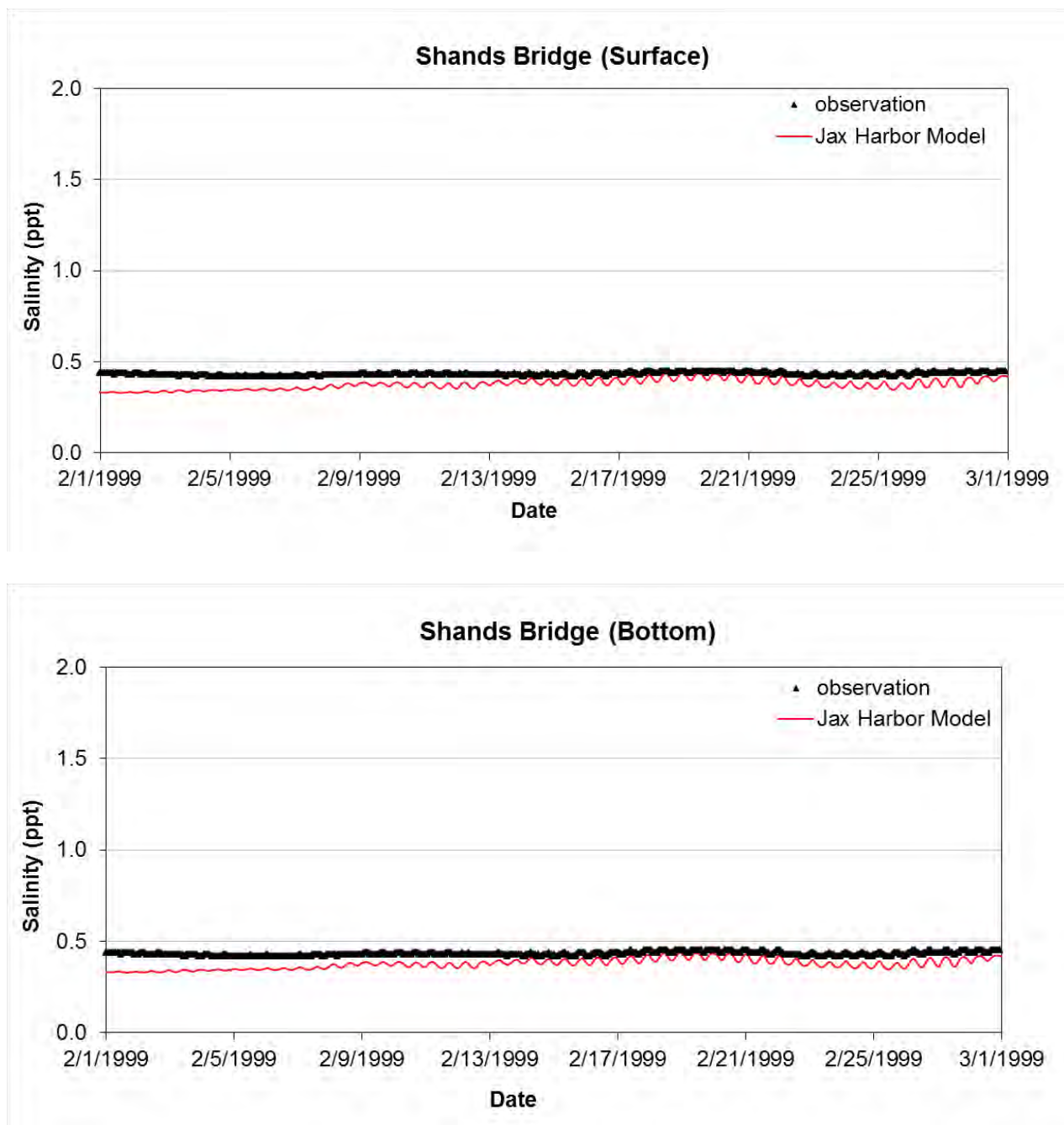
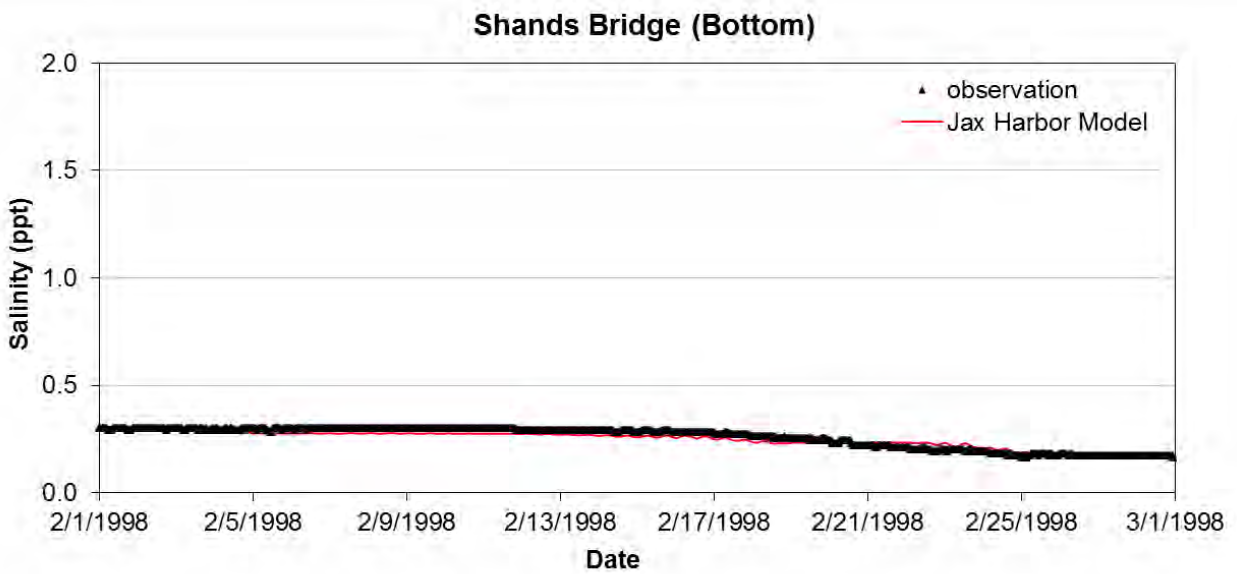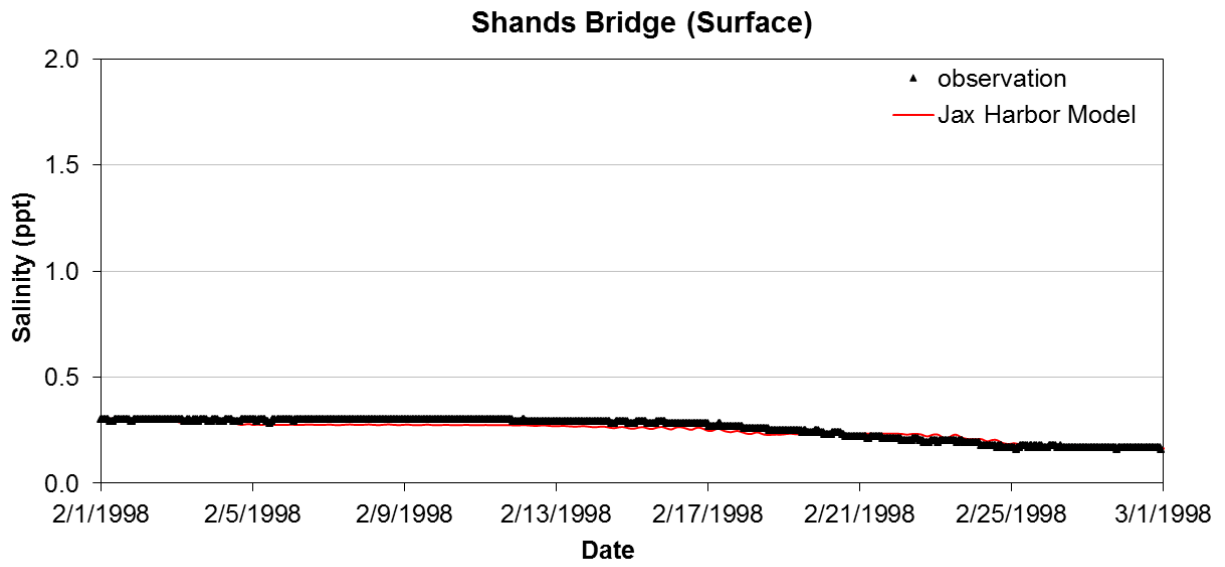**Figure 4.26** Comparison of Computed and Observed Salinity during Dry Period Calibration (Shands Bridge)

Table 4.5 Model Calibration Statistics for Salinity during Dry Period (12/1/1998 – 4/1/1999)

Parameters \ Station	Dames Point	Acosta Bridge	Buckman Bridge	Shands Bridge
Surface				
Correlation, R Coefficient	0.875	0.943	0.902	0.276
Root Mean Square Error (ppt), RMSE	2.204	1.649	0.555	0.078
Bottom				
Correlation, R Coefficient	0.832	0.943	0.845	0.280
Root Mean Square Error (ppt), RMSE	3.238	2.499	1.456	0.077

Figure 4.27 Comparison of Computed and Observed Salinity during a Portion of the Wind Condition Calibration Period (Dames Point)

Figure 4.28 Comparison of Computed and Observed Salinity during a Portion of the Wind Condition Calibration Period (Acosta Bridge)
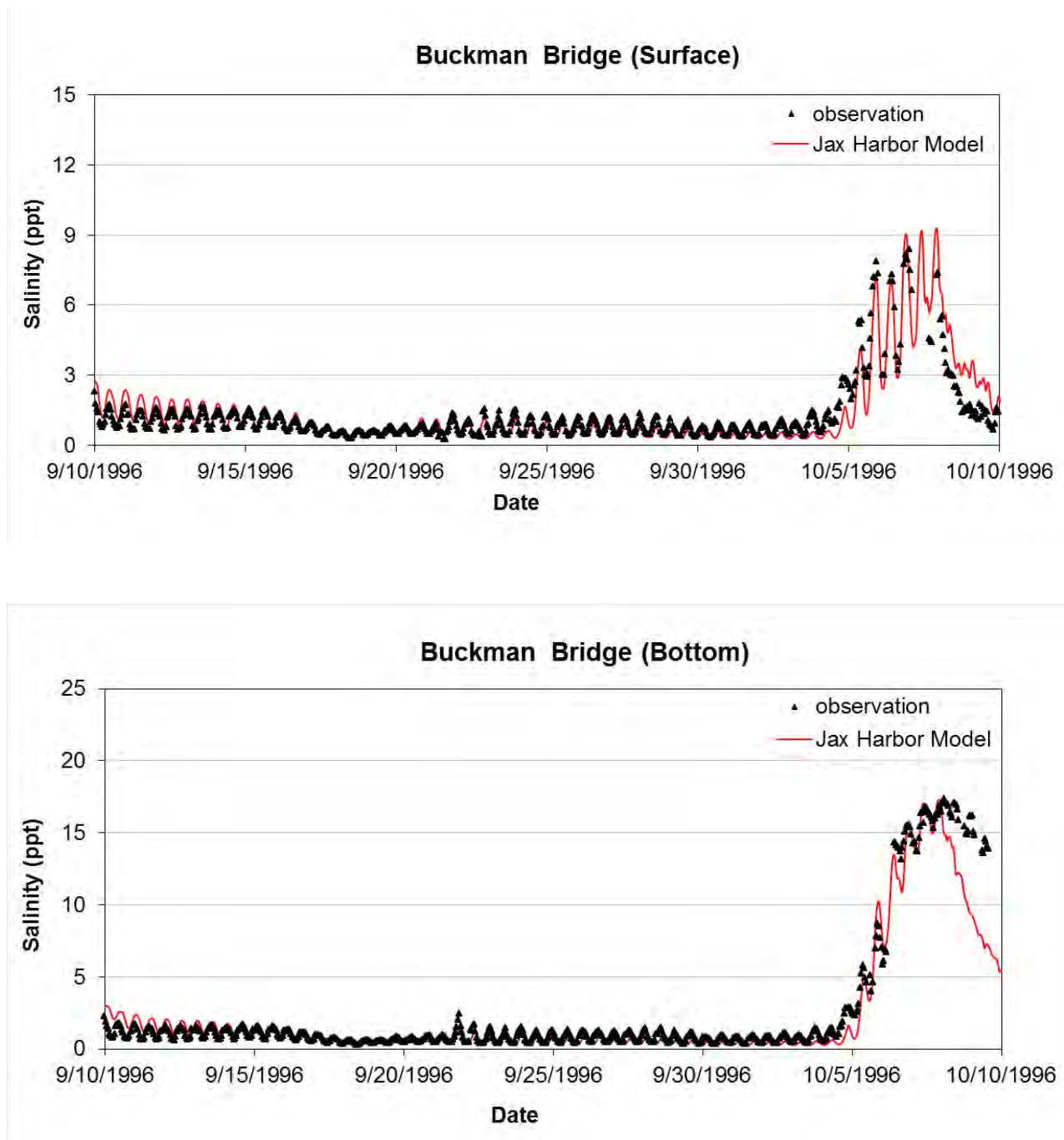
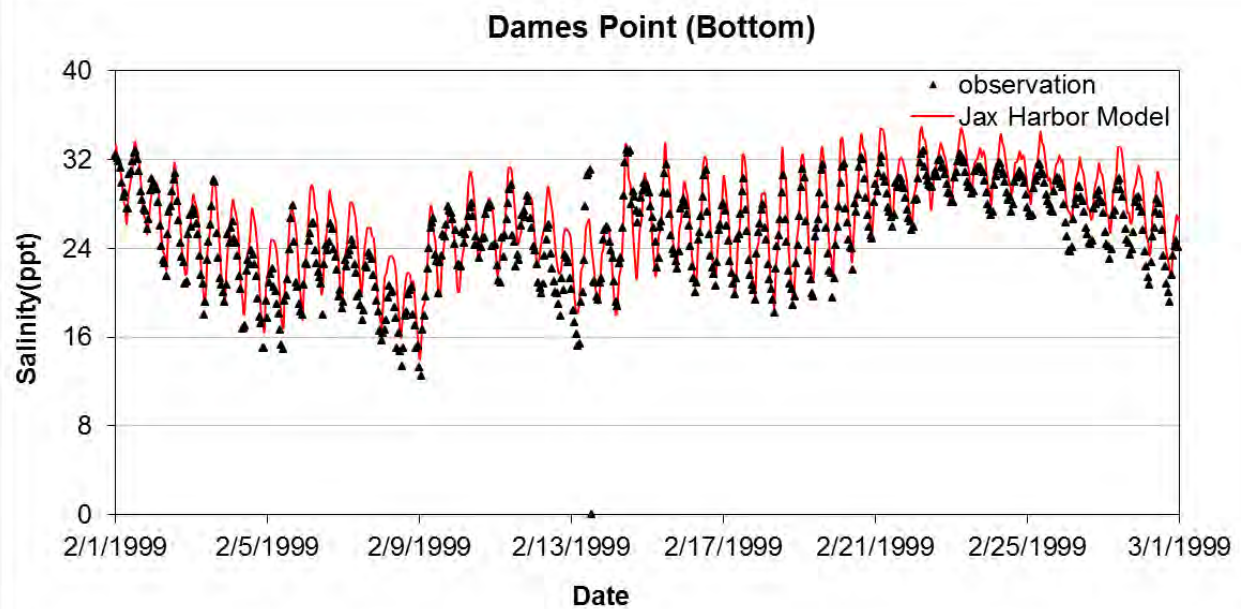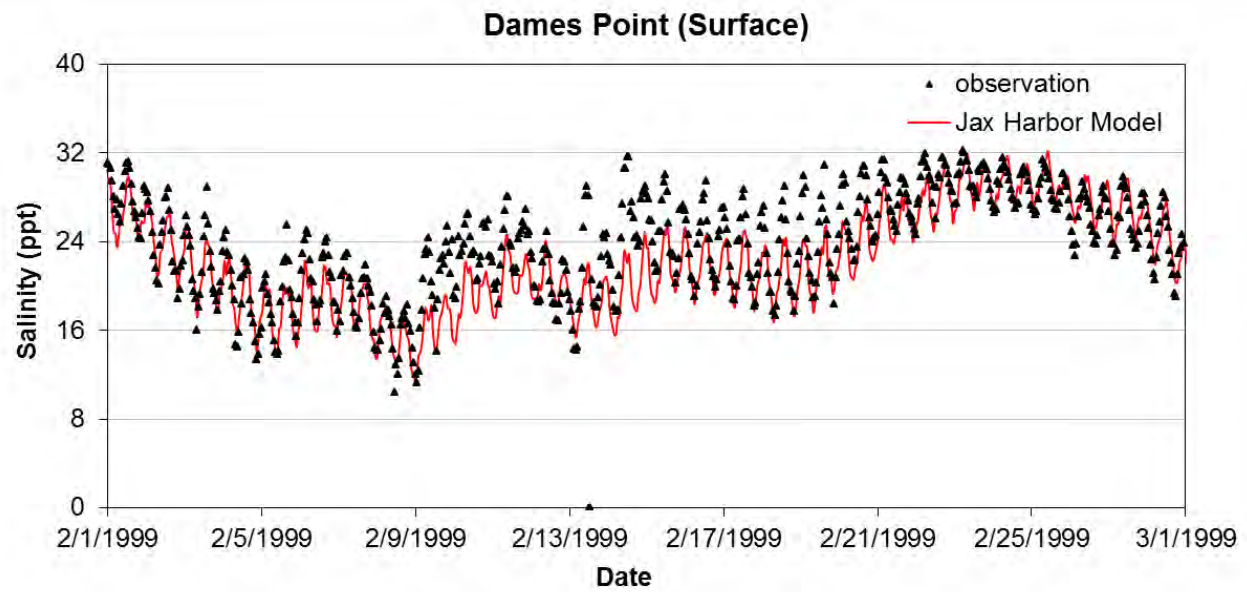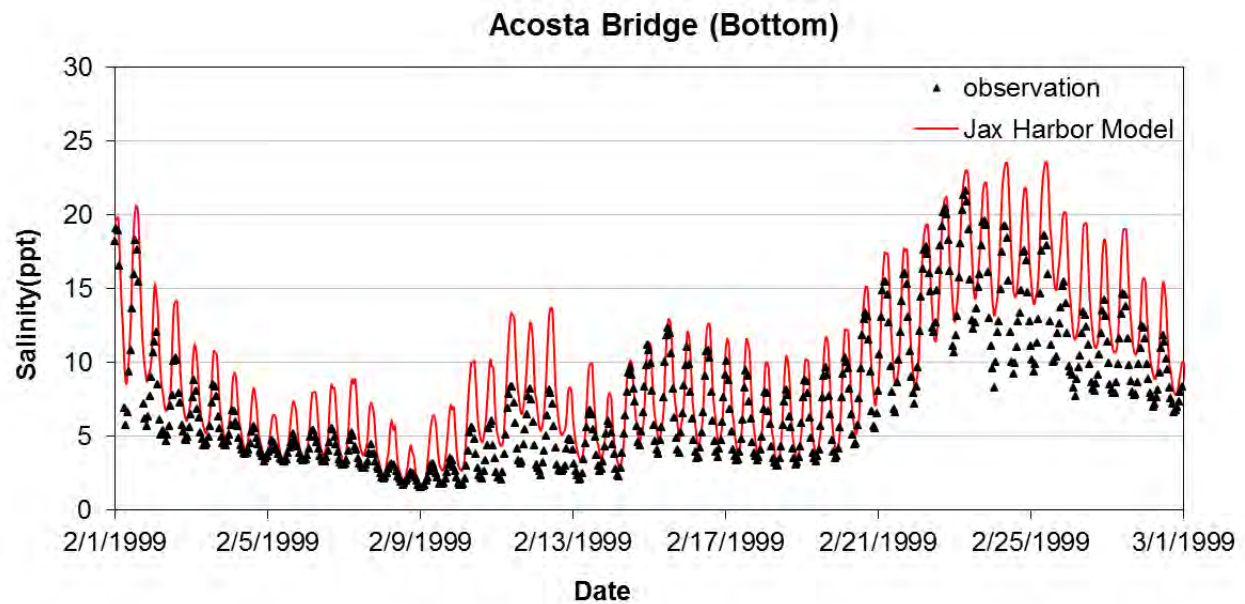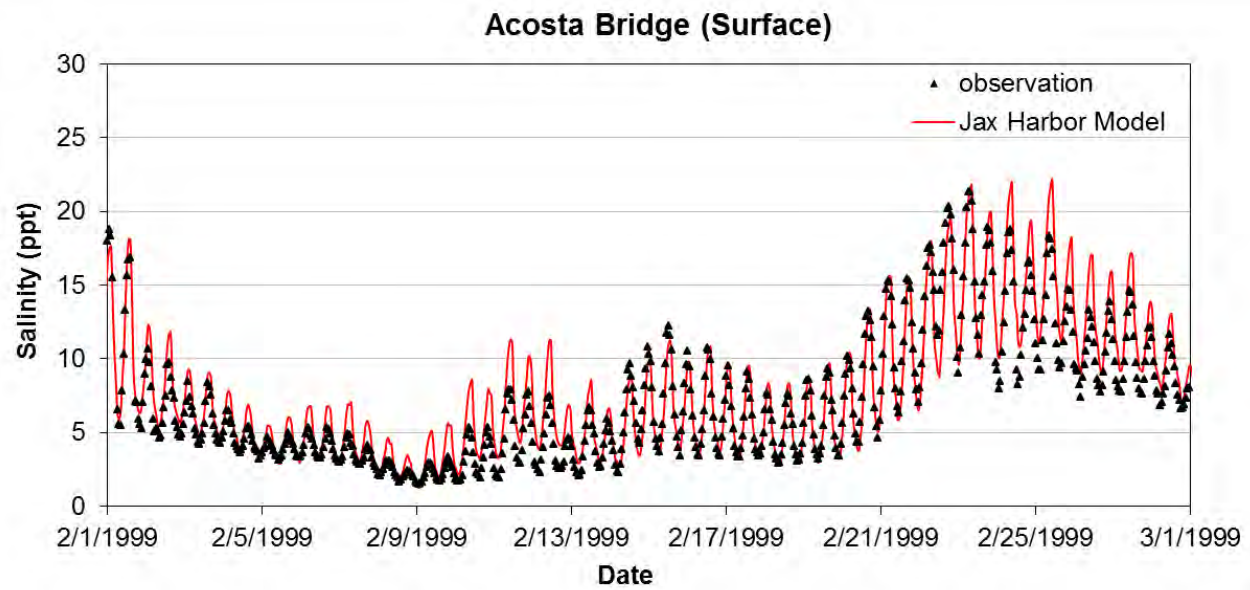**Figure 4.29** Comparison of Computed and Observed Salinity during a Portion of the Wind Condition Calibration Period (Buckman Bridge)
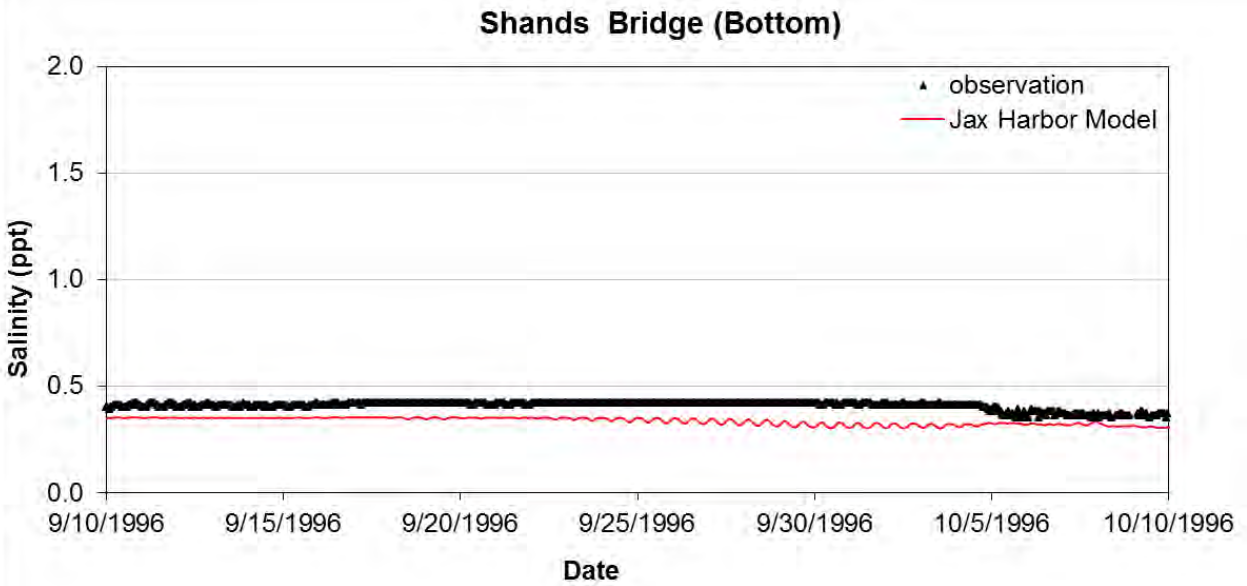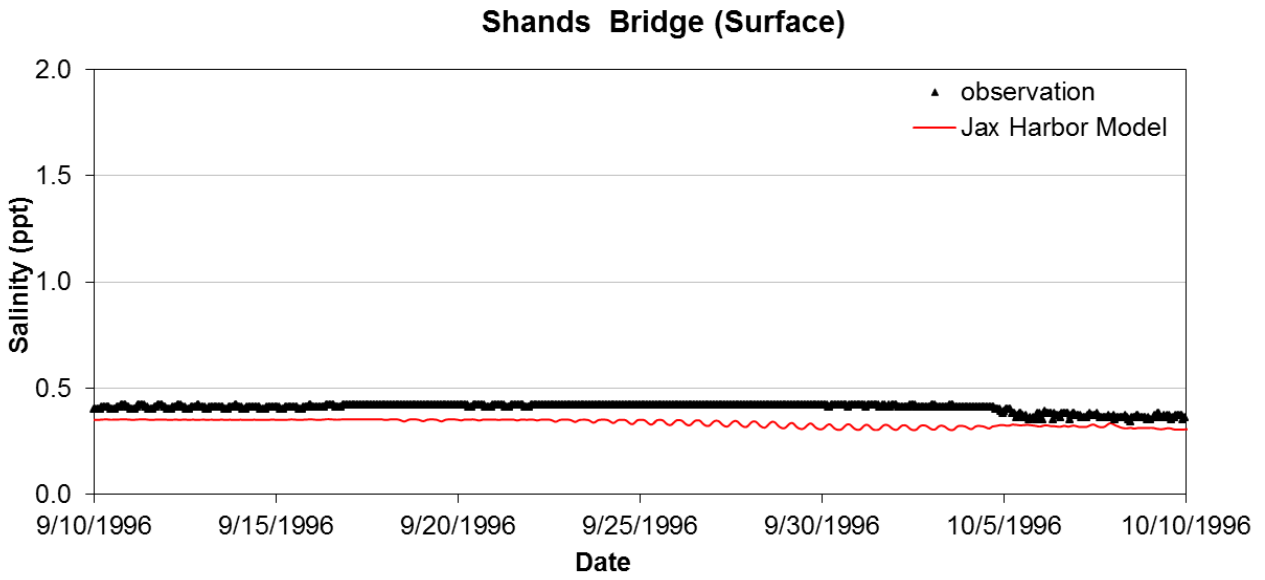
Figure 4.30 Comparison of Computed and Observed Salinity during a Portion of the Wind Condition Calibration Period (Shands Bridge)

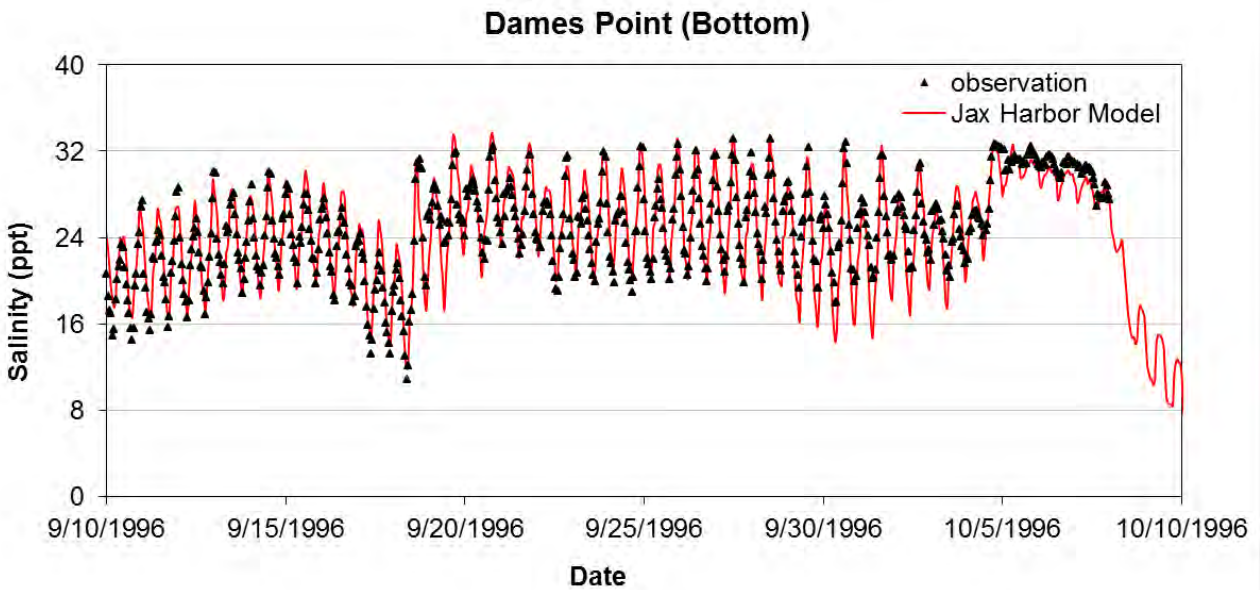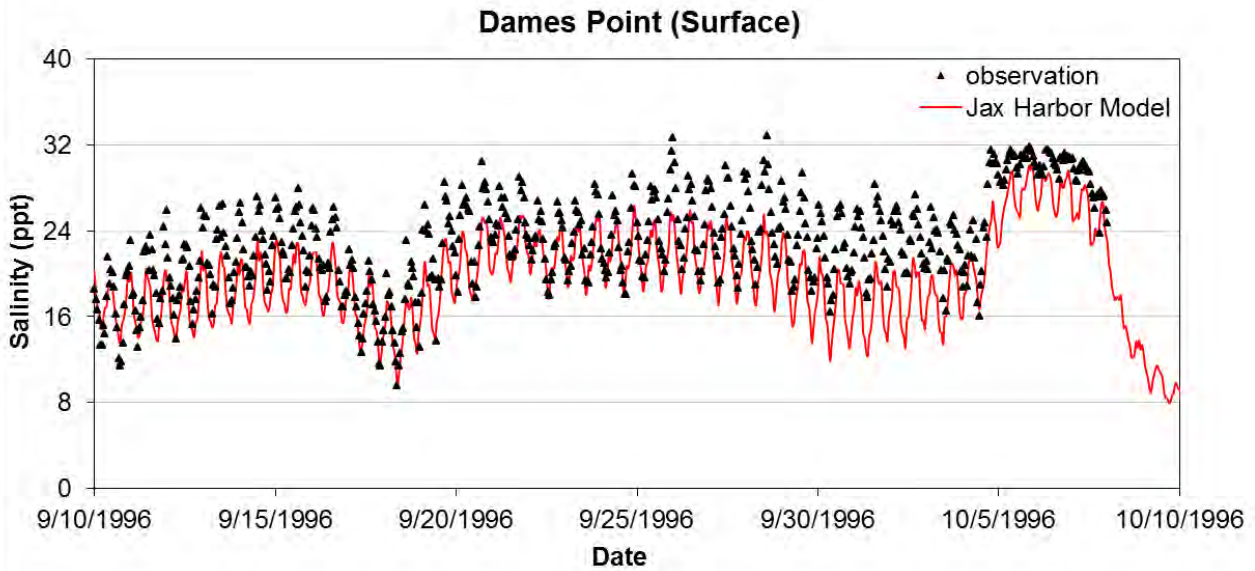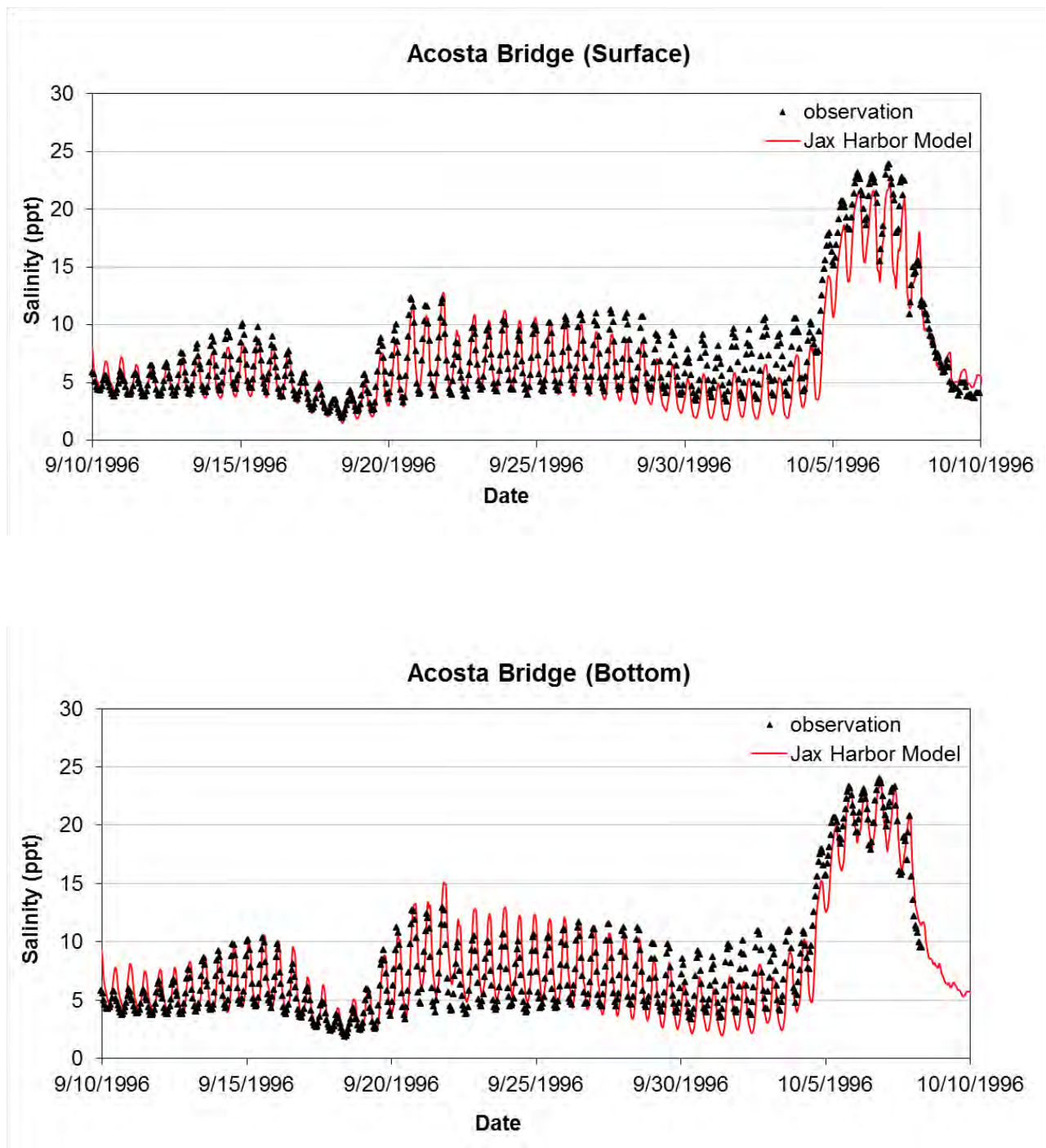**Table 4.6** Model Calibration Statistics for Salinity during Wind Condition Period (8/1/1996 –12/1/1996)

Station / Parameters	Dames Point	Acosta Bridge	Buckman Bridge	Shands Bridge
Surface				
Correlation Coefficient, R	0.922	0.937	0.808	0.062
Root Mean Square Error, RMSE (ppt)	3.394	1.849	0.831	0.041
Bottom				
Correlation Coefficient, R	0.934	0.928	0.827	0.182
Root Mean Square Error, RMSE (ppt)	2.272	2.004	1.981	0.047

4.4   USACE Model Verification

Model verification ensures that the model's calibrated parameters also apply for other data sets (i.e., data sets outside the calibration period). Model verification applied the same model parameters determined during model calibration and consisted of model simulations (with one-year model ramp up period) to reflect two typical conditions: wet period (8/1/2001 – 12/1/2001) and dry period (4/1/2001 – 8/1/2001). The following sections present graphical and statistical comparisons of model predictions to observed data for water level and salinity.

4.4.1   Water Level Verification

Simulated and measured hourly water levels were compared at the five water level stations along the Lower St. Johns River. Similar to comparisons during model calibration, the comparisons show overall good agreement between the measured and simulated water surface level for both wet and dry conditions.

Figure 4.31 through Figure 4.39 show the graphical comparisons between the measured and simulated values for a 30-day period. Notably, the comparisons at Long Branch are for another dry period as measured data is not available for the same dry period shown in the other figures. For the wet period, shown in Figure 4.31, excellent agreement between measured and simulated data occurs at Bar Pilot Dock. Although the model overestimates water levels by up to 0.3 ft at other stations, the ranges match very well. Lateral inflows likely provide larger inflow estimates that resulted in the overestimation of the water level during the wet period. In contrast to the wet period verification, Figure 4.36 through Figure 4.39 show that simulated values closely match measured values at all stations for the dry period. Table 4.7 and Table 4.8 present the statistics of water levels for measured and simulated data for the verification stations. Overall, the model results show good model verification as RMSE is less than 0.3 ft, and the correlation coefficient R is greater than 0.97 at all stations.
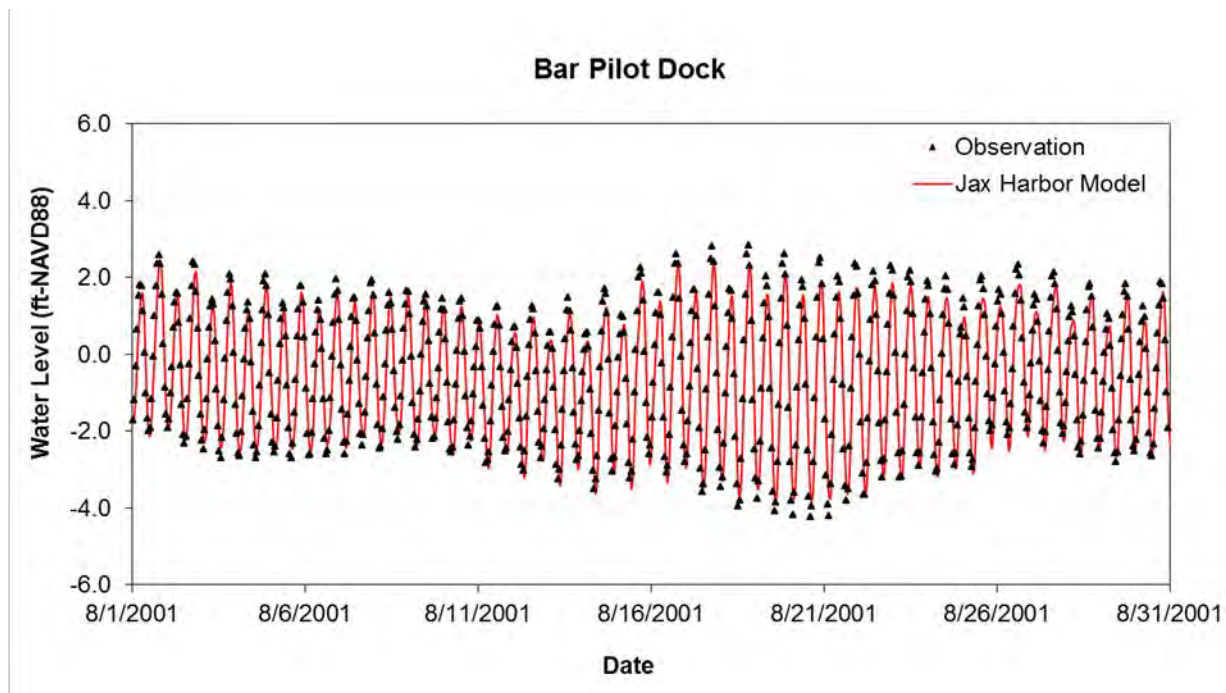
Figure 4.31 Comparison of Computed and Observed Water Level during a Portion of the Wet Period Verification (Bar Pilot Dock)

Figure 4.32 Comparison of Computed and Observed Water Level during a Portion of the Wet Period Verification (Long Branch)

Figure 4.33 Comparison of Computed and Observed Water Level during a Portion of the Wet Period Verification (Main Street Bridge)

Figure 4.34 Comparison of Computed and Observed Water Level during a Portion of the Wet Period Verification (Buckman Bridge)

Figure 4.35 Comparison of Computed and Observed Water Level during a Portion of the Wet Period Verification (Shands Bridge)

Table 4.7 Model Verification Statistics for Water Level during Wet Period (8/1/2001 –12/1/2001)

| Station / Parameters	Bar Pilot Dock	Long Branch Station	Main St. Bridge	Buckman Bridge	Shands Bridge
Correlation Coefficient, R	0.990	0.982	0.982	0.985	0.985
Root Mean Square Error, RMSE (ft)	0.246	0.266	0.249	0.223	0.186
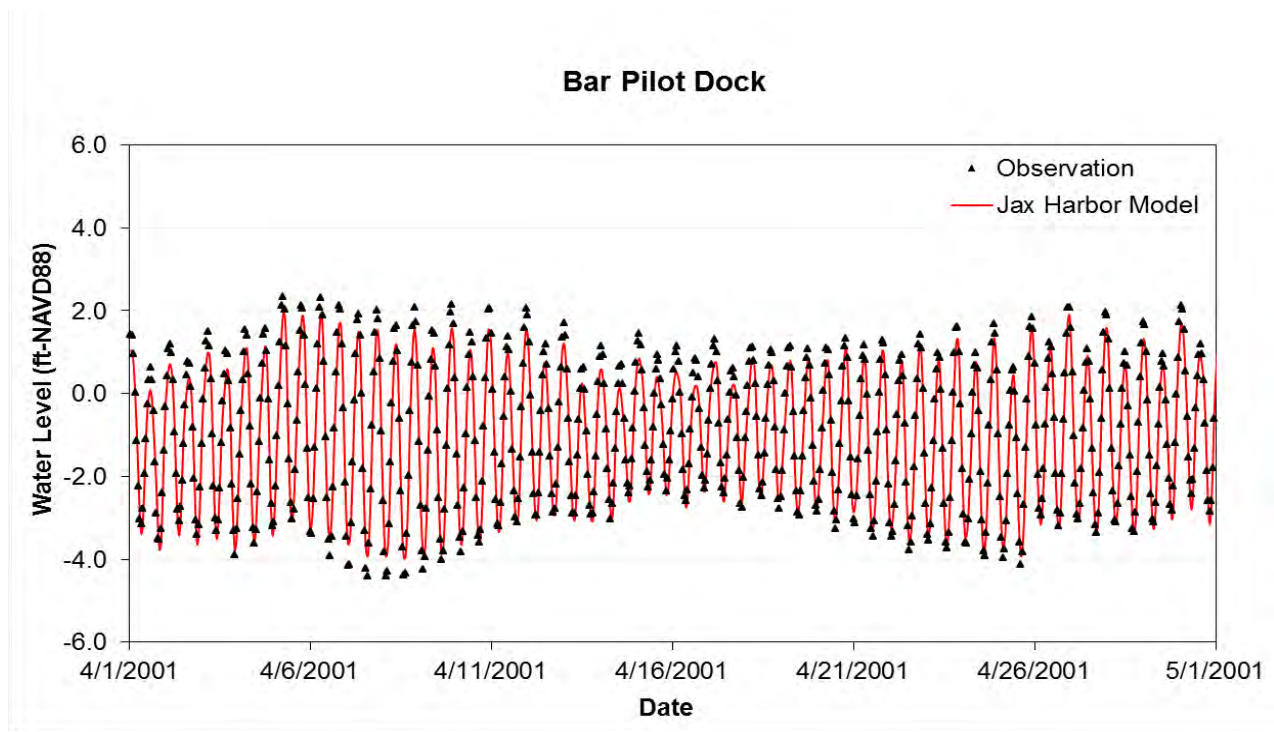
Figure 4.36 Comparison of Computed and Observed Water Level during a Portion of the Dry Period Verification (Bar Pilot Dock)
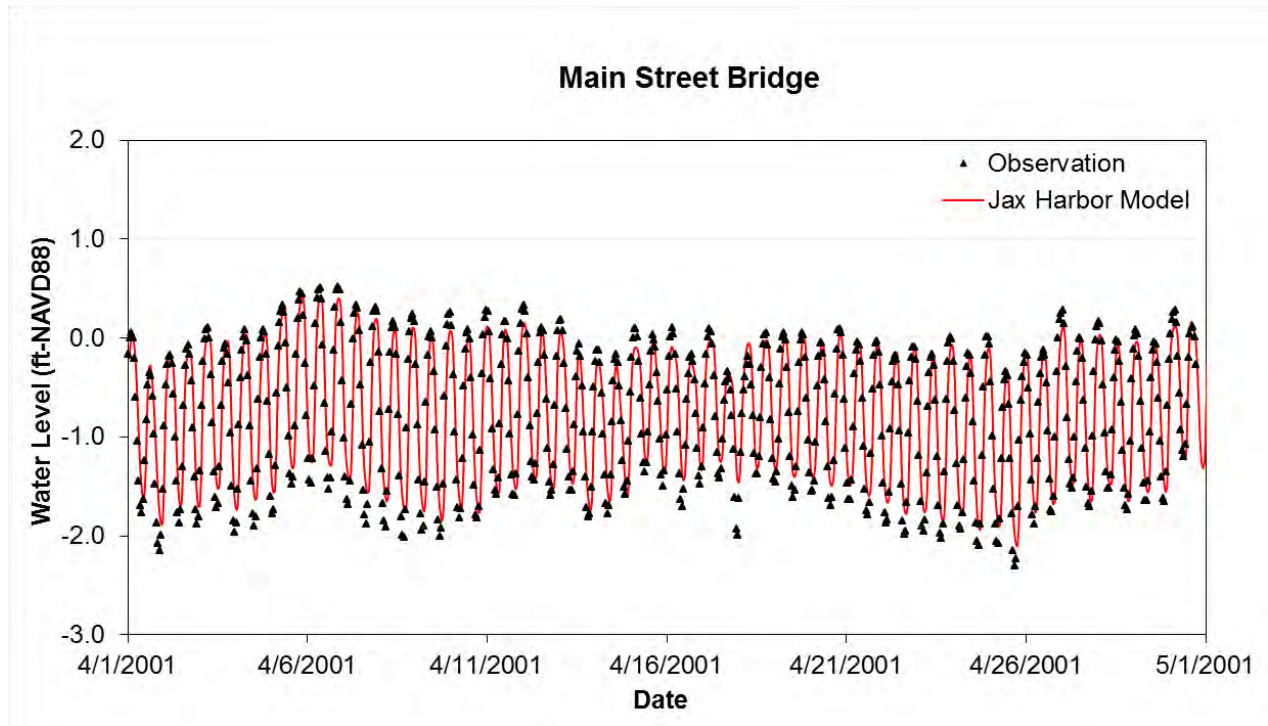
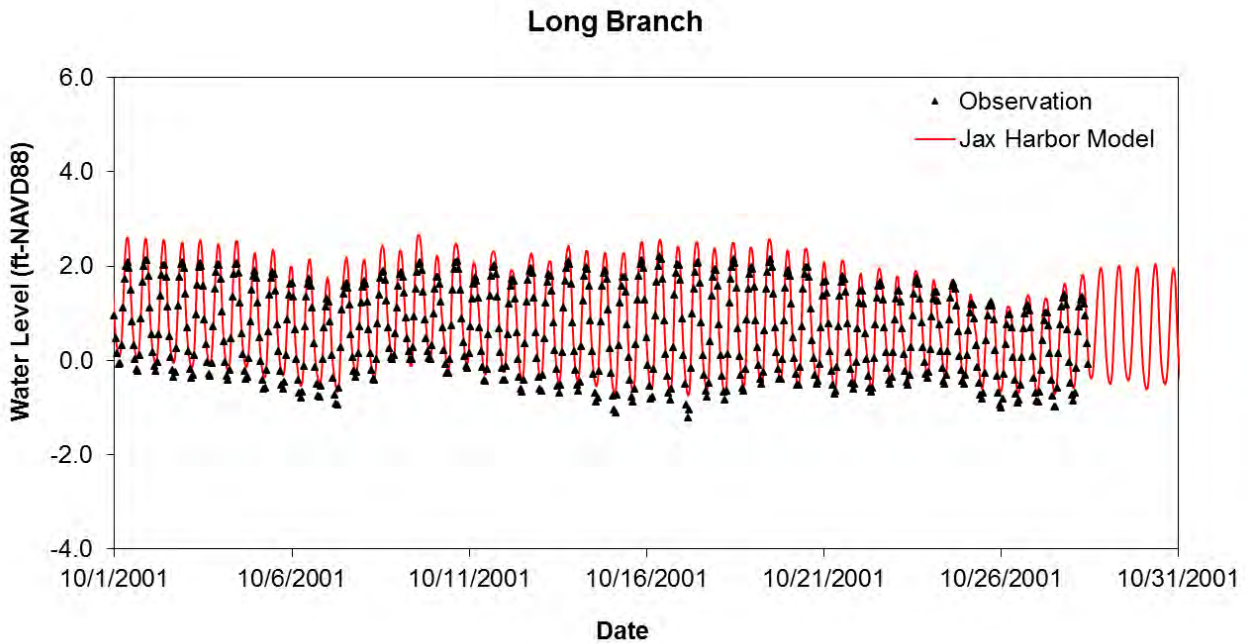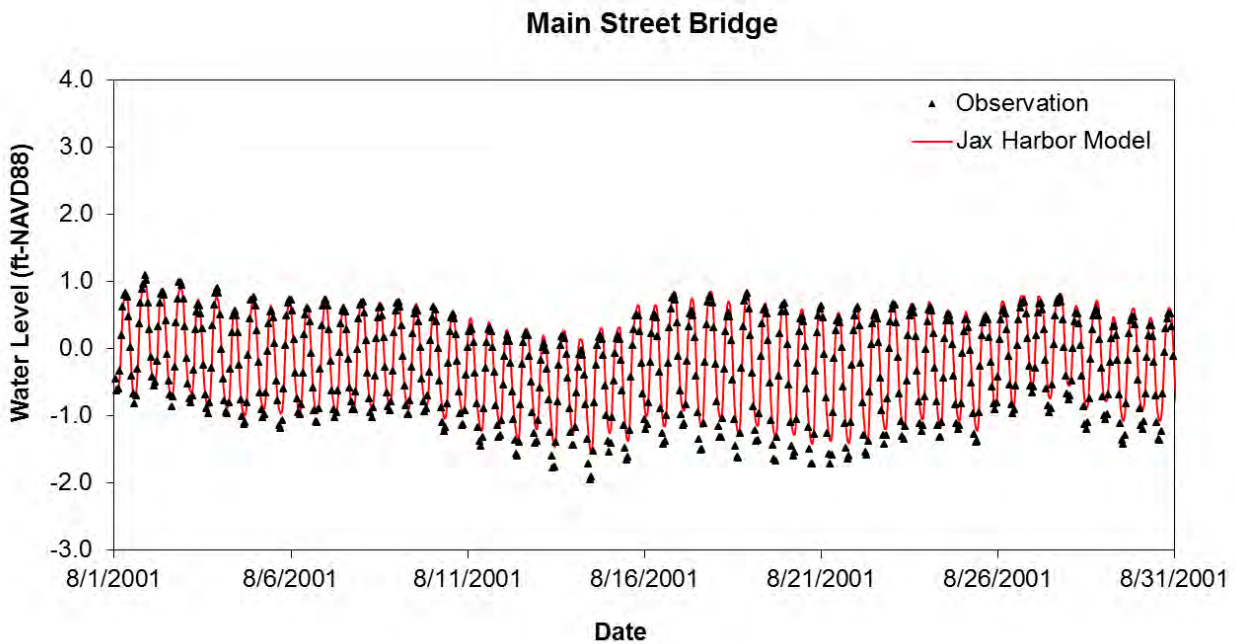**Figure 4.37** Comparison of Computed and Observed Water Level during a Portion of the Dry Period Verification (Main Street Bridge)

Figure 4.38 Comparison of Computed and Observed Water Level during a Portion of the Dry Period Verification (Buckman Bridge)

Figure 4.39 Comparison of Computed and Observed Water Level during a Portion of the Dry Period Verification (Shands Bridge)

Table 4.8 Model Verification Statistics for Water Level during Dry Period (4/1/2001 – 8/1/2001)

Station / Parameters	Bar Pilot Dock	Long Branch Station*	Main St. Bridge	Buckman Bridge	Shands Bridge
Correlation Coefficient, R	0.993	N/A	0.987	0.978	0.977
Root Mean Square Error, RMSE (ft)	0.290	N/A	0.129	0.105	0.096

* Note: Observation data unavailable at Long Branch Station for this period

4.4.2   Salinity Verification

Figure 4.40 through Figure 4.47 present comparisons of measured and simulated salinities for a one-month period. Overall, the model captures the salinity intrusion on the Lower St Johns River relatively well. During the wet period, shown in Figure 4.40 through Figure 4.43, the model underestimates the mean salinity, but the simulated ranges match very well. It appears that the model applied too much freshwater inflow. Notably, the freshwater inflow is an unadjustable model input (provided by SJRWMD) that is recognized as a limitation beyond the scope of this study. For the dry period, shown in Figure 4.44 through Figure 4.47, the simulated salinity is consistent with the measured data at all stations except Shands Bridge. Table 4.9 and Table 4.10 show salinity statistics for measured and simulated data. Overall, the most accurate results occur at Acosta Bridge and Buckman Bridge with RMSE less than 2.5 ppt and a correlation coefficient R greater than 0.89 at these two stations.

In general, the comparisons show that the model used in this study captures the general distribution of salinity along the Lower St. Johns River, and appears sufficiently calibrated and verified to evaluate the potential project-related hydrodynamic and salinity changes in the Lower St. Johns River.
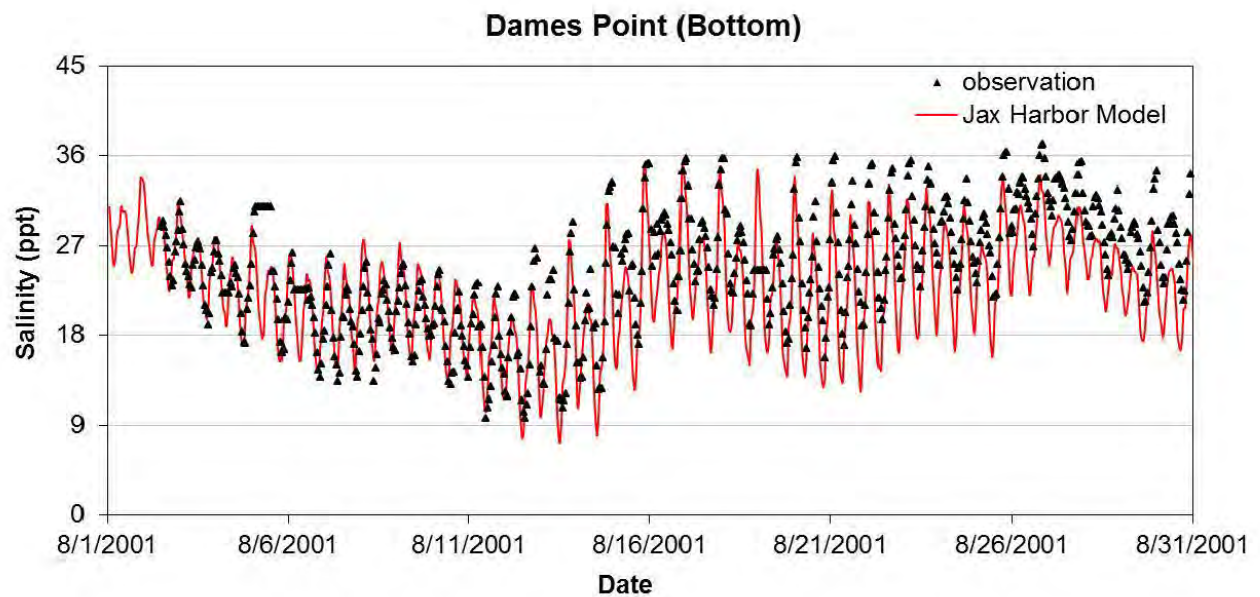
Figure 4.40 Comparison of Computed and Observed Salinity during a Portion of the Wet Period Verification (Dames Point)

Figure 4.41 Comparison of Computed and Observed Salinity during a Portion of the Wet Period Verification (Acosta Bridge)
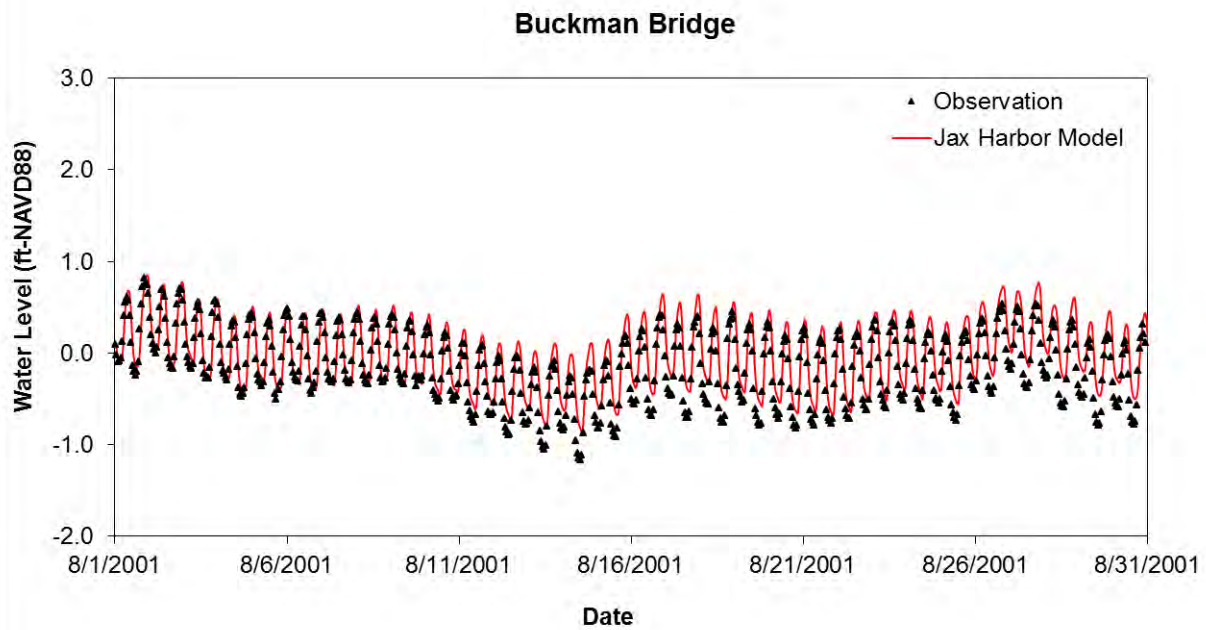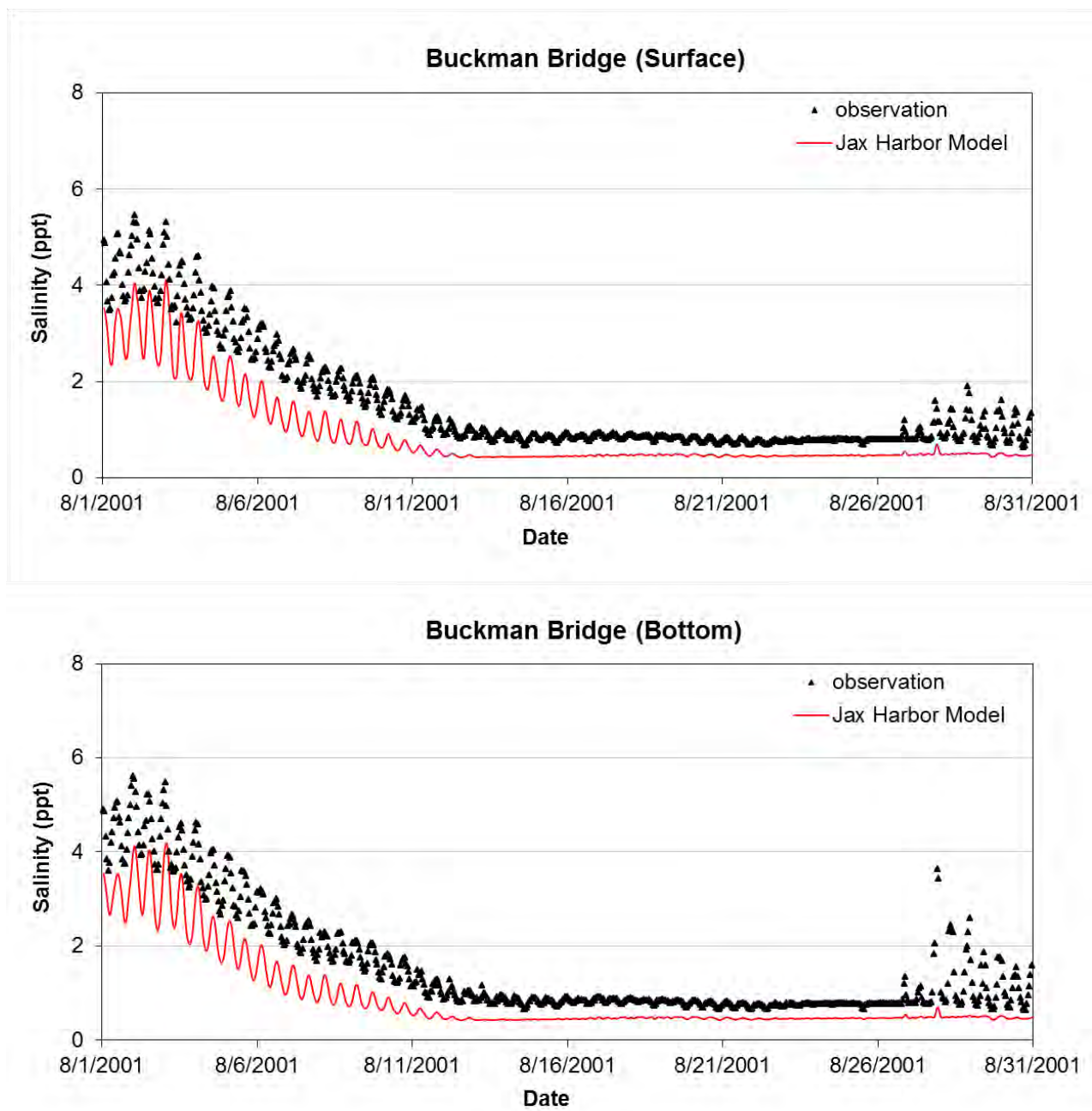
Figure 4.42 Comparison of Computed and Observed Salinity during a Portion of the Wet Period Verification (Buckman Bridge)
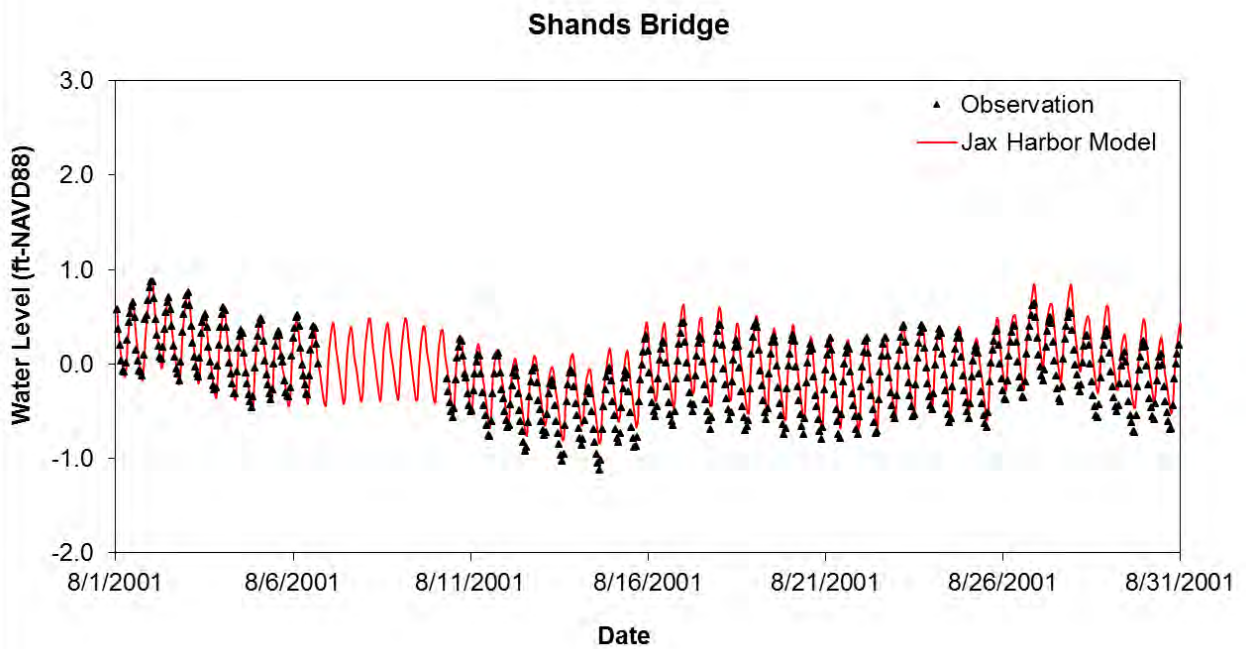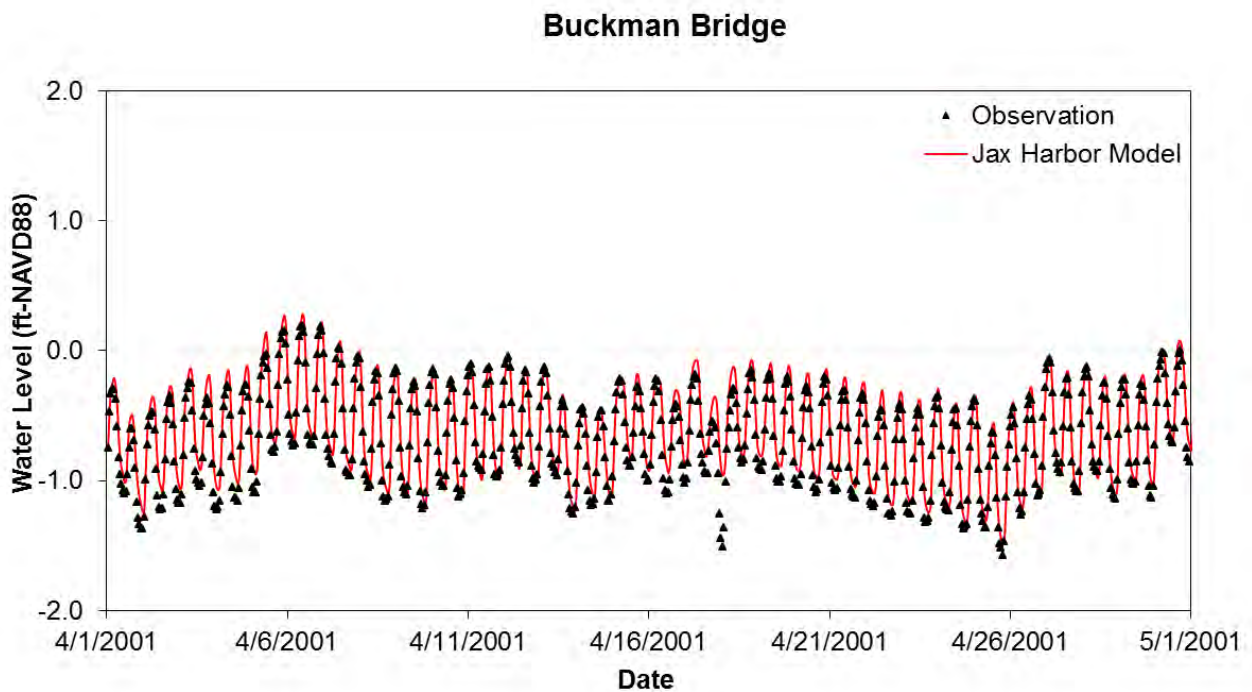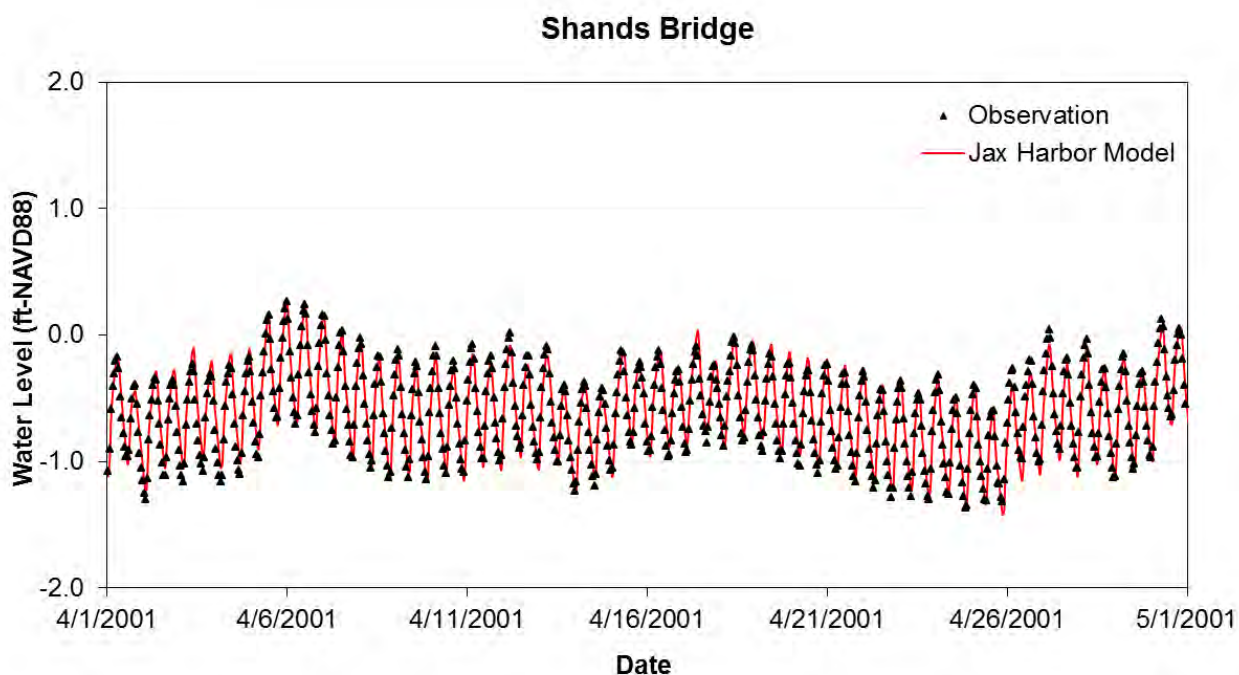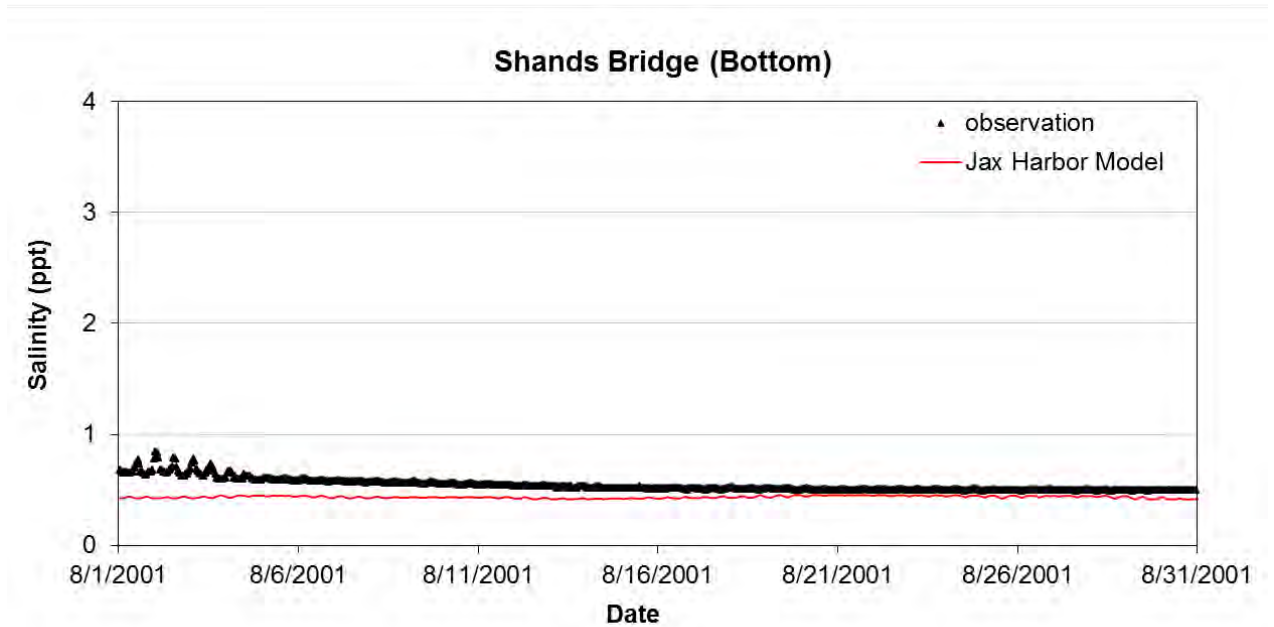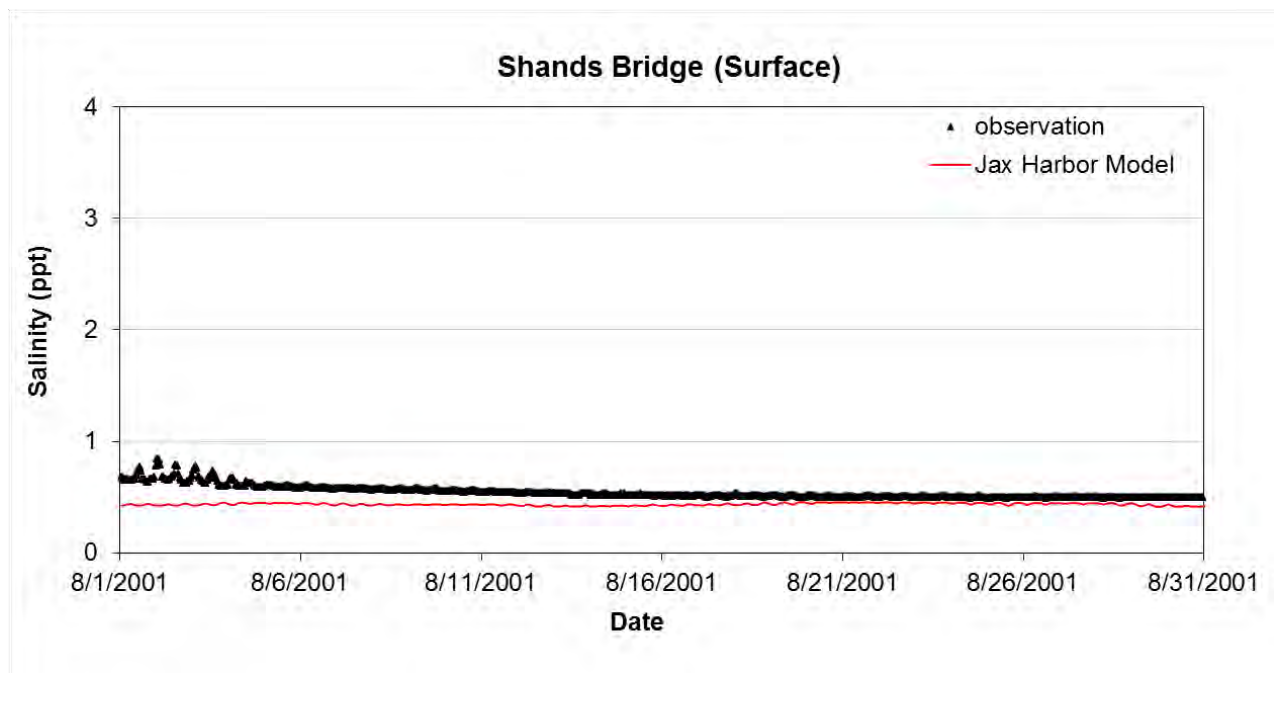
Figure 4.43 Comparison of Computed and Observed Salinity during a Portion of the Wet Period Verification (Shands Bridge)

Table 4.9 Model Verification Statistics for Salinity during Wet Period (8/1/2001 – 12/1/2001)

| Station / Parameters	Dames Point	Acosta Bridge	Buckman Bridge	Shands Bridge
Surface				
Correlation Coefficient, R	0.878	0.890	0.951	0.098
Root Mean Square Error, RMSE (ppt)	5.567	2.332	0.437	0.110
Bottom				
Correlation Coefficient, R	0.812	0.897	0.904	0.093
Root Mean Square Error, RMSE (ppt)	5.799	2.133	0.532	0.110
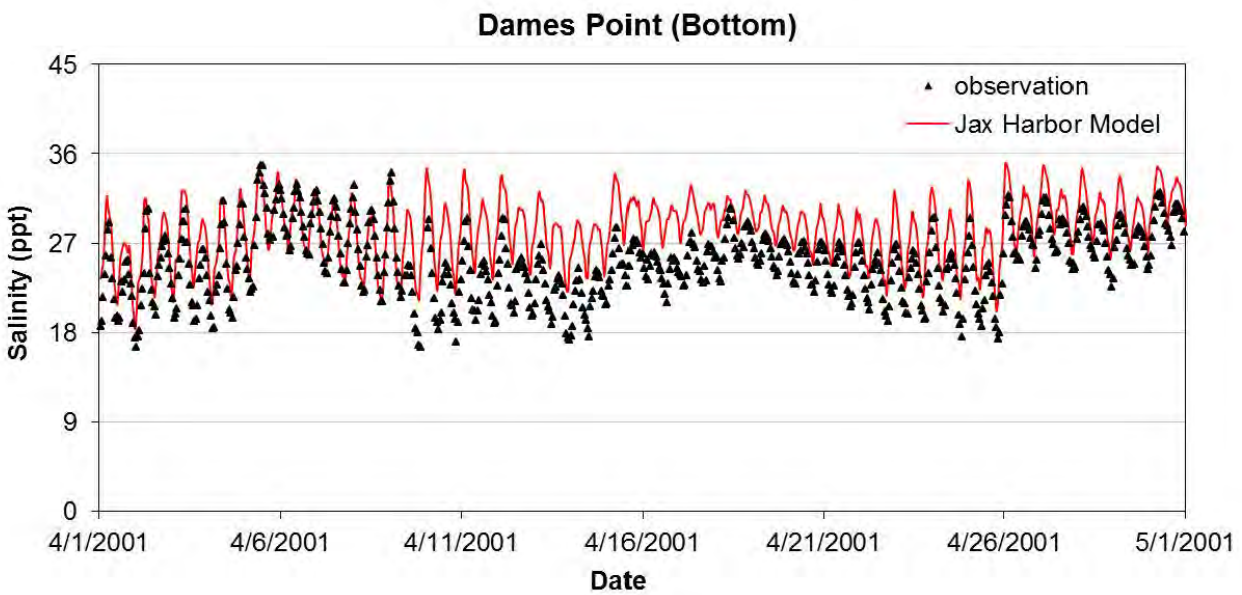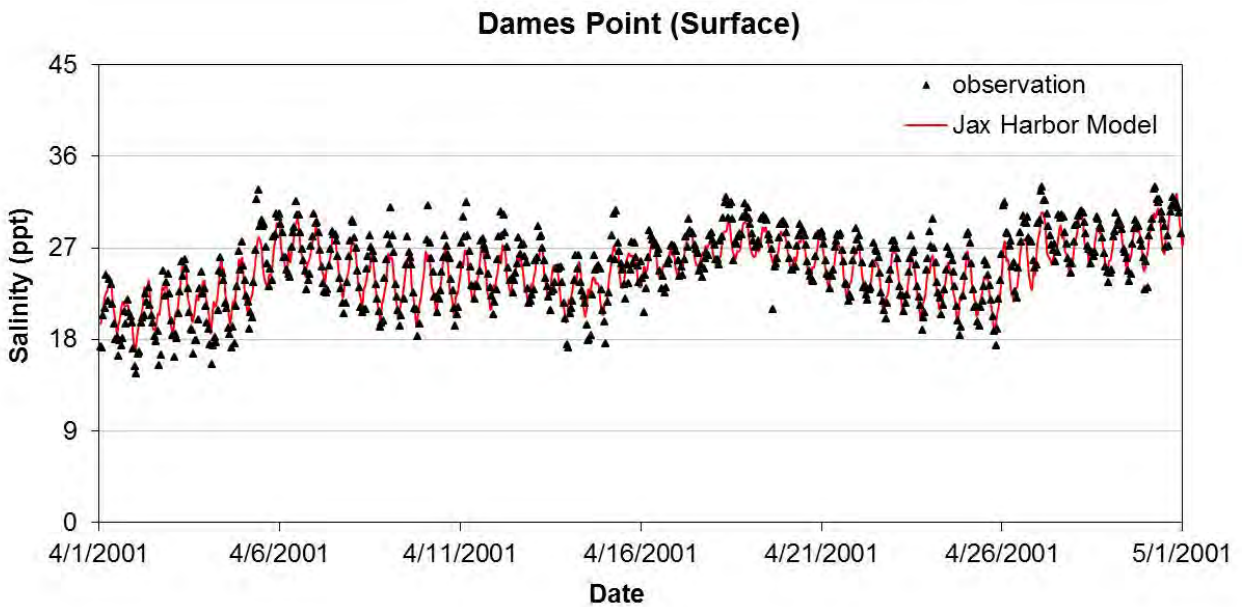
Figure 4.44 Comparison of Computed and Observed Salinity during a Portion of the Dry Period Verification (Dames Point)
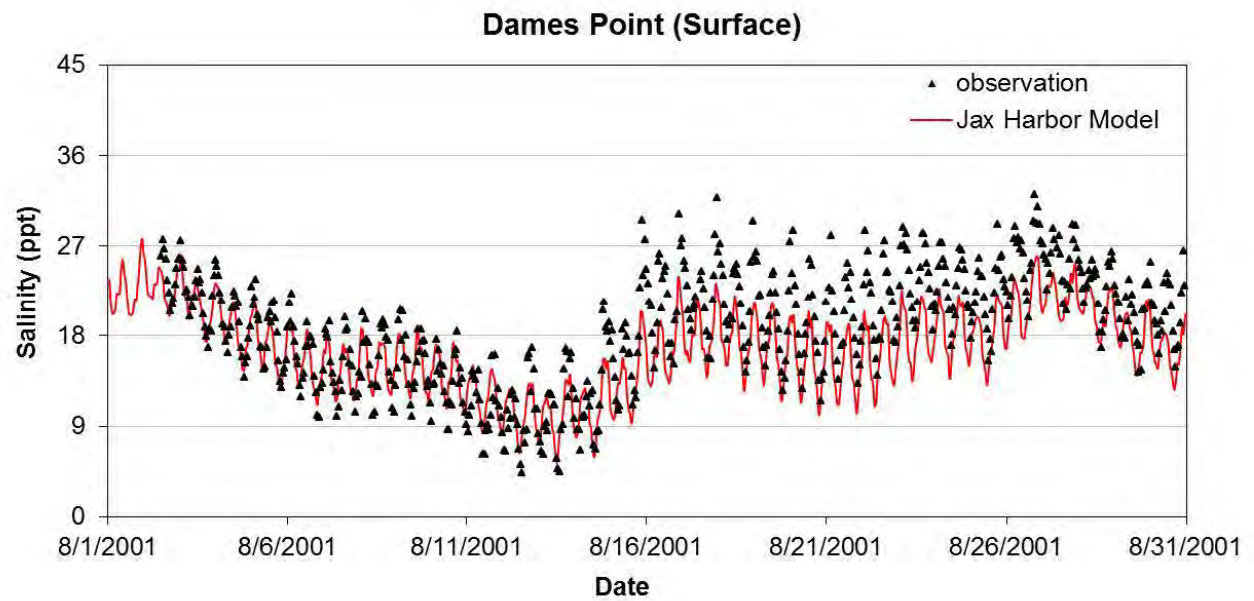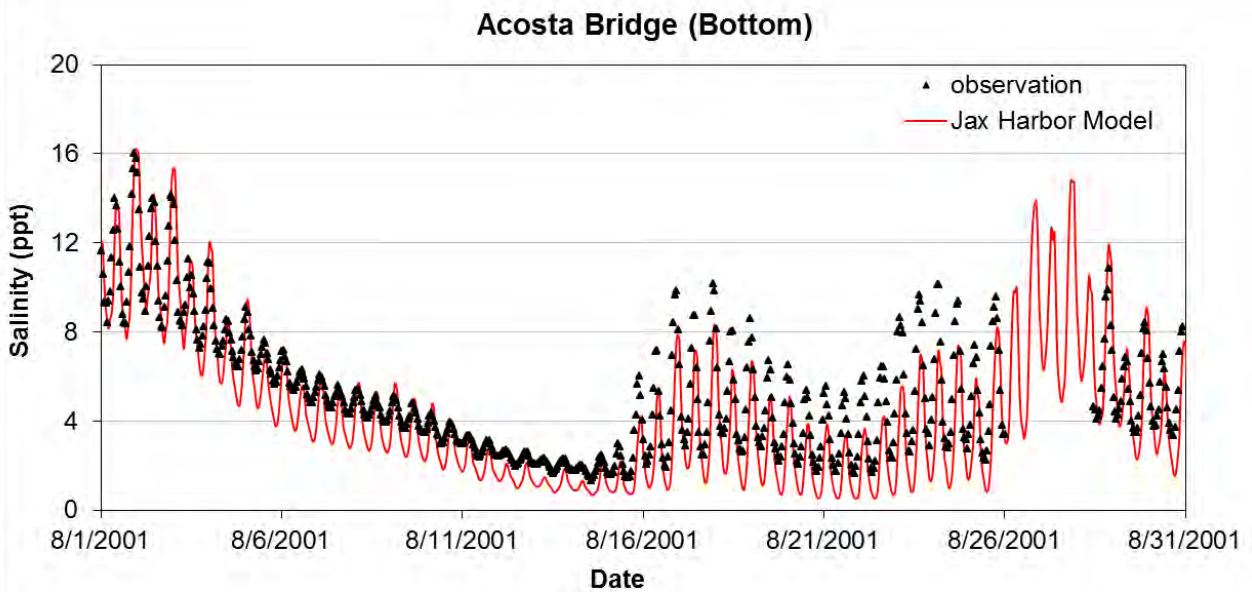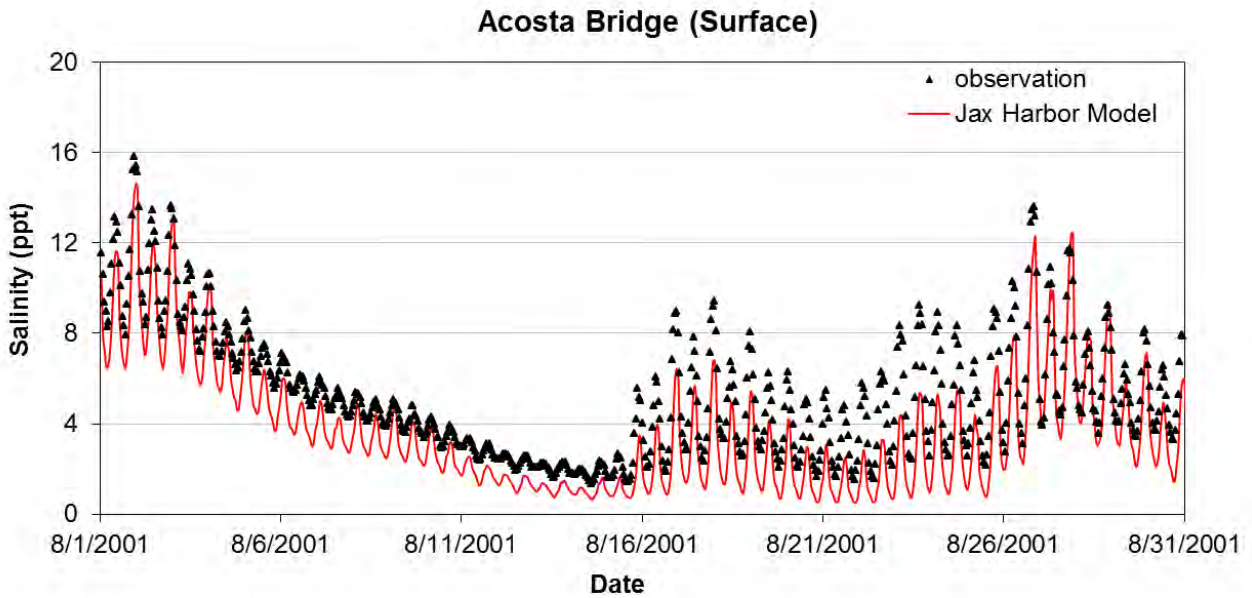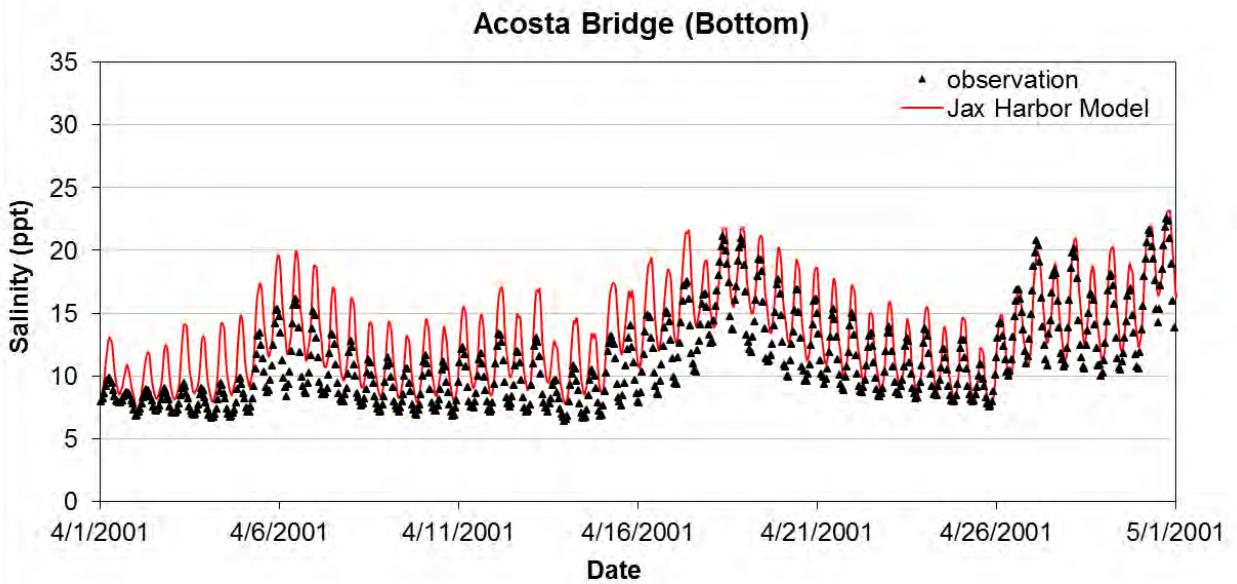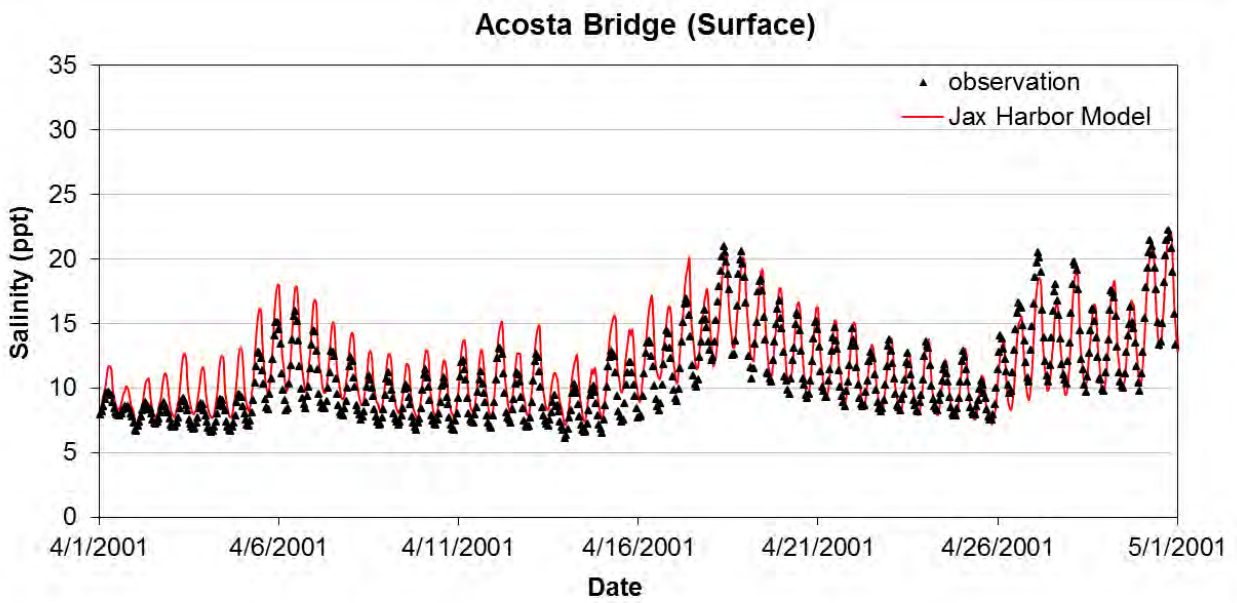
Figure 4.45 Comparison of Computed and Observed Salinity during a Portion of the Dry Period Verification (Acosta Bridge)
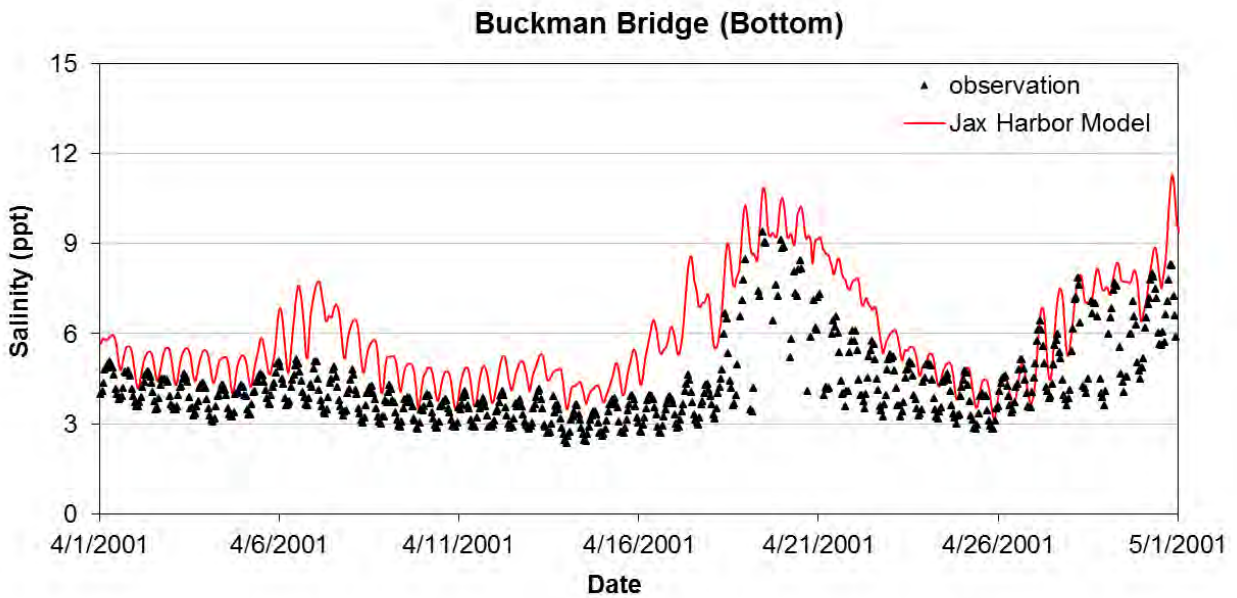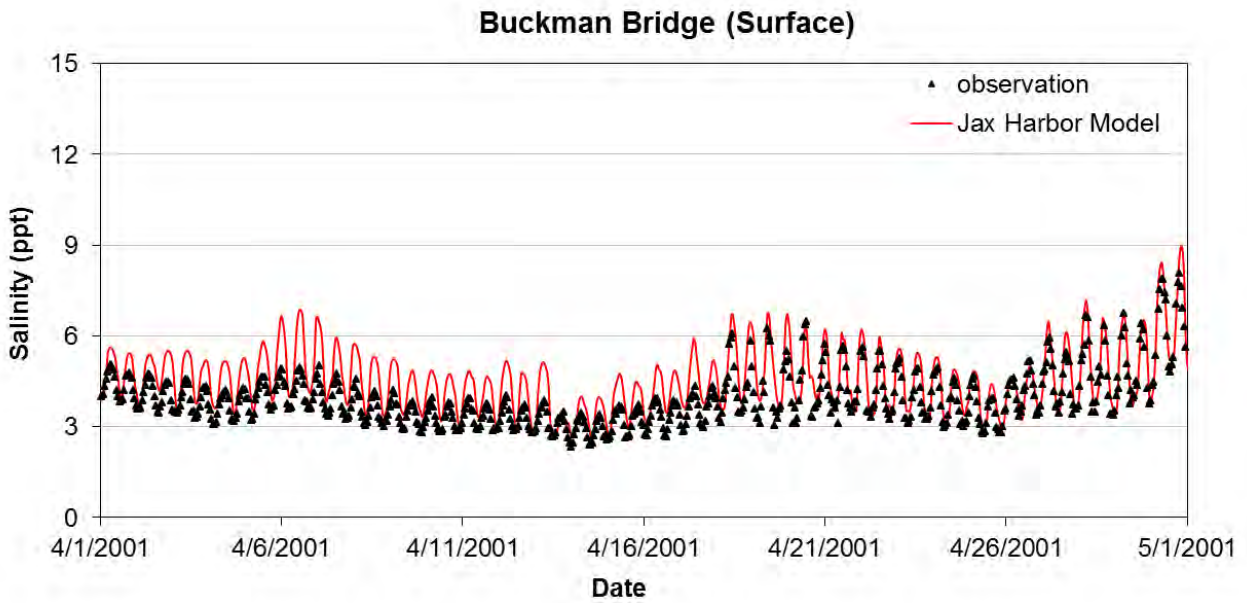
Figure 4.46 Comparison of Computed and Observed Salinity during a Portion of the Dry Period Verification (Buckman Bridge)
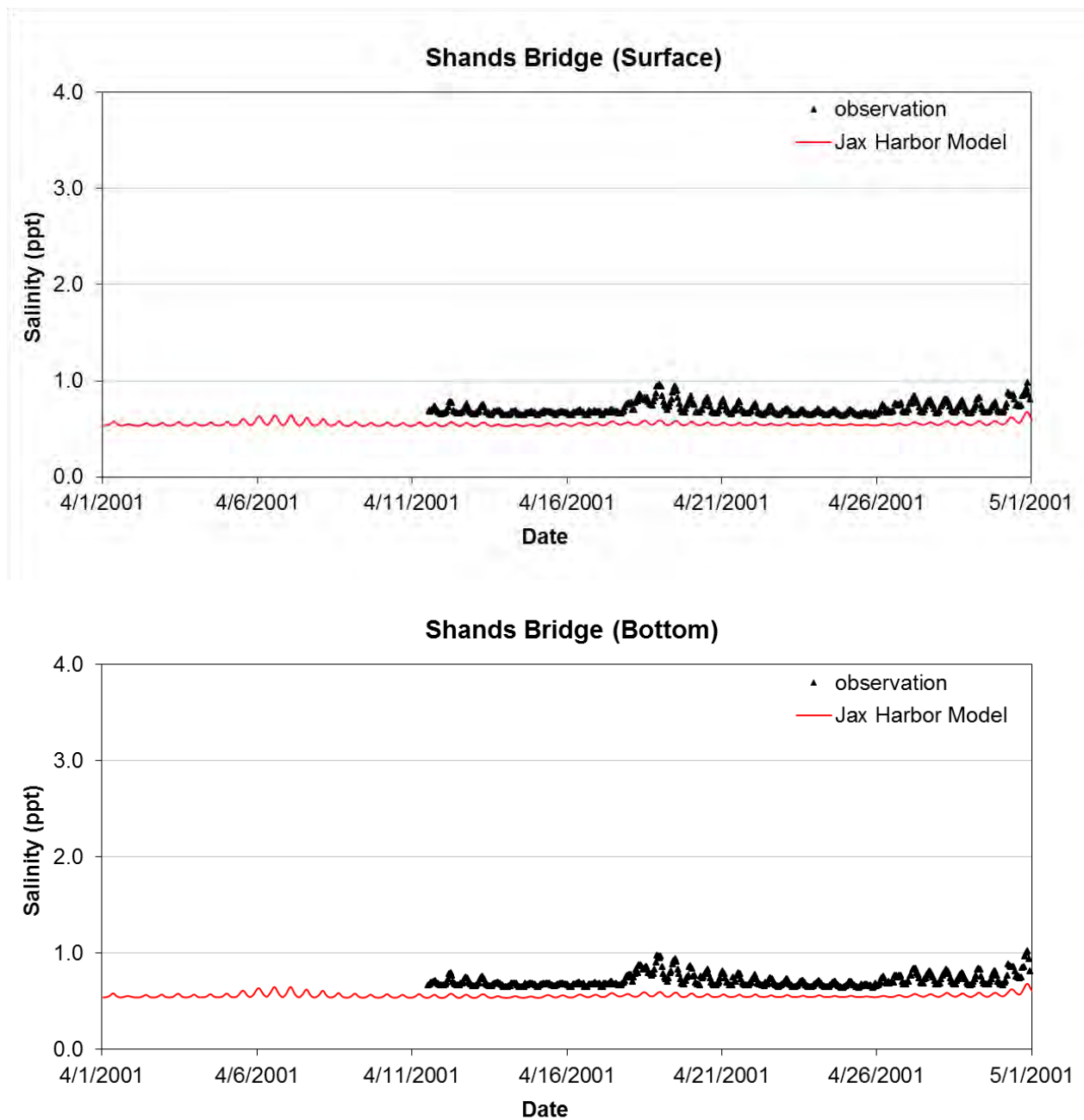
Figure 4.47 Comparison of Computed and Observed Salinity during a Portion of the Dry Period Verification (Shands Bridge)

Table 4.10 Model Verification Statistics for Salinity during Dry Period (4/1/2001 – 8/1/2001)

Station \ Parameters	Dames Point	Acosta Bridge	Buckman Bridge	Shands Bridge
Surface				
Correlation Coefficient, R	0.778	0.901	0.913	0.891
Root Mean Square Error, RMSE (ppt)	2.194	1.831	0.945	0.565
Bottom				
Correlation Coefficient, R	0.743	0.898	0.862	0.896
Root Mean Square Error, RMSE (ppt)	2.985	2.082	2.206	0.569

5.0   MODEL SCENARIOS AND IMPACTS

The USACE intends to use the calibrated and verified model to examine changes to salinity regime throughout the study area as a result of the proposed channel deepening and other actions (widening the channel at select locations and constructing a turning basin). The results should provide the data required for any assessment of dredging impacts on water quality or biological resources.

This chapter describes three model simulations: (1) 2009 Survey Condition, or Baseline Condition, (2) Alternative Plan A, and (3) Alternative Plan B. The 2009 Survey Condition model serves as a baseline model; the alternative plans represent two channel deepening scenarios. This chapter also presents a comparison of both scenarios, Alternative Plan A and Alternative Plan B, to baseline condition to evaluate the effects of both alternative plans on salinity.

5.1   Model Scenario Simulations

5.1.1   Baseline Condition (2009 Survey Condition)

Previous chapters detail the validation of the USACE model using the SJRWMD 2010 model bathymetry. The SJRWMD developed that bathymetry from various sources covering an 11-year period (1995 – 2005). However, since 2005 various dredging activities along the channel changed the channel bathymetry significantly. A 2009 USACE survey, conducted from the river mouth to JAXPORT Talleyrand Marine Terminal where the navigation channel ends, provides the most current and realistic bathymetry of the channel within the survey range. Thus, USACE-SAJ directed this study to incorporate the updated survey into the validated USACE model mesh from the river mouth to River Mile 23. The rest of the model domain maintains the same bathymetry as the SJRWMD 2010 model. As noted above, the resulting model (including the 2009 survey) provides baseline condition from which to compare the impacts from the simulated channel deepening scenarios (Alternative Plan A and Alternative Plan B).

5.1.2   Alternative Plan A

Alternative Plan A represents a composite of all the proposed dredging improvements. The proposed plan would involve dredging the navigation channel to 50 ft below mean lower low water (MLLW), widening some areas along the channel, and building new turning basins. Table 5. 1 and Figure 5.1 – Figure 5.3 present details of Alternative Plan A. These improvements were incorporated into the baseline model to create a new model – Alternative Plan A Model. Based on personal communications with the USACE Task Order Project Manager, the Adaptive Hydraulics Model (ADH) for the USACE's

hydro-modeling provided the proposed bathymetric data inside the navigation channel — that is, from the river mouth to JAXPORT Talleyrand Marine Terminal. No other changes were made to the baseline model bathymetry during the creation of Alternative Plan A Model.

Table 5. 1 Proposed Alternative Plan A

Location	Description	Note
Segment 1: Atlantic Ocean to Mile 14	1) Training Wall Reach Widening 2) St. John Bluff Reach Widening 3) Blount Island Terminal Turning Basin Modification 4) Southwest Blount Island Channel Widening 5) Broward Point Turning Widening	See Figure 5.1
Segment 2: Mile 11 to Mile 19	1) Drummond Creek Range Widening 2) Bartram Island Expansion 3) Trout River Cut Range Widening 4) Terminal Channel Turning Basin Modification 5) Terminal Channel Widening	See Figure 5.2
Segment 3: West Blount Island Channel	1) Cuts F & G Deepening 2) Southwest Blount Island Channel Widening	See Figure 5.3

Figure 5.1 Locations of the Dredging Improvement Areas in Segment # 1
(Source: USACE Jacksonville District)

Figure 5.2 Locations of Dredging Improvement Areas in Segment # 2
(Source: USACE Jacksonville District)
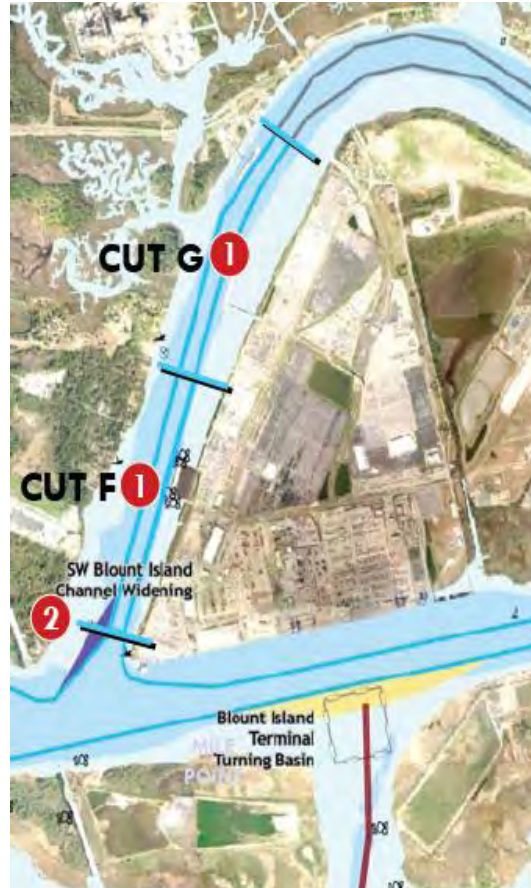
Figure 5.3 Locations of the Dredging Improvement Areas in Segment # 3
(Source: USACE Jacksonville District)

5.1.3   Alternative Plan B

Of the alternatives considered, Alternative Plan A would give the harbor the deepest channel. A modified plan, Alternative Plan B, involves deepening the navigation channel to 50 ft below MLLW for the first 14 miles from the river mouth only (Segment 1), widening some areas along the channel, and building new turning basins in this segment. Again, these improvements were incorporated into the baseline model bathymetry to create the Alternative Plan B Model. The Adaptive Hydraulics Model (ADH) provided the bathymetry inside the navigation channel from the river mouth to River Mile 14. No other changes were made to the model.

5.2   Effects on Salinity Concentration

The above models simulated the changes in hydrodynamics and salinity due to the proposed changes listed in Table 5. 1. Because the main goal of this study is to investigate the effect of proposed

alternative plans on salinity, this report discusses only salinity changes. The model for these simulations used the same boundaries as those used during model calibration (for the period between December 1, 1998 and April 1, 1999). The USACE-SAJ consider this period representative of typical dry conditions in the region.

Comparisons of simulations for the two alternatives with baseline simulations provided the means to evaluate the effects of proposed dredging improvements. Comparisons considered hourly salinity at three stations between Acosta and Shands bridges (Check Points #1, #9, and #16, Figure 5.4) selected by the USACE-SAJ along the Lower St. Johns River. Figure 5.5 – Figure 5.7 present comparison of model calculated salinity at each of the three stations. In summary, compared with the conditions simulated by the baseline model, Alternative Plan A clearly increases salinity at all three locations while Alternative Plan B shows small salinity increases at these three locations. For Alternative Plan A, salinity increases averages about 1.5 ppt at Check Point #1; average salinity changes then decrease upstream. Average salinity changes drop to about 0.8 ppt at Check Point #9 and to about 0.3 ppt at Check Point #16. Because Alternative Plan B will only dredge Segment 1, the downstream part of the channel, salinity does not change at these three locations in this scenario.
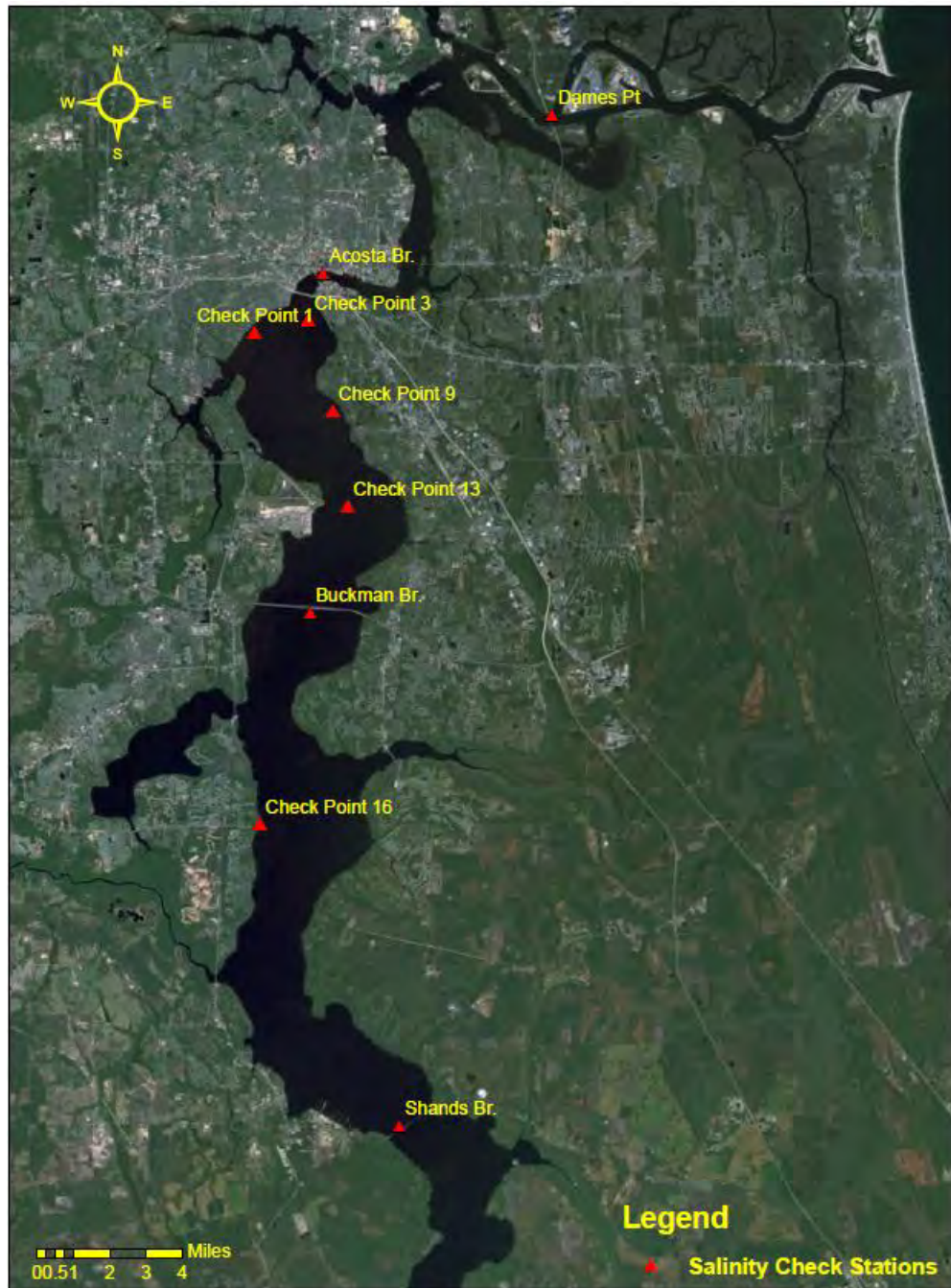
Figure 5.4 Salinity Station Locations

Figure 5.5 Comparison of Baseline, Alternative A, and Alternative B Models Computed Salinity during Dry Period Calibration (Check Point #1)

Figure 5.6 Comparison of Baseline, Alternative A, and Alternative B Models Computed Salinity during Dry Period Calibration (Check Point #9)
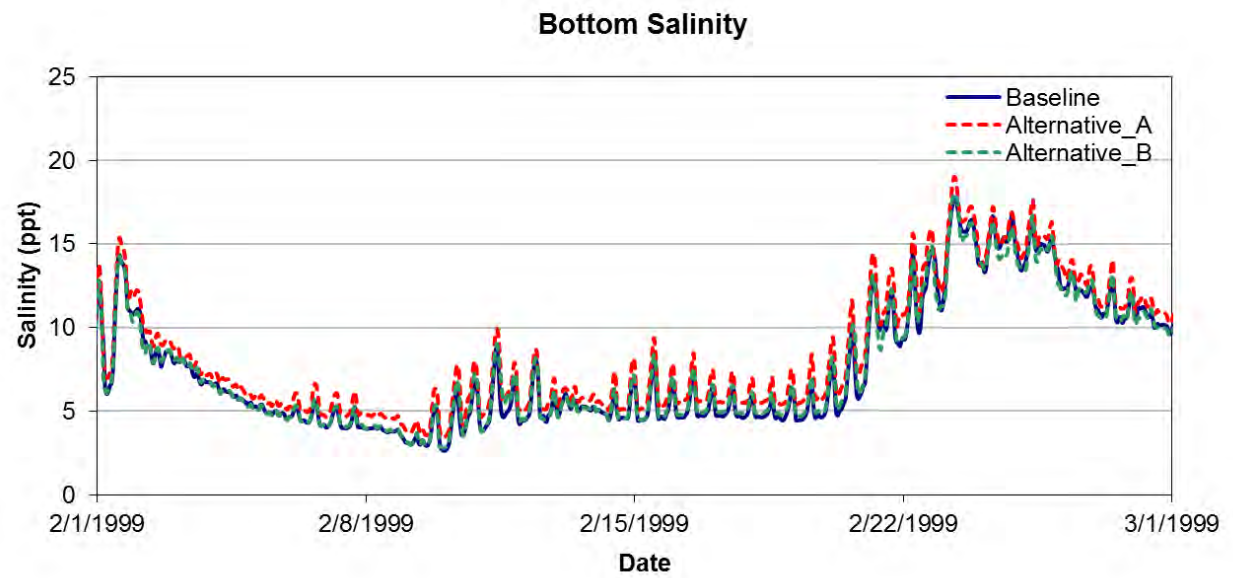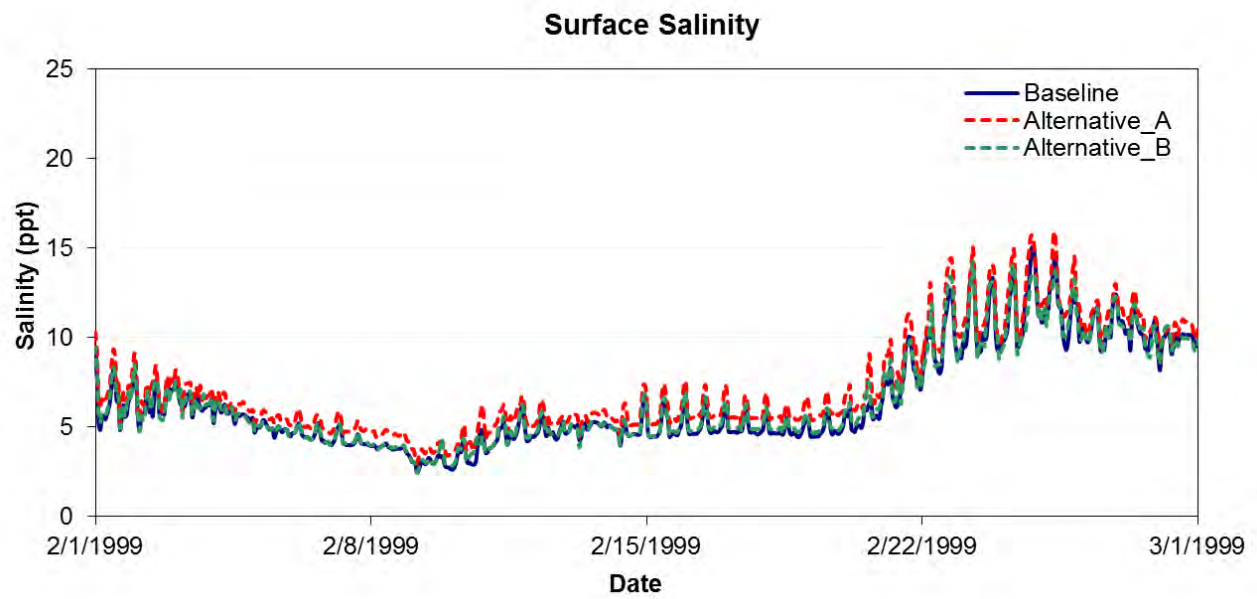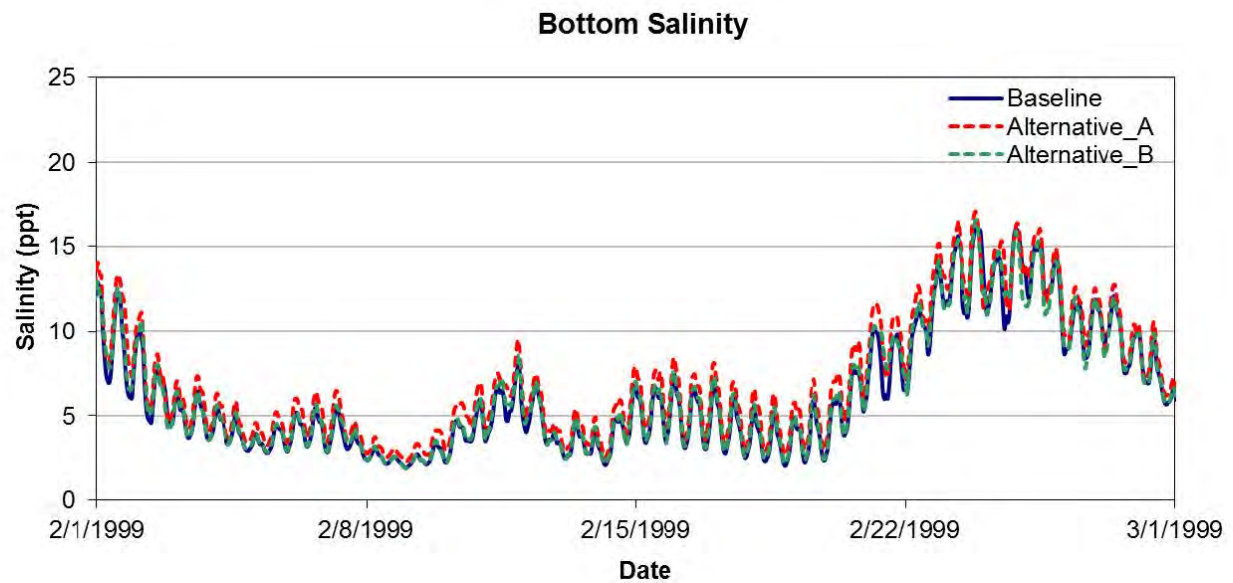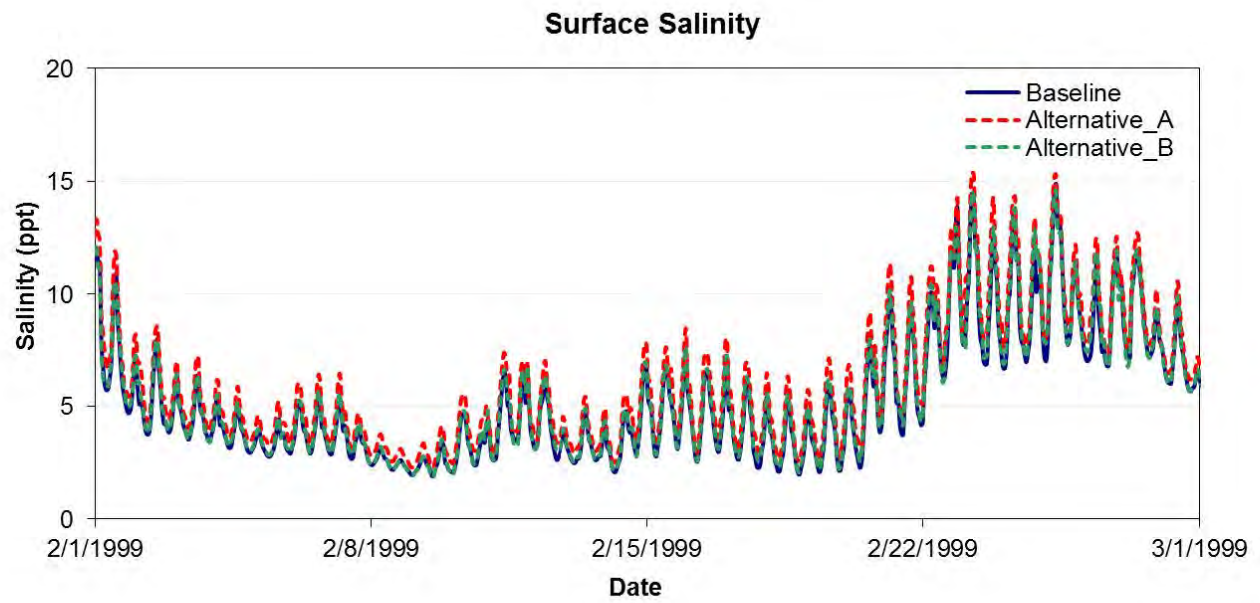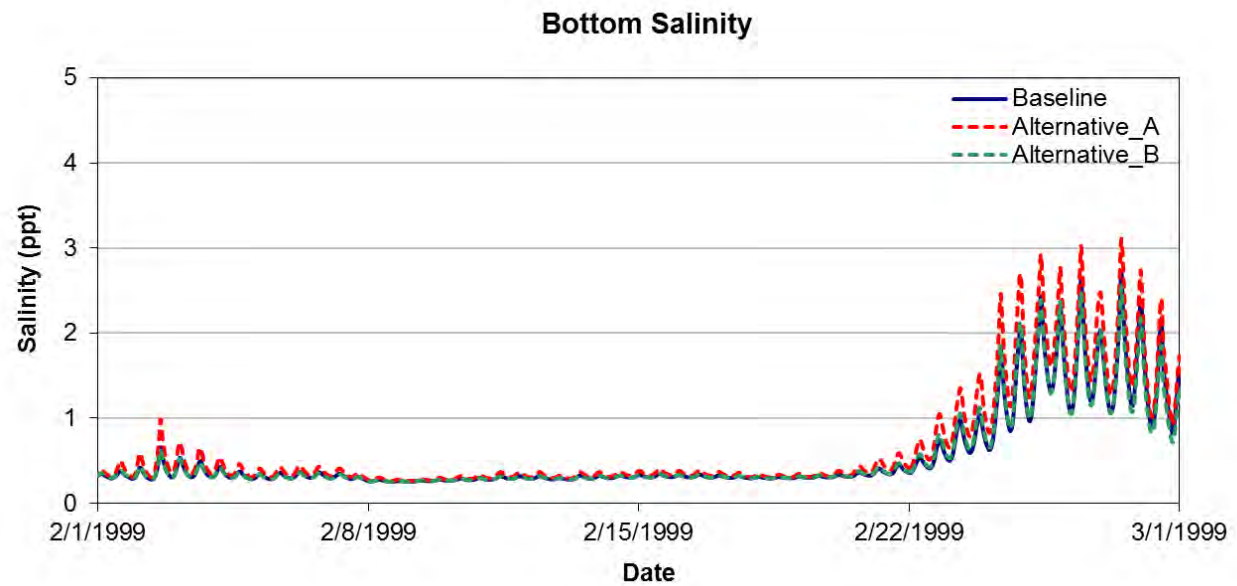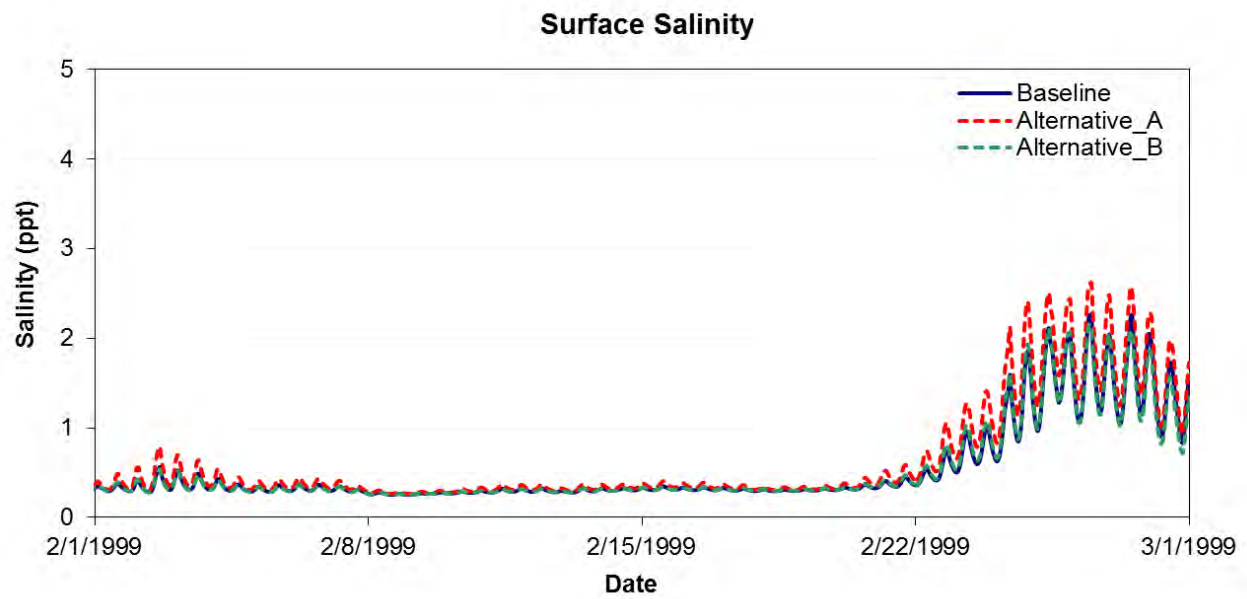
Figure 5.7 Comparison of Baseline, Alternative A, and Alternative B Models Computed Salinity during Dry Period Calibration (Check Point #16)

To investigate the possible effect on ecological systems in the Lower St. Johns River, the SJRWMD developed a predictive salinity exposure model for Vallisneria americana (Figure 5.8) based on field observation, experimental observation, and scientific literature (Dobberfuhl et al., 2011). The study used the daily average salinity for the surface and bottom model cells within the model domain. Seven, 30, 60, and 90 days of moving average salinity have been calculated as ecological model salinity inputs. Figure 5.9 – Figure 5.20 show the comparison of the baseline model and alternative models for 7, 30, 60, and 90 days moving average salinity over a four-month dry period. These plots show the number of days that the model salinity at the surface and bottom was above the indicated salinity concentration (e.g., 5 ppt, 10 ppt, 15 ppt, etc.). Overall, Alternative Plan A and B showed no significant impact at Check Point #16, and the results show little sensitivity to 90 days moving average salinity. Model results show that the greatest effects occur at Check Point #1. For example, counts of moving average salinity over 7, 30, 60, and 90 days during a four-month period for baseline condition show that the possibility of seven days moving average salinity above 5 ppt ranges from 62% at the surface and 70% at the bottom (or as Figure 5.9 shows 71 days and 80 days in a four-month period). For Alternative Plan A, the possibility increases to 73% (83 days) at the surface and 82% (94 days) at the bottom; for Alternative Plan B, the possibility drops to 65% (74 days) at the surface and 72% (82 days) at the bottom, but remains higher than baseline condition.
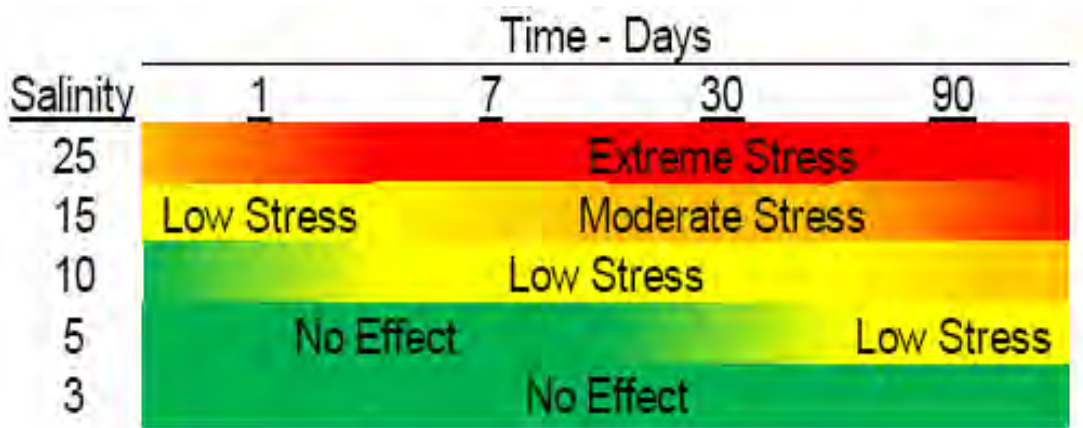
Figure 5.8 Salinity Exposure Model for *V*. Americana (Source: SJRWMD)

Figure 5.9 Comparison of Baseline Model and Alternative Models A and B, 7-Day Average Salinity Dry Period Calibration (Check Point #1)

Figure 5.10 Comparison of Baseline Model and Alternative Models A and B, 30-Day Average Salinity Dry Period Calibration (Check Point #1)

Figure 5.11 Comparison of Baseline Model and Alternative Models A and B, 60-Day Average Salinity Dry Period Calibration (Check Point #1)

Figure 5.12 Comparison of Baseline Model and Alternative Models A and B, 90-Day Average Salinity Dry Period Calibration (Check Point #1)
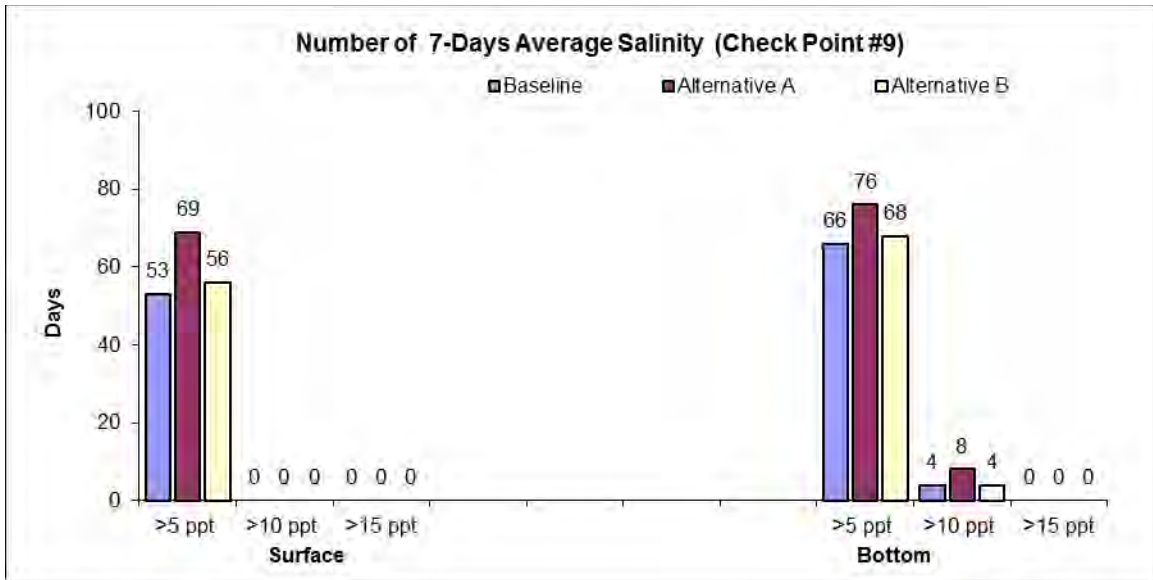
Figure 5.13 Comparison of Baseline Model and Alternative Models A and B, 7-Day Average Salinity Dry Period Calibration (Check Point #9)
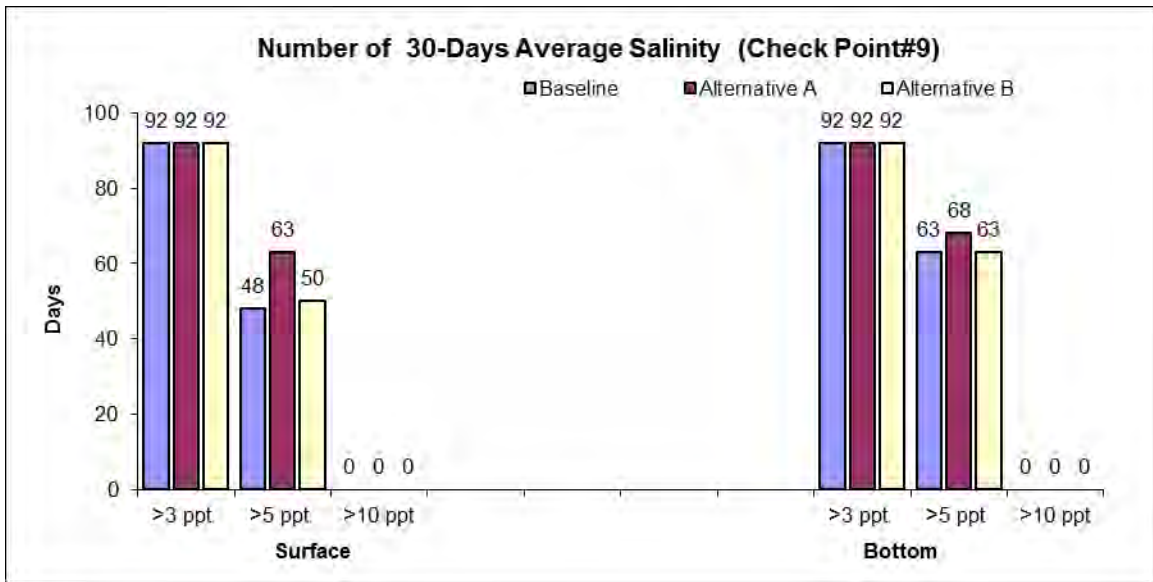
Figure 5.14 Comparison of Baseline Model and Alternative Models A and B, 30-Day Average Salinity Dry Period Calibration (Check Point #9)
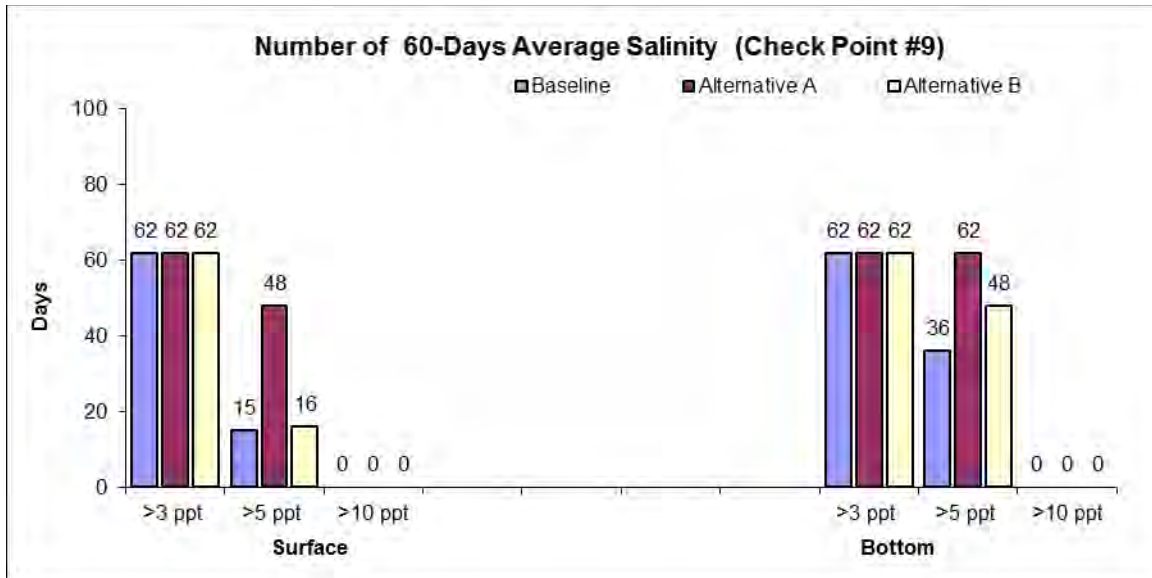
Figure 5.15 Comparison of Baseline Model and Alternative Models A and B, 60-Day Average Salinity Dry Period Calibration (Check Point #9)
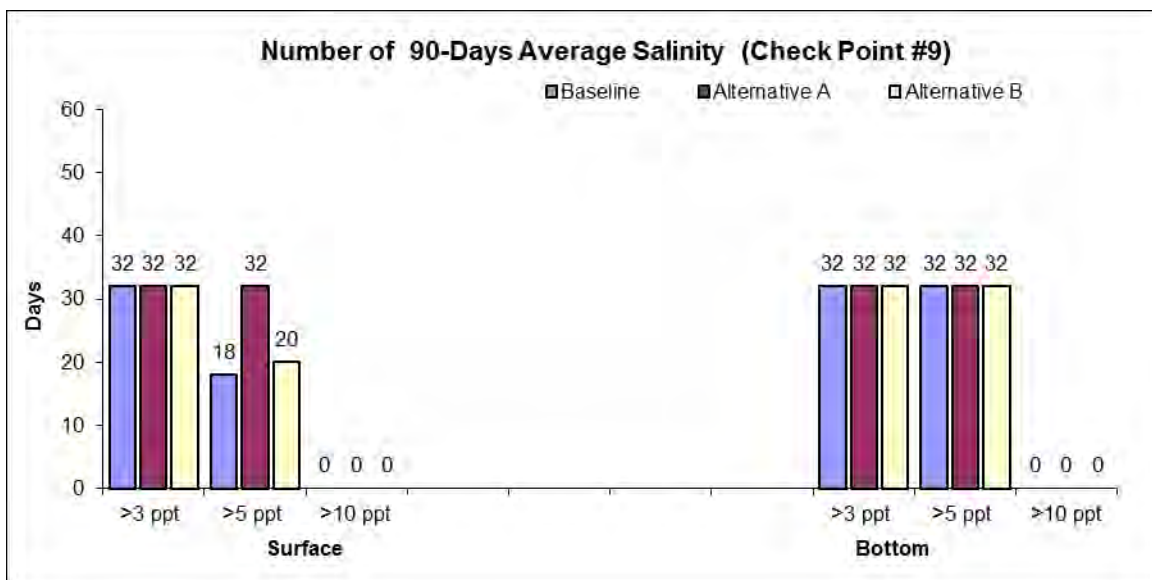
Figure 5.16 Comparison of Baseline Model and Alternative Models A and B, 90-Day Average Salinity Dry Period Calibration (Check Point #9)

Figure 5.17 Comparison of Baseline Model and Alternative Models A and B, 7-Day Average Salinity Dry Period Calibration (Check Point #16)

Figure 5.18 Comparison of Baseline Model and Alternative Models A and B, 30-Day Average Salinity Dry Period Calibration (Check Point #16)
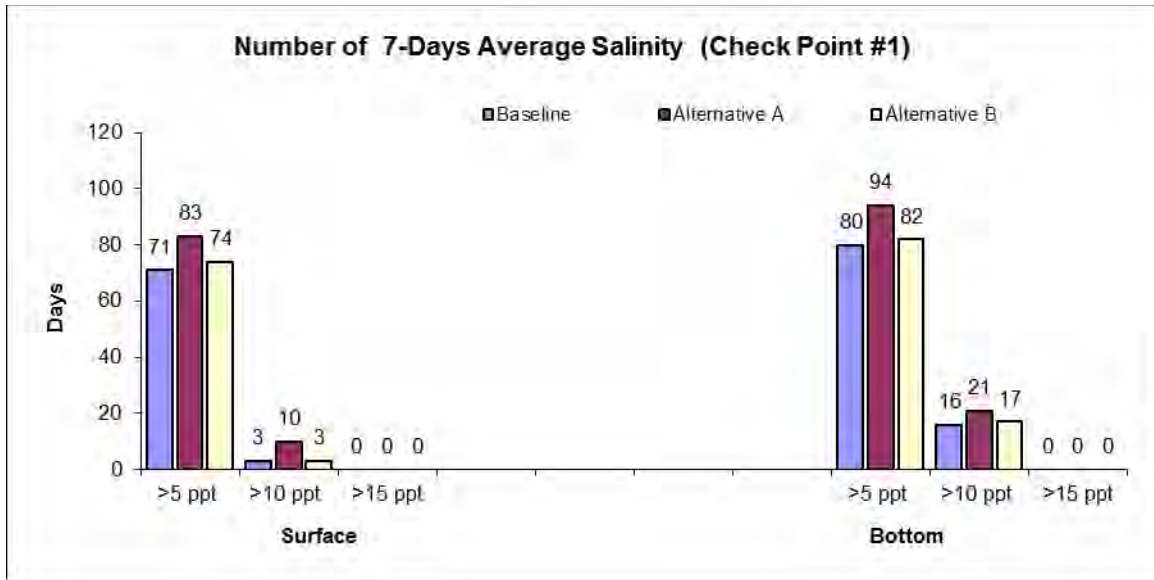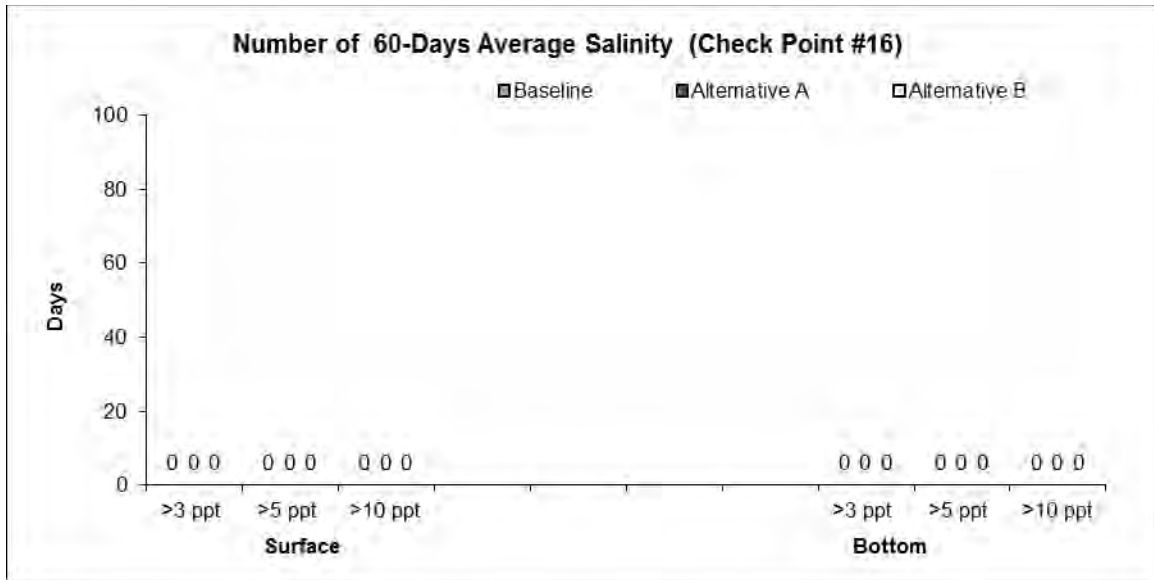
Figure 5.19 Comparison of Baseline Model and Alternative Models A and B, 60-Day Average Salinity Dry Period Calibration (Check Point #16)
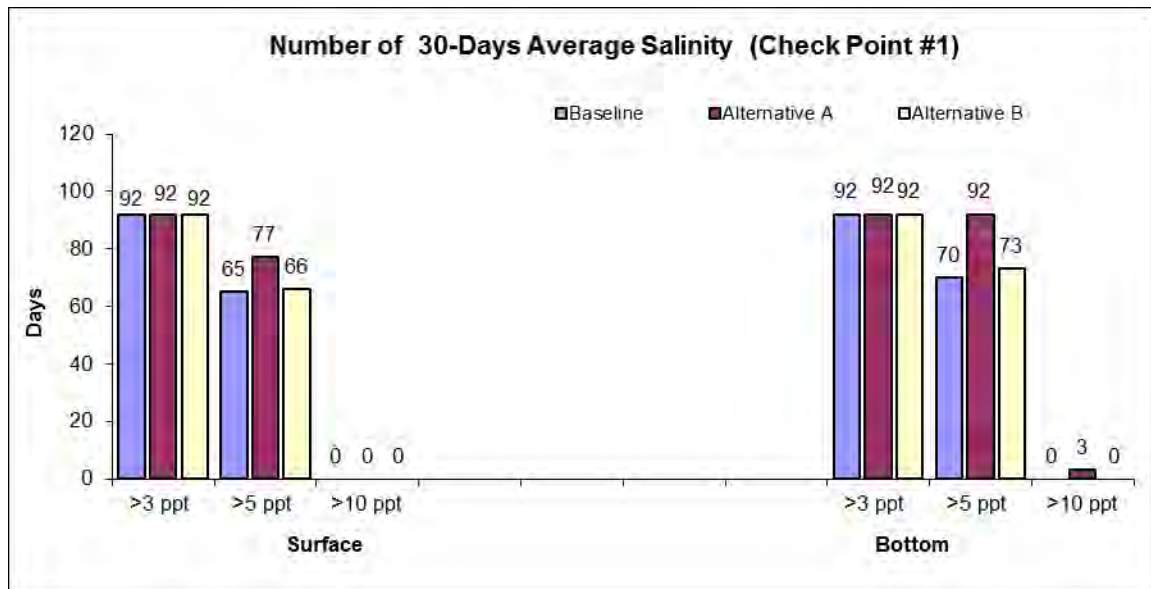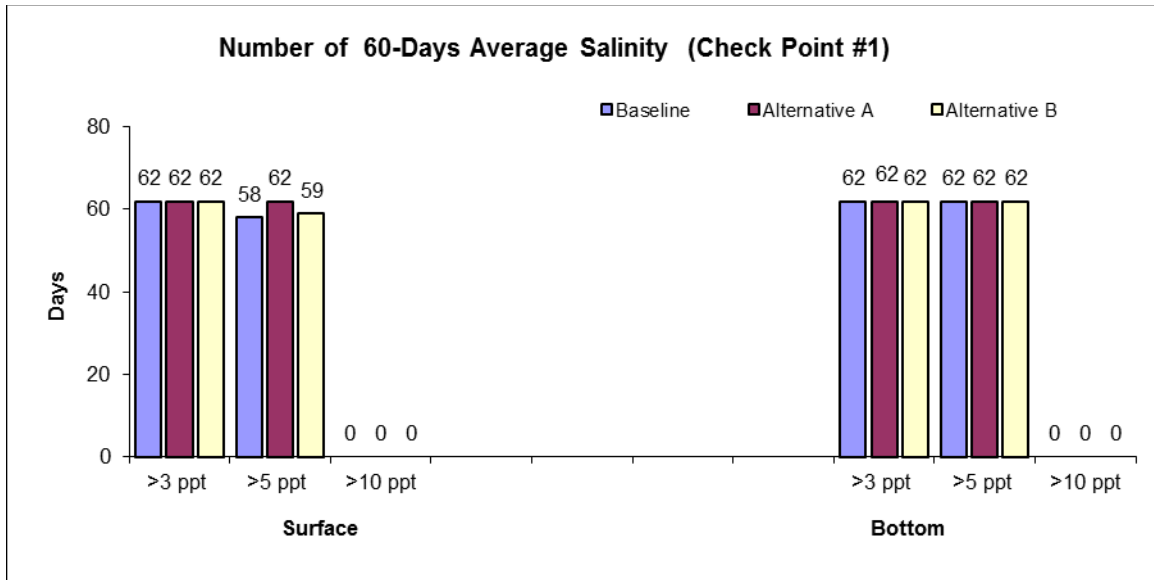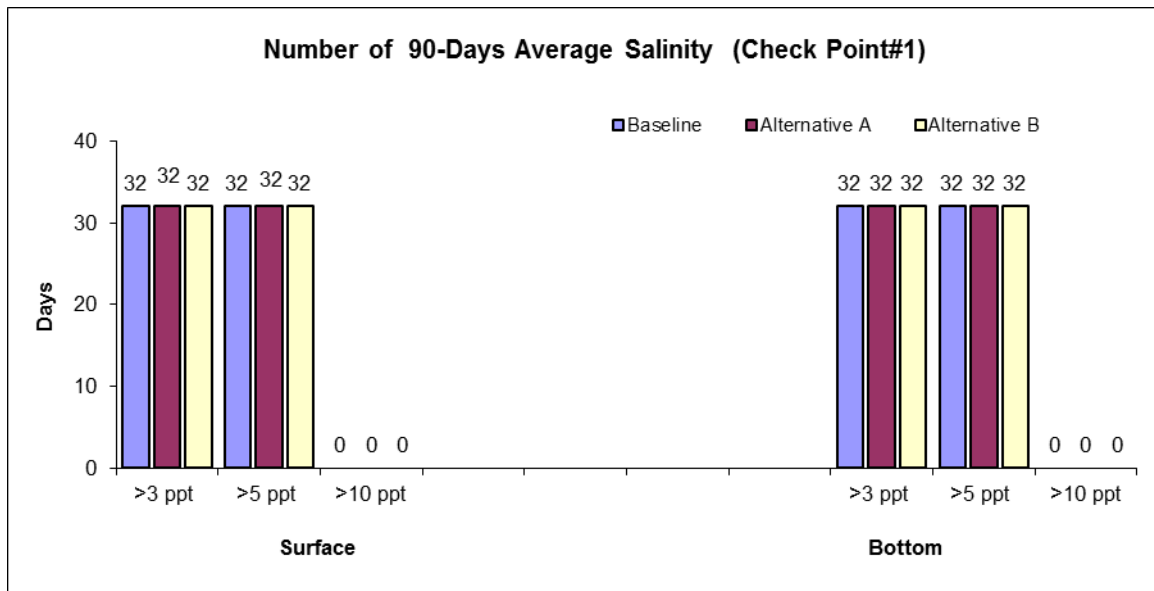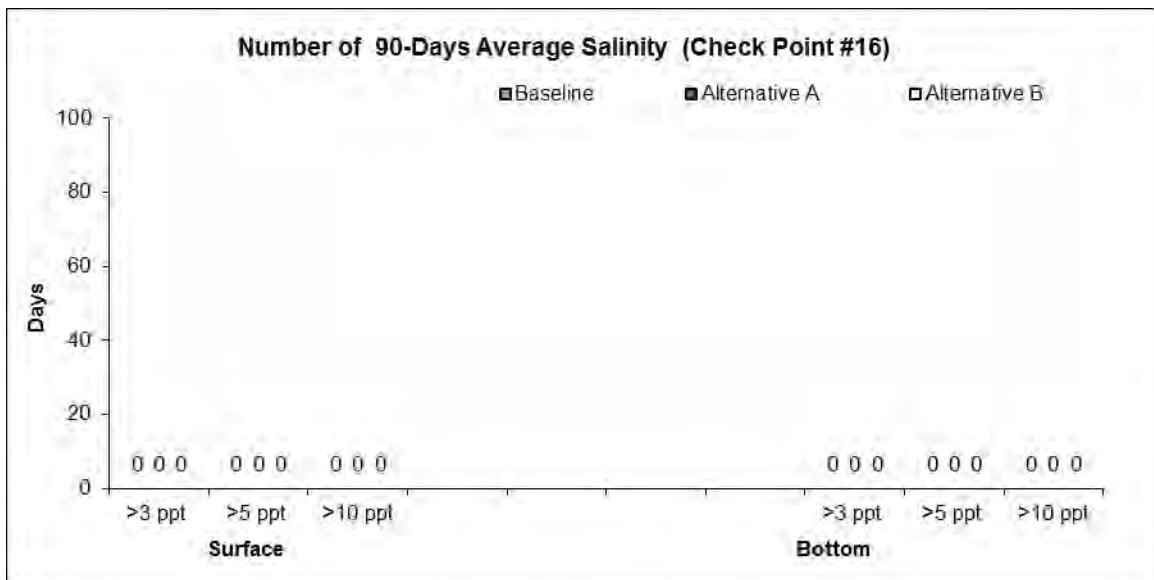

Figure 5.20 Comparison of Baseline Model and Alternative Models A and B, 90-Day Average Salinity Dry Period Calibration (Check Point #16)
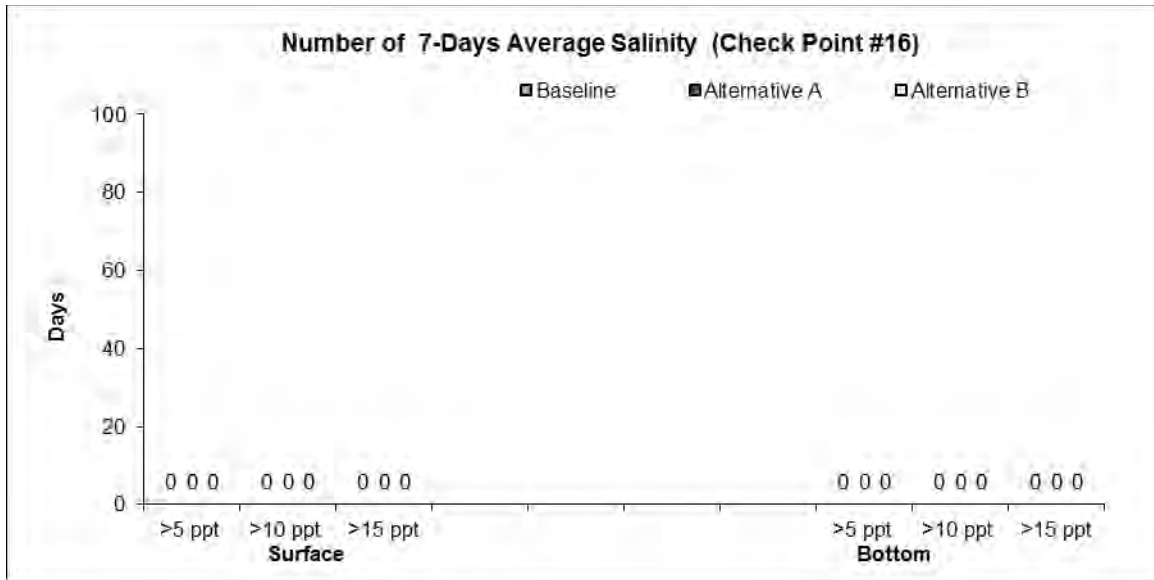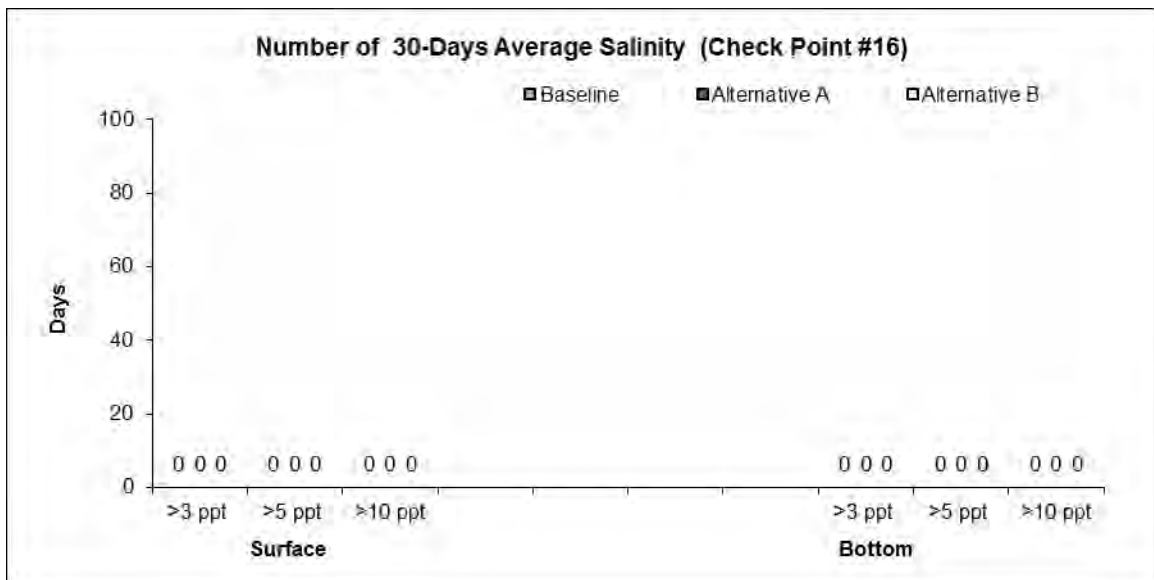
6.0 SUMMARY AND CONCLUSIONS

This study describes the setup, sensitivity analyses, and validation of a hydrodynamic and salinity model for assessing direct impacts to salinity of navigation channel modifications for the Jacksonville Harbor Deepening. The model sensitivity analyses provide six vertical layers and three elements across the navigation channel as most suitable for modeling efficiency and accuracy. The hydrodynamic model was calibrated and verified with monitoring data of water level and salinity collected during 1995 to 2005 for three conditions (wet period, dry period, and wind condition). The overall good agreement between simulated and observed water levels and salinity demonstrates the capability of the model to reasonably simulate these processes in the Lower St. Johns River. Based on the calibration and verification results and preliminary model application, the model is suitable for predicting hydrodynamic and salinity changes in the Lower St. Johns River from the potential channel deepening projects.

To test the model to evaluate the possible impacts from the potential channel dredging projects, this study simulated two preliminary project alternatives during a four-month dry period. To present the current condition of the channel more accurately, the study employed a model with 2009 survey bathymetric data to establish baseline conditions. This baseline model was then adjusted to reflect project modifications (dredging) in two additional models – one for Alternative Plan A and one for Alternative Plan B. Comparisons of simulation results from the models show that while potential dredging would not likely bring the ocean level salinity (35 ppt) any farther upstream, dredging could increase salinity along the river from its mouth to Buckman Bridge. Model results suggest small salinity changes at Shands Bridge and upstream.

REFERENCES

Belaineh, G. 2010. *Estimation of Volume and Chloride Flux from the Upper Floridan Aquifer to the St. Johns River Florida in Support of the Water Supply Impact Study*. St. Johns River Water Management District, Palatka, FL.

Blumberg, A. F., and Mellor, G. L. 1987. "A Description of a Three-dimensional Coastal Ocean Circulation Model." In: *Three-Dimensional Coastal Ocean Models, Coastal and Estuarine Science, Vol. 4.* (Heaps, N. S., ed.) American Geophysical Union, pp. 1-19.

Clark, T., and Hall, W. 1991. Multi-domain Simulations of the Time Dependent Navier-Stokes Equations: Benchmark Error Analysis of Some Nesting Procedures. *J. Comp. Phys*., 92, 456-481.

Cera, T., Smith, D., and Cullum, M. 2010. *Watershed Modeling and Hydrology of the St. Johns River Watershed*. St. Johns River Water Management District, Palatka, FL.

Dobberfuhl, D., Chamberlain, B., Hall., S., Jacoby, C,Mattson,R., Morris, L., and Slater, J. 2011. *Water Supply Impact Study: Littoral Zone Working Group Draft Final Report*. St. Johns River Water Management District, Palatka, FL.

Hamrick, J. M., Kuo, A. Y., and Shen, J. 1995. Mixing and dilution of the Surrey Nuclear Power Plant cooling water discharge into the James River. a report to Virginia Power Company, The College of William and Mary, Virginia Institute of Marine Science, Gloucester Point, VA, 76 pp.

Hamrick, J.M. 1996. User's Manual for the Environmental Fluid Dynamics Computer Code. Special Report No. 331 in *Applied Marine Science and Ocean Engineering*. Department of Physical Sciences, School of Marine Science, Virginia Institute of Marine Science, The College of William and Mary. Gloucester Point, VA.

Hamrick, J.M. 2011. Twenty Years of Estuary and Coastal Modeling with the Environmental Fluid Dynamic Code. (Presentation). *12th International Conference on Estuarine and Coastal Modeling*. Nov 7-9, St. Augustine, FL.

Hargreaves, H. G., and Allen, R.G. 2003. History of Evaluation of Hargreaves Evaporation Equation. *J. of Irrigation and Drainage Engineering ,* Vol. 129(1): 53-63.

Mellor, G, L., (1991). An Equation of State for Numerical Models of Oceans and Estuaries. *J. Atoms. Oceanic Tech*, 8, 609-611.

Jensen, M. E., Burman, R., and Allen, R. 1990. Evapotranspiration and Irrigation Water Requirements. *ASCE Manuals and Reports on Engineering Practice* No. 70: 350 pp.

Jin, K. R., J. M. Hamrick, and T. S. Tisdale, 2000: Application of a three-dimensional hydrodynamic model for Lake Okeechobee, *Journal of Hydraulic Engineering*, 106, 758-772.

St. Johns River Water Management District (SJRWMD). 2011. St. Johns River Water Supply Impact Study, Publication No. SJ2012-1, Palatka, FL.

Sucsy, P., Belaineh, G., Carter, E., Christian, D., Cullum, M., Stewart, J., and Zhang, Y. 2010. *Hydrodynamic Modeling Results*. St. Johns River Water Management District, Palatka, FL.

Sucsy, P., Christian, D., Zhang, Y., and Park, K. 2009. *Alternative Water Supply Cumulative Impact Assessment Interim Report*. St. Johns River Water Management District, Palatka, FL.

Sucsy, P. and Morris, F. 2002. "Calibration of a Three-Dimensional Circulation and Mixing Model of Lower St. Johns River." (Memorandum draft). St. Johns River Water Management District, Palatka, FL.

Toth, D. J. 1993. Volume 1 of the Lower St. Johns River Basin Reconnaissance: Hydrogeology. Tech. Rept. SJ93-7. St. Johns River Water Management District, Palatka, FL.

U.S. Environmental Protection Agency, 2007. *National Management Measures to Control Nonpoint Source Pollution from Hydromodification.* EPA 841-B-07-002, U.S. Environmental Protection Agency, Washington, D.C.

Wool, T. A., S. R. Davie, and H. N. Rodriguez, 2003: Development of three-dimensional hydrodynamic and water quality models to support TMDL decision process for the Neuse River estuary, North Carolina. *Journal of Water Resources Planning and Management*, 129, 295-306.

APPENDIX A

Governing Hydrodynamic

The computational schemes in the EFDC model are equivalent to the widely used Princeton Ocean Model (POM) by Blumberg and Mellor (1987) in many aspects. The EFDC model uses sigma vertical coordinate and curvilinear orthogonal horizontal coordinates. The EFDC model solves the 3-D, vertically hydrostatic, free surface, turbulent averaged equations of motions for a variable density fluid. Dynamically coupled transport equations for turbulent kinetic energy, turbulent length scale, salinity, and temperature are also solved.

To provide uniform resolution in the vertical, a time variable stretching transformation is applied. The stretching is given by

$$z = (z^* + h)/(\zeta + h) \tag{A.1}$$

where * denotes the original physical vertical coordinates and h and ζ are the physical vertical coordinates of the bottom topography and the free surface respectively. This so called "sigma" coordinate allows smooth representation of the bathymetry and same order of accuracy in shallow and deep waters.

In sigma coordinate, transforming the vertically hydrostatic boundary layer form of the turbulent equations of motion and utilizing the Boussinesq approximation for variable density results in the momentum and continuity equations and the transport equations for salinity and temperature, in the following form (John Hamrick ,1996):

$$\partial_t(mHu) + \partial_x(m_yHuu) + \partial_y(m_xHvu) + \partial_z(mwu) - (mf + v\partial_x m_y - u\partial_y m_x)Hv$$
$$= -m_yH\partial_x(g\zeta + P) - m_y(\partial_x h - z\partial_x H)\partial_z P + \partial_z(mH_1^{-1}A_v\partial_z u) + Q_u \tag{A.2}$$

$$\partial_t(mHv) + \partial_x(m_yHuv) + \partial_y(m_xHvv) + \partial_z(mwv) - (mf + v\partial_x m_y - u\partial_y m_x)Hu$$
$$= -m_xH\partial_y(g\zeta + P) - m_x(\partial_y h - z\partial_y H)\partial_z P + \partial_z(mH_1^{-1}A_v\partial_z v) + Q_v \tag{A.3}$$

$$\partial_z P = -gH(\rho - \rho_0)\rho_0^{-1} = -gHb \tag{A.4}$$

$$\partial_t(m\zeta) + \partial_x(m_yHu) + \partial_y(m_xHv) + \partial_z(mw) = 0 \tag{A.5}$$

$$\partial_t(m\zeta) + \partial_x(m_yH\int_0^1 udz) + \partial_y(m_xH\int_0^1 vdz) = 0 \tag{A.6}$$

$$\rho = \rho(P,S,T) \tag{A.7}$$

$$\partial_t(mHS) + \partial_x(m_yHuS) + \partial_y(m_xHvS) + \partial_z(mwS) = \partial_z(mH^{-1}A_b\partial_z S) + Q_S \tag{A.8}$$

$$\partial_t(mHT) + \partial_x(m_yHuT) + \partial_y(m_xHvT) + \partial_z(mwT) = \partial_z(mH^{-1}A_b\partial_z T) + Q_T \tag{A.9}$$

In the above equations, u and v are the horizontal velocity components in the curvilinear, orthogonal coordinates x and y, m_x and m_y are the square roots of the diagonal components of the metric tensor, $m = m_x m_y$ is the Jacobian or square root of the metric tensor determinant. The vertical velocity, with physical units, in the stretched, dimensionless vertical coordinate z is w, and is related to the physical vertical velocity w* by:

$$w = w^* - z(\partial_t \zeta + u m_{x-1} \partial_x \zeta + v m_{y-1} \partial_y \zeta) + (1-z)(u m_{x-1} \partial_x h + v m_{y-1} \partial_y h) \qquad (A.10)$$

The total depth, $H = \zeta + h$, is the sum of the depth below and the free surface displacement relative to the undisturbed physical vertical coordinate origin, z* = 0. The pressure p is the physical pressure in excess of the reference density hydrostatic pressure, $\rho_0 g H(1-z)$, divided by the reference density ρ_0. In the momentum equations (Equations A.2 and A.3), f is the Coriolis parameter, A_v is the vertical turbulent or eddy viscosity, and Q_u and Q_v are momentum source-sink terms which will be later modeled as subgrid scale horizontal diffusion. The density ρ_0, is in general a function of temperature, T, and salinity or water vapor, S, in hydrospheric and atmospheric flows respectively and can be a weak function of pressure, consistent with the incompressible continuity equation under the anelastic approximation (Mellor, 1991, Clark and Hall, 1991). The buoyancy, b, is defined in Equation (A.4) as the normalized deviation of density from the reference value. The continuity equation (Equation A.5) has been integrated with respect to z over the interval (0,1) to produce the depth integrated continuity equation (Equation A.6) using the vertical boundary conditions, w = 0, at z = (0,1), which follows from the kinematic conditions and equation (Equation A.10). In the transport equations for salinity and temperature equations (Equations A.8 and A.9) the source and sink terms, Q_S and Q_T include subgrid scale horizontal diffusion and thermal sources and sinks, while A_b is the vertical turbulent diffusivity.